의학박사 학위논문

A Study of Fertility Preservation Options Using Mouse Ovarian Tissue

생쥐 난소조직을 이용한
가임력보존 방법에 관한 연구

2016 년 2 월

서울대학교 대학원
의학과 분자유전체의학 전공

이 재 왕

A Thesis of the Degree of Doctor of Philosophy

생쥐 난소조직을 이용한 가임력보존 방법에 관한 연구

A Study of Fertility Preservation Options Using Mouse Ovarian Tissue

February 2016

The department of Molecular Genomic Medicine

Seoul National University

College of Medicine

Jaewang Lee

A Study of Fertility Preservation Options Using Mouse Ovarian Tissue

생쥐 난소조직을 이용한 가임력보존 방법에 관한 연구

지도교수 서 창 석

이 논문을 의학박사학위논문으로 제출함

2016년 02월

서울대학교 대학원

의학과 분자유전체의학 전공

이 재 왕

이재왕의 박사학위논문을 인준함

2016년 02월

위 원 장 김 나 영 (인)

부 위 원 장 서 창 석 (인)

위 원 김 진 욱 (인)

위 원 전 진 현 (인)

위 원 지 병 철 (인)

ABSTRACT

Introduction: As the diagnosis and treatment of cancer have been dramatically improved, fertility preservation in female cancer patients has been up in light to improve their quality of life. Oocyte banking and embryo cryopreservation commonly used as fertility preservation options, however, they cannot be applied to pre-pubertal girls and unmarried women. Fertility preservation with ovarian tissue (OT) can provide alternative instead of oocyte and embryo while there are major hurdles to enhance the efficiency of the procedures. First, cryoinjury is usually occurred during cryopreservation process. Second, ischemic injury is also spontaneously happened until re-vascularization, such as 2 days and 5 days are needed to initiate the re-vascularization. Finally, OT has a risk to re-implant the malignant cells after transplantation. This study was aimed to 1) compare the deleterious effects of cryoinjury and ischemic injury on the quality of OT after cryopreservation and transplantation process 2) decrease the cryoinjury after vitrification-warming process using several types of antifreeze proteins 3) diminish the ischemic injury via enhancement of re-vascularization after auto-transplantation 4) optimize the two-dimensional follicle culture system using mouse model.

Methods: For the comparison of cryoinjury and ischemic injury (Exp I), a total of 160 ovaries were harvested from 6-week-old female B6D2F1 mice. Ovaries were randomly divided into eight different groups consisting of two

control groups (fresh and vitri-con) and six experimental groups according to the presence or absence of vitrification and transplantation. (fresh OT [FrOT]-day [D] 2, FrOT-D7, FrOT-D21, vitrified OT [VtOT]-D2, VtOT-D7, and VtOT-D21). In the fresh control group, OT was fixed immediately after ovariectomy, and in the vitri-con group, OT was fixed after the vitrification-warming procedure. All six experimental groups were auto-transplanted with fresh or vitrified-warmed OT, and then the mice were sacrificed by cervical dislocation at 2, 7, or 21 days after grafting. To investigate the detrimental impacts of these injuries, histology, cell-death, blood vessel distribution in OT and ELISA for FSH level

For decrease cryoinjury during vitrification-warming process (Exp II.), a total of 140 mice were sacrificed to collect sexually mature ovaries from 6-week-old aged female B6D2F1 mice. In Exp II-I, a total of 240 whole ovaries were randomly distributed to one of three groups: the fresh control group, the vitrification control group, or the AFP-treated group. The AFP-treated group was further divided into nine subgroups according to AFP type (e.g., FfIBP, LeIBP, and type III AFP) and dose (0.1, 1.0, and 10 mg/mL). After two-step vitrification and four-step warming process, the quality of ovary was assessed. Then, auto-transplantation of ovary was carried out to determine whether the cryoprotective effects of LeIBP could also be seen in OT after transplantation (Exp II-II). A total of 20 B6D2F1 mice were randomly divided into two groups: one group that received 10mg/ml of LeIBP-treated ovaries and another that received the vitrification control ovaries. We used only 10 mg/ml of LeIBP-treated group for this experiment because this group showed the

best results in Experiment II-I. The quality was evaluated by histology, TUNEL, immunohistochemistry and serum FSH level on each evaluation days (Day 2, 7 and 21 days after transplantation).

Next, a combination of simvastatin and/or methylprednisolone was treated to diminish of ischemic injury during avascular period after transplantation (Exp III). Following comparison study, the mice were treated with 5 mg/kg of simvastatin and/or methylprednisolone 2 h before ovareictomy and then the ovaries were cryopreserved by two-step vitrification process as previously described in Exp I. One week later, vitrified OTs were warmed by four-step warming process and then auto-transplanted under bilateral kidney capsules. Similar to the Exp II-II, the mice were sacrificed by cervical dislocation on 2^{nd}, 7^{th} or 21^{st} of the transplantation period to assess the quality of OT. Macroscopic and microscopic examination, immunohistochemistry for blood vessel, flow cytometry for CD45, serum AMH ELISA were carried out on each evaluation days. Moreover, oocyte retrieval from graft and further *in vitro* fertilization were also performed to evaluate the drug safety on gametogenesis and embryogenesis.

Finally, Pre-antral follicles were mechanically isolated from 2-week-old BDF-1 mice and randomly assigned into two groups according to the culture methods (with or without oil layer, Exp IV). *In vivo* matured oocytes were collected using superovulation to compare the growth, cytoplasmic normality, gene expression and embryonic development. Ovarian follicles were *in vitro* cultured for 10 days and cumulus-oocyte complexes were harvested at 16-18 hours after hCG and EGF treatment. Mature oocytes were assessed their

maturational ability and developmental competence *in vitro*.

Results: In Exp I, The vitrification-warming procedure decreased the intact (grade 1, G1) follicle ratio in the vitri-con and FrOT-D2 groups compared with that in the fresh control, and this ratio was reduced more by ischemic injury after transplantation (fresh: 64.2%, vitri-con: 50.3%, and FrOT-D2: 42.5%). The percentage of apoptotic follicles was significantly increased in the vitrified-warmed ovarian tissue than in the fresh control, and it increased more after transplantation without vitrification (fresh: 0.9%, vitri-con: 6.0%, and FrOT-D2: 26.8%). The mean number of follicles per section and CD31-positive area was significantly reduced after vitrification and transplantation. (the number of follicles, fresh: 30.3 ± 3.6, vitri-con: 20.6 ± 2.9, and FrOT-D2: 17.9 ± 2.1; CD31-positive area, fresh: 10.6 ± 1.3%, vitri-con: 5.7 ± 0.9%, and FrOT-D2: 4.2 ± 0.4%). Regarding the G1 follicle ratio and CD31-positive area per graft, only the FrOT groups significantly recovered with time after transplantation (G1 follicle ratio, FrOT-D2: 42.5%, FrOT-D7: 56.1%, and FrOT-D21: 70.7%; CD31-positive area, FrOT-D2: 4.2 ± 0.4%, FrOT-D7: 5.4 ± 0.6%, and FrOT-D21: 7.5 ± 0.8%).

In Exp II-I, the percentage of grade 1 total follicles was significantly higher in only the 10 mg/mL LeIBP group than in the vitrification control while all of AFP-treated groups had significantly improved grade 1 primordial follicle ratio compared with the vitrification control. The apoptotic (TUNEL-positive) follicle ratio was significantly decreased in the 1 and 10 mg/ml of LeIBP treated groups. The proportion of τH2AX positive follicles was significantly

reduced in all AFP-treated groups while the Rad51-positive follicle ratio was significantly decreased in only FfIBP and LeIBP treated groups.

In ExpII-II, after auto-transplantation of OT vitrified with 10 mg/ml of LeIBP, the percentage of total Grade 1 follicles and primordial Grade 1 follicles, the extent of the CD31-positive area were significantly increased. Moreover, the level of serum FSH and the percentage of TUNEL-positive follicles were significantly lower in the LeIBP-treated group than in the control group.

In Exp III, The group that received simvastatin and methylprednisolone showed a significantly improved intact (G1) follicle ratio (D2: $p<0.001$, D7: $p<0.05$ and D21: $p<0.001$), apoptotic follicle ratio (D21: $p<0.05$), CD31-positive area (D7: $p<0.05$ and D21: $p<0.05$), and serum AMH level (D7: $p<0.001$) after transplantation when compared with the sham control. However, no difference was noted in the fertilization and blastocyst formation rate, the number of total and apoptotic blastomere per blastocyst and ICN/TE ratio among the four transplantation groups.

In Exp IV, With respect to the follicular growth, the diameter of follicles in oil layer culture was significantly higher than that of without oil layer. In addition, maturational criteria including survival in oil layer, pseudo-antral like cavity formation, ovulation and oocyte maturation, also significantly increased compared with the without oil layer. Late stage of culture, estradiol on D10 and progesterone on D11 in spent medium of oil layer was statistically significant different between without oil layer culture condition. When comparing the mRNA expression in matured oocytes, no significant difference was observed between *in vivo* and *in vitro* derived oocytes. On the

other hand, *in vitro* grown and matured oocytes increased the level of reactive oxygen species and decreased the mitochondrial activity when compared with the *in vivo* mature oocytes with statistical significance. Moreover, cortical granules of both *in vitro* derived oocytes seemed to be more clumped and unevenly distributed than *in vivo* control. However, no significant difference was noted in actin filament configuration and spindle normality between *in vitro* and *in vivo* derived oocytes.

Conclusions: Cryoinjury and ischemic injury are main cause of follicular depletion during fertility preservation process using ovarian tissue. Inevitable post-transplantation ischemia seems to be more deleterious than cryoinjury during cryopreservation process. Then, cryoinjury and ischemic injury could be decreased by use of AFPs and a combination of simvastatin and methylprednisolone. It can improve the quality of OT via promotion of vessel integrity in OT after cryopreservation and transplantation process. Therefore, minimizing cryoinjury and ischemic injury by enhancing vascularization is needed to improve the ovarian function after fertility preservation. Finally, optimization of two-dimensional *in vitro* follicle culture method was also attempted to avoid the re-implantation of residual malignancy cells in OT after transplantation and found the cause of reduction in embryonic development competence from *in vitro* derived oocytes.

Keywords: Fertility preservation/ ovarian tissue / vitrification/ cryoinjury/ transplantation/ ischemic injury/ *in vitro* follicle culture

CONTENTS

LIST OF TABLES

LIST OF FIGURES

LIST OF ABBREVIATIONS

4-PL: Four-parameter logistic

AFP: Antifreeze protein

α-MEM: α-minimum essential medium

AMH: Anti-Mullerian hormone

ANOVA: Analysis of variance

bFGF: Basic fibroblast growth factor

BSA: Bovine serum albumin

CG: Cortical granule

COC: Cumulus-oocyte complex

CPA: Cryoprotective agent

Ct: Threshold cycle

DAPI: 4',6-diamidino-2-phenylindole

DMSO: Dimethyl sulfoxide

D-PBS: Dulbecco's phosphate-buffered saline

E2: Estradiol

ECM: Extracellular matrix

EG: Ethylene glycol

EGF: Epidermal growth factor

ELISA: Enzyme-linked immunosorbent assay

EM: Electron microscope

ES: Equilibration solution

FBS: fetal bovine serum

FfIBP: Antifreeze protein from Flavobacterium frigoris

FrOT: Transplantation of fresh ovarian tissue

FSH: Follicle-stimulating hormone

GV: Germinal vesicle

GVBD: Germinal vesicle breakdown

H&E: hematoxylin-eosin

H_2O_2: Hydrogen dioxide

hCG: Human chorionic gonadotropin

hMG: Human menopausal gonadotropin

HRP: Horse-radish peroxidase

ICM: Inner cell mass

IHC: Immunohistochemistry

IR: Ice-recrystallization

IRI: Ischemic reperfusion injury

ITS: Insulin-transferrin-selenium

IVC: *In vitro* culture

IVF: *In vitro* fertilization

IVM: *In vitro* maturation

KL: Kit-ligand

LeIBP: Antifreeze protein from Leucosporidium sp.

LN_2: Liquid nitrogen

M.P.: Methylprednisolone

MII: Metaphase II

mTF: Modified tubal fluid

OT: Ovarian tissue

OTC: Ovarian tissue cryopreservation

OTT: Ovarian tissue transplantation

P/S: Penicillin-streptomycin

P4: Progesterone

PMSG: Pregnant mare's serum gonadotropin

qRT-PCR: Quantitative reverse transcription polymerase chain reaction

ROCK: RhoA/Rho-kinase

ROS: Reactive oxygen species

RT: Room temperature

S+M: A combination of simvastatin and methylprednisolone

S-1-P: Sphingosine-1-phosphate

Simv.: Simvastatin

SPSS: The statistical package for the social sciences

TE: Trophoectoderm

TH: Thermal hysteresis

TUNEL: Terminal deoxynucleotidyl transferase dUTP nock-end labeling

VEGF: Vascular endothelial growth factor

VS: Vitrification solution

VtOT: Transplantation of vitrified-warmed ovarian tissue

INTRODUCTION

Over the past decades, the survival rate of cancer patients has dramatically increased because the diagnosis and treatment of cancer has improved, and survivors have tried to carry their own babies to enhance their quality of life after cancer treatment. Mature oocyte and embryo banking are generally recommended before cancer treatment and its safety have been confirmed by American society for reproductive medicine. However, gamete or zygote banking are not feasible options for pre-pubertal girls or fertile women who cannot delay therapy [1-4]. Alternatively, only the transplantation of cryopreserved ovarian tissue (OT) is possible in such patients. To date, >60 babies have been born from female cancer patients who preserved their fertility with ovarian tissue transplantation (OTT) after overcoming cancer [5]. Therefore, ovarian tissue cryopreservation (OTC) and OTT have attracted attention to preserve fertility before/after cancer treatment.

Even though OTC and OTT have some advantages in terms of application, there are still two major hurdles to improve the tissue quality after OTC and OTT. First, cryoinjury occurs during the cryopreservation-warming procedure, and it may cause follicular loss and destruction of stromal cells in the ovary [6-8]. Since protecting the ovary from cryoinjury is crucial to preserve ovarian follicles and improve ovarian function, various attempts have been reported to decrease cryoinjury. This includes the use of different cryodevices [9], cryoprotectant agents [10], transport time and temperature [11], additives such as

antifreeze proteins (AFPs) [12], and genetic manipulation [13].

Second, when OTT without any vascular anastomosis is performed, ischemic injury will occur, causing a drastic depletion of follicles in the grafts. Newton et al. demonstrated that at least 25% of primordial follicles are reduced due to ischemia after xeno-transplantation [14]. Based on this previous study, eliminating or decreasing the ischemic period after avascular transplantation is suggested to reduce ischemic injury to improve graft quality. Therefore, many researchers have attempted to reduce ischemic injury by enhancing re-vascularization after OTT [15-19]. However, which type of injury is more detrimental to OT quality after cryopreservation and transplantation has not been fully investigated. To improve the efficiency of OT cryopreservation and transplantation, it is important to compare these two major causes in terms of OT quality before and after cryopreservation and transplantation.

Since damage that occurs during the cryopreservation procedure may cause follicular depletion, the prevention of chilling injury is the most important requirement for maintaining ovarian function. Recently, there has been much research on developing methods to prevent ovarian follicle depletion and improve ovarian function after ovarian tissue cryopreservation: these methods include using computerized freezing and vitrification procedures, various slow freezing protocols and vitrification procedures [7], genetic manipulation [20], different cryodevices [9], different transport times and temperatures [11], several different cryoprotectant agents [10], and other approaches [21]. Despite these efforts, cryodamage still occurs, resulting in the impairment of ovarian function.

Antifreeze proteins (AFPs) lower the freezing point of a solution in a noncolligative manner and lead to an increase in the difference between the melting point and the freezing point, a phenomenon known as thermal hysteresis (TH), by binding to the surfaces of ice crystals [22]. In 1969, DeVries and his colleague isolated the first AFP from Antarctic fish [23]; since then, AFPs (or ice-binding proteins [IBPs]) that permit survival in subzero environments have also been found in vertebrates, insects, plants, fungi, and bacteria [24]. Moreover, AFPs inhibit ice recrystallization (IR), thus protecting cellular membranes in polar organisms [25]. IR refers to the growth of larger ice grains at the expense of smaller ones, a phenomenon that is fatal to cells and leads to cold damage and cell death [26,27]. Except fish, most psychrophilic organisms use IR inhibition to protect their cell membranes from cryodamage in order to survive extremely icy conditions.

So far, many different types of AFPs have been identified, with different amino acid sequences, molecular weights, ice-binding affinities, TH activities, origins, and structural difference. AFPs are classified as hyperactive and moderately active according to their levels of TH activity. Most fish AFPs exhibit moderate TH activity at about 1℃ [28], while hyperactive AFPs, found in many insects, plants, and bacteria, exhibit TH activities at more than 1℃ [29,30].

The ischemic injury occurring promptly after transplantation without vascular anastomosis is involved in the dramatic follicular depletion observed in grafted OT. At least 25% of the primordial follicles are lost as a result of transplantation of cryopreserved xenografts of human OT into mice [14].

Moreover, Kim et al. revealed that post-transplantation ischemia is much more detrimental to OT than freezing/thawing injury [31]. Prevention of this ischemic injury is therefore critical for preserving the ovarian follicles after transplantation of OT. To date, several studies have attempted to reduce ischemic damage and enhance re-vascularization after OT transplantation using treatments of with various agents such as human menopausal gonadotropin (hMG), vascular endothelial growth factor (VEGF) and basic fibroblast growth factor (bFGF), vitamin E and sphingosine-1-phosphate (S-1-P) [15-19].

Simvastatin is a well-known cholesterol-lowering drug and 3-hydroxy-3-methyl-glutaryl (HMG)-CoA reductase inhibitor, and its main target diseases are hyperlipidemia and coronary artery diseases. In addition, simvastatin also exerts diverse effects, such as angiogenesis, anti-inflammatory effects, and apoptosis inhibition. Lefer et al. and Wolfrum et al. demonstrated that preoperative statin administration protects the myocardium from ischemia-reperfusion injury (IRI) in a cholesterol-independent fashion [32,33]. Moreover, Tuuminen et al. reported that donor simvastatin treatment targets microvascular intracellular RhoA/Rho-kinase (ROCK)-mediated cytoskeleton contraction and promotes endothelial integrity and microvascular reperfusion in rat cardiac allografts [34,35].

Methylprednisolone is a synthetic glucocorticoid or corticosteroid drug that is well-known for its anti-inflammatory properties. It exerts anti-inflammatory effects via inhibition of nuclear factor kappa B transcription factor [35] and by other mechanisms targeting the inflammatory processes. These mechanisms

include dampening of the inflammatory cytokine cascade, inhibiting the activation of T cells, decreasing extravasation of immune cells into the central nervous system, facilitating apoptosis of activated immune cells, and indirectly decreasing the cytotoxic effects of nitric oxide and tumor necrosis factor alpha [36].

Ovarian follicle culture has been up in light to obtain developmentally competent oocytes from *in vitro* system to preserve fertility in cancer patients. Ovarian tissue (OT) cryopreservation and transplantation could be also used as an alternative option to adolescent cancer patients instead of mature oocyte and embryo cryopreservation. However, OT cryopreservation and transplantation has the fatal risk about cancer re-implantation after transplantation of OT, because the malignancy cells could be still resided in cryopreserved OTs. On the other hand, ovarian follicle culture system is seems to be free from such concerns.

Since the first literature of Eppig and Schroeder [37], a diversity of culture method have been used in the follicle culture system, such as absence or presence of oil layer under two-dimensional culture, group culture and even three-dimensional follicle culture [38-41]. In particular, two-dimensional culture system have been mostly applied to harvest the *in vitro* grown and matured oocytes in mice [42-44], rats [45], bovine [46], monkey [47], and human [48]. Mature oocytes, embryos and even live birth have been reported by conventional follicle culture system. However no study has been reported to compare between conventional culture systems.

Even though follicle culture system is thought to be useful method for

mature oocyte collection, maturational and developmental competence of *in vitro* grown oocytes decreased compared with the *in vivo* grown and matured oocytes. Many researchers have made great efforts to improve the quality of oocytes grown *in vitro* while the main cause of decreased quality is not fully understood, yet.

Based on these backgrounds, the aims of this study were to investigate the ovarian damage during fertility preservation process and a minimization of tissue damages through inhibition of those two main injuries using mouse ovarian tissue. Moreover, the present study have tried to improve the efficiency of conventional follicle culture via comparing different culture methods.

MATERIALS AND METHODS

I. Ovarian Injury during Cryopreservation and Transplantation: A Comparative Study between Cryoinjury and Ischemic Injury

Experimental animals and ethics

In total, 80 6-wk-old B6D2F1 female mice (Orient Co., Seongnam, South Korea) were housed under a 12-h light/dark cycle at 22℃ and fed ad libitum. The experimental protocols and animal handling procedures were performed under the approval of the Institutional Animal Care and Use Committee of Seoul National University Bundang Hospital (approval no.:BA1301-120-004-01). Figure 1 shows a schematic figure of the experimental design for chapter I. The mice were divided into eight groups consisting of two control groups (fresh and vitri-con) and six experimental groups (fresh ovarian tissue [FrOT]-day [D] 2, FrOT-D7, FrOT-D21, vitrified ovarian tissue [VtOT]-D2, VtOT-D7, and VtOT-D21). In the fresh control group, OT was fixed immediately after ovariectomy, and in the vitri-con group, OT was fixed after the vitrification-warming procedure. All six experimental groups were auto-transplanted with fresh or vitrified-warmed OT, and then the mice were sacrificed by cervical dislocation at 2, 7, or 21 days after grafting. In previous studies, re-vascularization in mice was initiated within 2 days, and the oxygen saturation of the graft in transplanted mice normalized to control levels 7 days after the transplantation stage [49]. In addition, activated primordial follicles

need 19–21 days to become pre-ovulatory follicles in a murine model[50]. Accordingly, we selected various evaluation days in the present study.

OT vitrification and warming

To obtain the whole ovaries, the mice were anesthetized by an intraperitoneal injection of zoletil (30 mg/kg; Virbac, Carros, France) and Rompun (10 mg/kg; Bayer, Leverkusen, Germany) before ovariectomy. All process including ovariectomy, vitrification-warming, transplantation, suture and even sacrifice was performed by expert researcher (J. Lee). When we did ovariectomy and transplantation, we used fine forcep and scissors to minimize the tissue damage and bleeding. And we did not artificial coagulation due to we thought it could also negatively effect on adjacent tissue such as oviduct, uterus and fat pad. Mouse whole ovaries were cryopreserved using vitrification and warming processes. In accordance with our previous protocol [10], the vitrification and warming processes were respectively subjected to two-step and four-step processes, and Dulbecco's phosphate-buffered saline (D-PBS) containing 20% heat-inactivated fetal bovine serum (FBS, Gibco, Carlsbad, CA, USA) was used as a basic medium. In brief, the whole ovaries were firstly equilibrated in D-PBS containing 20% FBS, 7.5% (v/v) ethylene glycol (EG, Sigma-Aldrich, St. Louis, MO, USA), and 7.5% (v/v) dimethyl sulfoxide (DMSO, Sigma-Aldrich) for 10 min at room temperature (RT). Then the equilibrated whole ovaries were transferred to the vitrification solution, which was composed of D-PBS supplemented with 20% FBS, 20% EG, 20% DMSO, and 0.5 M sucrose (Sigma-Aldrich) for 5 min at RT. To

improve heat conductivity, remaining water was removed with sterilized gauze, and each whole ovary was laid on the top of an electron microscopic copper grid. The whole ovaries were directly plunged into liquid nitrogen (LN_2) and then the cryovials (Nunc, Roskilde, Denmark) stored in LN_2 tank in a cryovial. Vitrified whole ovaries were stored in an LN_2 tank for at least 1 wk.

One week later, the vitrified whole ovaries were warmed. Firstly, the ovaries were allowed to warm spontaneously at RT for 10 sec, and then they were serially incubated with 1.0 M, 0.5 M, 0.25 M, and 0 M of sucrose solutions at RT for 5 min for each step to minimize osmotic shock.

Auto-transplantation of fresh or vitrified-warmed ovaries

The auto-transplantation procedures were performed as previously described[51]. The mice were anesthetized by an intraperitoneal injection of zoletil (30 mg/kg) and Rompun (10 mg/kg; Bayer) before the auto-transplantation procedure was performed. In the FrOT groups, fresh whole ovaries were removed and immediately implanted into both kidney capsules under anesthetic condition. In the VtOT groups, vitrified whole ovaries were warmed and instantly transplanted into both kidney capsules 1 wk after vitrification. The transplantation of fresh or vitrified-warmed whole ovary was performed simultaneously to synchronize with the sacrifice day. After auto-transplantation, the incision site and skin were closed and sutured with 4-0 suture silk in 3 min.

Preparation of the OT sample and blood serum level

To assess the histology and immunohistochemical analysis of OTs, non-transplanted OTs from two control groups and grafts from six experimental groups were collected, and the ovaries were immediately fixed with 4% paraformaldehyde. Whole blood was obtained from each of the eight groups to investigate the restoration of ovarian function by measuring the serum follicle-stimulating hormone (FSH) level.

Follicle classification and morphological analysis

Paraffin sections (5 μm) of each tissue were mounted on slides and stained with hematoxylin and eosin (Merck, Darmstadt, Germany), and the follicles were classified and graded by the following criteria [52,53].

The developmental stages of the ovarian follicles were classified as follows: 1) primordial: single layer of flattened pre-granulosa cells; 2) primary: single layer of granulosa cells, one or more of which is cuboidal; 3) secondary: two or more layers of cuboidal granulosa cells, without the antrum; or 4) antral: multiple layers of cuboidal granulosa cells with the antrum.

The morphological integrity of the follicles was defined as follows: 1) primordial/primary follicle: grade 1 (G1), spherical with even distribution of the granulosa cells; grade 2 (G2), granulosa cells are pulled away from the edge of the follicle, but the oocytes are still spherical; and grade 3 (G3), pyknotic nuclei, misshapen oocytes, or vacuolation; and 2) secondary/antral follicle: G1, intact spherical follicle with evenly distributed granulosa and theca cells, small spaces, and spherical oocytes; G2, intact theca cells,

disrupted granulosa cells, and spherical oocytes; and G3, disruption and loss of granulosa and theca cells, pyknotic nuclei, and missing oocyte.

The number of ovarian follicles was counted from the entire section under a high power field (×400). The follicles were counted and classified in only one section per each OT when they contained oocytes to avoid miscounting.

Analysis of apoptosis

To compare the apoptotic effects of cryoinjury and ischemic injury, apoptotic follicles in the OT from each of the eight groups was detected by terminal deoxynucleotidyl transferase dUTP nick end labeling (TUNEL, Roche, Switzerland) assay. Briefly, the sections were deparaffinized and rehydrated to perform TUNEL assay, and then the slides were incubated with 0.8% proteinase K (Dako, Glostrup, Denmark) for 15 min at RT. Following incubation of the proteinase K solution, the sections were treated with a TUNEL reaction mixture under humidified and dark conditions for 1 h at 37℃. To visualize the nucleus, the slides were mounted using the Vectashield mounting medium with 4',6-diamidino-2-phenylindole (Vector Laboratories, Burlingame, CA, USA) and examined under the inverted Zeiss AX10 microscope (Carl Zeiss, Göttingen, Germany). Negative and positive controls were respectively used as an untreated TUNEL mixture and treated mixture with 100 U/mL of DNase I. When the percentage of TUNEL-positive follicles was >30%, we regarded the follicle as an apoptotic follicle, according to our previous study [54].

Immunohistochemistry (IHC) of ovarian tissues

To evaluate the distribution of blood vessels in OTs, CD31-positive areas in OTs were detected by immunohistochemistry. In brief, antigenic retrieval was subjected to microwave heating for signal enhancement and slide cool down at RT for 30 min. Then the slides were treated with a horseradish peroxidase (HRP) blocking solution to inactivate the endogenous HRP and were incubated overnight at 4℃ with primary CD31 antibody (PECAM; 1:200; Abcam, Cambridge, UK). The next day, the sections were incubated with EnVision+ HRP (Dako) for 30 min at RT. Following HRP incubation, the enzyme was reacted with liquid DAB+ substrate (Dako) for 10 min at RT. To counterstain, the slides were stained with hematoxylin and serially dehydrated with ethanol and xylene. Finally, the slides were mounted and examined under an inverted Zeiss AX10 microscope (Carl Zeiss). After examining the overall OTs, we imaged the ovaries under ×100 magnification and automatically merged them using Adobe Photoshop CS3 (San Jose, CA, USA). The brown colored-CD31 blood vessels in the merged images were quantified by the i-solution image analysis program (IMT Technology Inc., Seoul, Korea).

Enzyme-linked immunosorbent assay for FSH

To investigate ovarian function, whole blood samples were collected by cardiac puncture, and serum separation was performed by centrifugation at 13,000 revolutions per min for 3 min. Blood sera from the fresh controls were immediately collected from the mice after sacrifice. In the vitri-con group,

mice were ovariectomized for OT vitrification and sacrificed 1 wk after ovariectomy to evaluate the serum FSH level. The six experimental groups were sacrificed to obtain blood sera on each evaluation day (2, 7, and 21 days). Following serum separation, enzyme-linked immunosorbent assay (ELISA; Endocrine Technologies, Newark, CA, USA) for FSH was used to measure the eight different groups in accordance with the manufacturer's instructions. The optical density was read at 450 nm, and the concentrations were converted using a standard curve. The intra- and inter-assay coefficients of variation were 6.35% and 5.88%, respectively. The sensitivity of the ELISA kit was 0.5 ng/mL.

Statistical analysis

A chi-square test (for follicle grading and the TUNEL assay) or ANOVA (for the number of follicles, proportion of CD31-positive areas, and serum FSH level) was performed. SPSS, version 12.0 software (IBM Corp., Armonk, NY, USA) and GraphPad Prism 6.0 (Graphad Software, La Jolla, CA, USA) were used to perform statistical analysis. Values of $p < 0.05$ were considered to indicate statistically significant differences.

II. Effects of Three Different Types of Antifreeze Proteins on Mouse Ovarian Tissue Cryopreservation and Transplantation

Experimental animals

Five-week-old B6D2F1 female mice (Orient Co., Seongnam, South Korea) were housed under a 12 h light/dark cycle at 22℃ and fed ad libitum. The experimental protocols and animal handling procedures were performed with the approval of the Institutional Animal Care and Use Committee of Seoul National University Bundang Hospital (BA1304-126-029-01).

Vitrification and warming of whole mouse ovaries (Experiment II-I)

Figure 2 contains a schematic diagram that shows the design for Experiment II-I. Whole ovaries were obtained from mice after cervical dislocation by expert to treat experimental animals (J. Lee) and were randomly assigned to one of three groups: the fresh control group, the vitrification control group, or the AFP-treated group. The AFP-treated group was further divided into nine subgroups according to AFP type (e.g., FfIBP, LeIBP, and type III AFP) and dose (0.1, 1.0, and 10 mg/mL). A total of 240 whole ovaries were obtained from 120 mice. We had shown previously in a pilot study that type III AFPs could have beneficial effects on OT vitrification and warming when used at 5 mg/mL [12].

The ovaries were vitrified using a two-step process as follows [10]. First, they were equilibrated in Dulbecco's phosphate-buffered saline (D-PBS) supplemented with 20% (v/v) fetal bovine serum (FBS; Gibco, Carlsbad,

California, US), 7.5% (v:v) ethylene glycol (EG; Sigma, St.Louis, Missouri, US), and 7.5% (v/v) dimethylsulfoxide (DMSO, Sigma) for 10 min at room temperature. Then they were transferred into the vitrification medium, which consisted of D-PBS containing 20% FBS, 20% EG, 20% DMSO, and 0.5 M sucrose (Sigma), for 5 min at room temperature. To enhance heat conductivity and eliminate the remaining water, each ovary was then put on an electron microscopic copper grid (JEOL, Tokyo, Japan); then the ovaries were plunged directly into liquid nitrogen. The vitrified ovaries were then placed into 1.5 mL cryovials (Nunc, Roskilde, Denmark) filled with liquid nitrogen.

At least one week after vitrification, the ovaries underwent warming as follows. First, the ovaries were exposed to air for 10 sec. Then, they were rehydrated via sequential equilibration in 1.00, 0.50, 0.25, and 0.00 M sucrose solutions at room temperature, for 5 min each time. D-PBS supplemented with 20% FBS was used as the basal medium for both vitrification and warming. For the AFP-treated groups, the medium was supplemented with AFP during both vitrification and warming. The charcateristics of AFPs used in this study was summarized in Table 1.

Auto-transplantation of cryopreserved ovaries (Experiment II-II)

We performed Experiment II to determine whether the cryoprotective effects of LeIBP could also be seen in OT after transplantation (Fig 2.1). A total of 20 B6D2F1 mice were randomly divided into two groups: one group that received 10mg/ml of LeIBP-treated ovaries and another that received the vitrification control ovaries. We used only 10 mg/ml of LeIBP-treated group

for this experiment because this group showed the best results in Experiment I. The mice were anesthetized by intraperitoneal injection of 30 mg/kg of Zoletil (Virbac, Carros, France) and 10 mg/kg of Rompun (Bayer, Leverkusen, Germany). After analgesia, the ovaries were removed through bilateral incisions in the dorsal flank. All the operating procedures were finished after suturing the incisions by 4-0 silk suture silk in 10 minutes. Then the ovaries were vitrified as described for Experiment I. Seven days after the ovariectomy, the vitrified ovaries were warmed as described above and then auto-transplanted underneath the kidney capsules.

Sample preparation

In Experiment I, the ovaries were warmed and fixed immediately with 4% paraformaldehyde. In Experiment II, quick and humane sacrifice of mice was performed by cervical dislocation 7 days after transplantation to obtain the grafts and whole blood from each mouse, respectively. The collected ovaries were prepared for paraffin embedding, and the blood serum was separated by centrifugation to perform enzyme-linked immunosorbent assay (ELISA) for mouse follicle stimulating hormone (FSH).

Morphological assessment and classification of ovarian follicles

The tissues were dehydrated, paraffin embedded, serially sectioned at 4-μm thickness, and the first 5th section of tissue was mounted onto glass slides. The slides were stained with hematoxylin and eosin (Merck, Darmstadt, Germany) and then analyzed for follicle count and grading. Each slide was

read twice by a single experienced inspector (J. Lee), and the average of the follicle counts was used for the results. Only follicles with a visible nucleus in the oocyte were counted, to avoid double counting of follicles. Each follicle was classified according to the following categories [52]:

primordial: single layer of flattened pregranulosa cells;

primary: single layer of granulosa cells, one or more of which was cuboidal;

secondary: two or more layers of cuboidal granulosa cells, with the antrum absent

antral: multiple layers of cuboidal granulosa cells, with the antrum present.

The integrity of each follicle was evaluated using the following criteria [53]:

primordial/primary follicle: Grade 1 (G1), spherical with even distribution of the granulosa cells; Grade 2 (G2), granulosa cells pulled away from the edge of the follicle but with the oocytes still spherical; Grade 3 (G3), pyknotic nuclei, misshapen oocytes, or vacuolation;

secondary/antral follicle: G1, intact spherical follicle with evenly distributed granulosa and theca cells, small space, and spherical oocytes; G2, intact theca cells, disrupted granulosa cells, and spherical oocytes; G3, disruption and loss of granulosa and theca cells, pyknotic nuclei, and missing oocyte.

Atretic follicles were characterized by the presence of eosinophilia of the ooplasm, contraction and clumping of chromatin material, and wrinkling of the nuclear membranes in the oocytes.

Assessment of apoptotic follicles

Apoptosis of follicles in the warmed and transplanted ovaries was evaluated

as previously described [10]. Following deparaffinization and rehydration, the slide was treated with 0.8% proteinase K (Dako, Denmark) at room temperature for 15 min, incubated with a TUNEL reaction mixture (1:9 enzyme:label) for 1 hour at 37°C in a humidified chamber in the dark, and then rinsed with D-PBS. The slides were then mounted in VECTASHIELD® Mounting Medium with 4′, 6-diamidino-2-phenylindole (DAPI) (Vector Laboratories, Burlingame, California, US), and examined under an inverted Zeiss AX10 microscope (Carl Zeiss, Oberkochen, Germany). Slides incubated without the TUNEL reaction mixture were used as the negative control and those incubated in 100 U/mL of DNase I was used as the positive control. Cells that were positive for the TUNEL assay were indicated by green fluorescence. A follicle containing over 30% cells positive for green fluorescence was considered to be an apoptotic follicle.

Immunohistochemical analysis

Following TUNEL assay, immunohistochemical analysis was carried out to investigate DSB and DDR using τH2AX and Rad51 antibodies [55]. The paraffin slides (4 μm) of the ovaries were baked and then dewaxed and rehydrated in xylene, ethanol, and water. Rehydrated slides were microwave-heated in an appropriate heat-induced epitope retrieval solution for 20 min in order to block the endogenous peroxidase activity with peroxidase blocking solution (Dako) for 10 min. Then, the slides were incubated with appropriate concentrations of τH2AX (1:100; Millipore, US), Rad51 (1:100; Bioworld Technology, St.Louis, Missouri), and CD31 (1:100; Abcam Cambridge, UK)

primary antibodies at room temperature for 1 hour. Following incubation with the τH2AX and Rad51 antibodies, the slides were then incubated in Alexa 594 conjugated anti-rabbit secondary antibody in blocking buffer (1:1000; Invitrogen, Carlsbad, California, US) at room temperature for 1 hour. Then, the slides were mounted with VECTASHIELD® Mounting Medium containing DAPI (Vector Labs) and examined using a Zeiss AX10 fluorescence microscope (Carl Zeiss). Following incubation with CD31 antibody, the sections were treated with EnVision™+ HRP (Dako, Carpinteria, CA, US) for 30 min at room temperature and then treated with Liquid DAB+ Substrate (Dako, Denmark) for 10 minutes at room temperature. Then all sections were counterstained with hematoxylin (Dako, Denmark) and dehydrated in ethanol and xylene. Finally, the slides were mounted with Mounting Medium (Dako, Denmark) and examined under an inverted Zeiss AX10 microscope (Carl Zeiss). Follicles containing at least one nucleus stained with τH2AX were considered to contain DNA DSB, and follicles containing at least one nucleus stained with Rad51 were regarded as undergoing DNA DDR. In 2009, Brown and Holt already demonstrated that the expression of Rad 51 was up-regulated by irradiation within 10 min [56]. Because the warming process in the present study took more 20 min, this is sufficient for DNA repair and express Rad51 expression to start.

Measurement of serum FSH level

We used an ELISA kit (Endocrine Technologies, Newark, NJ, US) to measure the concentration of serum FSH in the two different transplant

groups (vitrification control vs. LeIBP-treated). According to the manufacturer's instructions, FSH was measured by extrapolating the optical density reading of the ELISA plate at 450 nm, and concentrations were calculated using serial standard dilutions.

Statistical analysis

The distribution of the follicle stages and normality in each sample were evaluated for each group. Data were analyzed by Student's t-test, the Mann–Whitney test, the chi-square test, and ANOVA, as appropriate. SPSS version 12.0 software (SPSS Inc., Chicago, US) was used for statistical analysis, and a p value of <0.05 was considered to indicate a statistically significant difference.

III. A Combination of Simvastatin and Methylprednisolone Improves the Quality of Vitrified-warmed Ovarian Tissue after Auto-transplantation

Experimental animals and administration

A total of 232 six-week-old B6D2F1 female mice (Orient Co., South Korea) were housed under a 12-h light/dark cycle at 22℃ and fed *ad libitum*. The experimental protocols and animal-handling procedures were performed with approval of the Institutional Animal Care and Use Committee (IACUC) of Seoul National University Bundang Hospital (BA1407-156/028-01). Dissection, vitrification, warming, and auto-transplantation of whole mice ovaries were performed according to the IACUC-approved method.

Experiment III-I (Auto-transplantation of fresh OT)

Forty mice (n=10 per group) were used for a preliminary experiment to evaluate the beneficial effects of simvastatin and/or methylprednisolone on transplantation of fresh OT. The mice were randomly assigned to each group and administered 5 mg/kg of simvastatin perorally, 15 mg/kg of methylprednisolone intravenously, or a combination of the two drugs 2 h before ovariectomy (Simv., M.P., and S+M groups, respectively). The same volume of saline was orally gavaged 2 h before ovariectomy in the sham control group. Two hours later, the mice were anesthetized by intraperitoneal injection of a solution of 30 mg/kg of ketamine (Virbac, Carros, France) and 10 mg/kg of xylazine (Bayer, Leverkusen, Germany) for ovariectomy and

auto-transplantation. Dorsal fur of mice was shaved and the skin was swabbed with 70% (v/v) alcohol. A 1-cm incision was made on the dorsal skin, and both ovaries removed and auto-transplanted beneath the bilateral kidney. And then, the incision site and skin were closed and sutured. The mice were sacrificed with cervical dislocation 7 days after auto-transplantation. Following sacrifice, the OTs were fixed for histological and immunohistochemical assessment.

Experiment III-II (Auto-transplantation of vitrified-warmed OT)

The experimental design of experiment III-II is schematically presented in Figure 3. The mice were divided into six groups as fresh control (n=10), vitrified-warmed control (n=10), sham control (n=43), simvastatin (n=43), methylprednisolone (n=43) and a combination of simvastatin and methylprednisolone combination (n=43) treated groups in experiments II. In fresh and vitrified-warmed control groups, OTs were immediately fixed after ovariectomy and vitrification-warming procedures, respectively. To compare the efficacy of treatment during transplantation, the mice were administered 5 mg/kg of simvastatin perorally, 15 mg/kg of methylprednisolone intravenously, or a combination of the two drugs 2 h before ovariectomy and vitrification. The same volume of saline was orally gavaged 2 h before ovariectomy in the sham control group. After vitrification-warming the OTs were auto-transplanted. The transplanted OTs were evaluated after 2, 7, and 21 days.

Ten mice per group were used for evaluation of histology,

immunohistology and serum anti-Mullerian hormone (n=120), and 3 mice per group were used for flow cytometric analysis (n=36) for the four experimental groups at each evaluation day. To validate the embryonic developmental competence using retrieved oocytes, 4 mice per group were used 21 days after transplantation (n=16).

In the previous studies, re-vascularization in murine model occurred within 48 hours, oxygen saturation returned to nearly normal levels in control mice 7 days after transplantation and it took up to 19-21 days for the development of an activated follicle to reach the pre-ovulatory stage [49,50]. Based on these previous studies, we chose the 2, 7 and 21 day time points for the evaluation of ovarian follicle development and function.

Cryopreservation of whole mice ovaries by two-step vitrification method

The mice were anesthetized by intraperitoneal injection of a solution of ketamine (0.15 mg/g of body weight) and xylazine (0.016 mg/g of body weight) to remove whole ovaries. For OT collection, the ovaries were categorized into four treatment groups and vitrified in accordance with the protocols described elsewhere [10]. Briefly, OTs were serially incubated in equilibration solution (ES) for 10 min and vitrification solution (VS) for 5 min, respectively. [Composition of ES: Dulbecco's phosphate-buffered saline (D-PBS) supplemented with 20% (v/v) fetal bovine serum (FBS; Gibco, US), 7.5% (v/v) ethylene glycol (EG; Sigma, US), and 7.5% (v/v) dimethylsulfoxide (DMSO; Sigma). Composition of VS: D-PBS containing 20% FBS, 20% EG, 20% DMSO, and 0.5 M sucrose (Sigma)]. After immersion, each ovary was

placed on the copper grid of the electron microscope (EM) in order to improve the cooling rate, and the remaining VS was removed by filtering through sterilized filter papers. The EM grid containing the adhered OTs was immediately plunged into liquid nitrogen, and the vitrified ovaries were placed in 1.5-mL cryovial (Nunc, Denmark) filled with liquid nitrogen.

Warming and auto-transplantation of cryopreserved ovaries

A week after ovariectomy and vitrification, the cryopreserved OTs were exposed to room temperature (RT) for 10–20 s in order to warm the vitrified ovaries. They were then immediately incubated with gradually decreasing concentrations of sucrose solution (1.0, 0.5, 0.25, and 0 M) for 5 min each. D-PBS supplemented with 20% FBS was used as the basic medium. The mice were anesthetized by intraperitoneal injection of a solution of 30 mg/kg of ketamine and 10 mg/kg of xylazine. Dorsal fur of mice was shaved and the skin was swabbed with 70% (v/v) alcohol. A 1-cm incision was made on the dorsal skin, and both the kidneys were externalized through the incision site. Each ovary was placed inside both bilateral kidney capsules, and the incision site and skin were closed and sutured.

Histological and immunohistochemical analysis of OTs

The OTs were fixed with 4% paraformaldehyde and embedded in paraffin wax for making sections (5-μm-thick). Sections were mounted on slides and stained with hematoxylin and eosin (H&E; Merck, Germany). Ovarian follicles were classified by Lundy's [52] and Gandolfi's criteria [53].

The developmental stages of ovarian follicles were classified in accordance with Lundy's criteria

1) primordial: single layer of flattened pregranulosa cells;
2) primary: single layer of granulosa cells, one or more of which is cuboidal;
3) secondary: two or more layers of cuboidal granulosa cells, with the antrum absent; or
4) antral: multiple layers of cuboidal granulosa cells, with the antrum present.

Morphological integrity of follicles was defined by Gandolfi's methods

1) primordial/primary follicle: Grade 1 (G1), spherical with even distribution of the granulosa cells; Grade 2 (G2), granulosa cells pulled away from the edge of the follicle but with the oocytes still spherical; Grade 3 (G3), pyknotic nuclei, misshapen oocytes, or vacuolation;
2) secondary/antral follicle: G1, intact spherical follicle with evenly distributed granulosa and theca cells, small space, and spherical oocytes; G2, intact theca cells, disrupted granulosa cells, and spherical oocytes; G3, disruption and loss of granulosa and theca cells, pyknotic nuclei, and missing oocyte.

Atretic follicles were characterized by the presence of eosinophilia of the ooplasm, contraction and clumping of chromatin material, and wrinkling of the nuclear membranes in the oocytes. We evaluated the follicles in only one oocyte-containing section per OT to avoid miscounting.

In addition, the density of blood vessels was evaluated by immunohistochemical analysis, and the CD31-positive area of each ovary was determined by using i-solution image analysis program (I-solution DT, IMT Technology Inc., Korea). Briefly, the paraffin slides were incubated overnight at 4℃ with anti-CD31 antibody (PECAM; 1:200; Abcam, UK) and sections were treated with EnVision™+ HRP (Dako, Denmark) for 30 min at RT and then with Liquid DAB+ Substrate (Dako) for 10 min at RT. Following this, all sections were counterstained with hematoxylin (Dako) and dehydrated in ethanol and xylene. Finally, the slides were mounted with the Mounting Medium (Dako) and examined under inverted Zeiss AX10 microscope (Carl Zeiss, Germany).

Terminal deoxynucleotidyl transferase dUTP nick-end labeling (TUNEL) assay for the assessment of apoptosis

Apoptosis of follicles in the control and transplanted groups was evaluated as described previously [51]. After deparaffinization and rehydration, the sections were treated with 0.8% proteinase K (Dako) in PBS for 15 min at RT, followed by incubation with a TUNEL reaction mixture (enzyme: label solution = 1:9) for 1 h at 37℃ in a humidified chamber in dark, followed by rinsing with DPBS. The slides were mounted with Vectashield® Mounting Medium with 4′,6-diamidino-2-phenylindole (DAPI) (Vector Laboratories, USA) and examined under inverted Zeiss AX10 microscope. An untreated TUNEL reaction mixture was used as the negative control and a slide treated with 100 U/mL of DNase I was used as the positive control. The presence of

more than 30% apoptotic cells in a follicle was considered to be apoptosis-positive in accordance with the previous study [54].

Flow cytometry

A total of 36 mice (3 mice/group) were killed by cervical dislocation to analyze CD45-positive populations in the grafts. Ovarian cells were isolated by using the Cell Dissociation Sieve-tissue Grinder Kit (Sigma), and red blood cells were removed by treatment with RBC lysis buffer at RT for 10 min (Biolegend, US). The ovarian cells were then incubated with purified anti-mouse CD16/32 (Biolegend) for 10 min to block the nonspecific antibody. Following this, the cells were first incubated with anti-mouse CD45R monoclonal antibodies (Abcam) for 30 min and then with APC goat anti-rat IgG antibody for 10 min (Biolegend). The cells were then analyzed by the FACS Calibur Flow Cytometer (BD Biosciences, US) and FlowJo software (Tree Star, US).

Enzyme-linked immunosorbent assay (ELISA) for anti-Mullerian hormone (AMH)

Whole blood was collected for serum collection from OT-transplanted mice 2, 7, and 21 days after transplantation. ELISA was performed to detect AMH (Cusabio, China) in blood sera of the transplanted mice. Briefly, blood samples were obtained by cardiac puncture, and serum was separated by centrifugation and used for AMH measurement by ELISA. The absorbance was measured at 450 nm and the concentration of serum AMH was calculated.

The intra- and inter-assay coefficients of variation were found to be <15% and 15%, respectively, with a sensitivity of 0.38 ng/mL.

A standard curve was plotted on reducing the data using a software capable of generating a four parameter logistic (4-PL) curve-fit and the AMH levels were calculated by the professional software "Curve Expert 1.3".

Oocyte retrieval, *in vitro* maturation (IVM), *in vitro* fertilization (IVF), and *in vitro* culture (IVC)

Three weeks after OT transplantation, 16 transplanted mice (4 mice/group) were hyper-stimulated via intraperitoneal injection of 7.5 IU of pregnant mare's serum gonadotropin (PMSG), followed by 7.5 IU of human chorionic gonadotropin (hCG). After 10 h, cumulus–oocytes complexes (COCs) were obtained by ovary puncture and then matured *in vitro* in a commercial IVM medium (TCM-199; Invitrogen, USA) supplemented with 20% FBS (Invitrogen), recombinant follicle-stimulating hormone FSH/hCG (75 mIU/mL and 0.5 IU/mL) (Serono, Switzerland), and recombinant epidermal growth factor (10 ng/mL; Sigma) for 6 h. After IVM, all COCs were completely denuded by treatment with 85 IU/mL hyaluronidase, and nuclear maturation was examined. Extrusion of the first polar body was used as the maturation criterion and was scored under an inverted microscope (50× magnification). After IVM, mature MII oocytes were inseminated with epididymal sperm for 4 h [57], and the fertilized embryos obtained were washed with fertilization medium (mTF supplemented with 0.4% BSA) and cultured in it for 24 h. Fertilization status was assessed by the formation of two cells 24

h after insemination, after which, the cleaved embryos were placed in cleavage medium (Global media, Life Global, Belgium) supplemented with 0.4% BSA for further development. The blastulation rate was assessed 72 h after insemination.

Differential staining of blastocysts

Mouse preimplantation blastocysts were immediately fixed with 4% paraformaldehyde in PBS for 30 min at RT. The embryos were then permeabilized with 0.5% Triton X-100 in PBS for 30 min and placed in blocking solution composed of 3% BSA in PBS for 1 h. Following the blocking procedure, the embryos were incubated overnight with primary OCT4 (1:100; Abcam) at 4℃. Alexa 594-conjugated secondary anti-rabbit antibody was treated overnight at 4℃. After 2nd antibody incubation, the embryos were incubated with the TUNEL reaction mixture (enzyme:label solution = 1:9) for 1 h at 37℃ in a humidified chamber in the dark, followed by rinsing with DPBS. The slides were then mounted with Vectashield® Mounting Medium with DAPI and examined under the inverted Zeiss AX10 microscope.

Statistical analyses

Data were analyzed by one-way ANOVA (CD31, CD45, serum AMH and the number of total and apoptotic blastomeres) or Chi-square test (grade 1 follicle ratio, MII oocyte, two cell cleavage and blastocyst formation rate). The SPSS version 12.0 software (SPSS Inc., US) and GraphPad Prism 5.0

(GraphPad Software, US) were used for statistical analysis. Values were considered significant at $p < 0.05$.

IV. Comparison Conventional Follicle Culture Methods and Developmental Competence of an *in vitro* Grown and Mature Oocytes

Animals and collection of ovarian tissue

Female B6D2F1 mice (F1 hybrid, C57BL/6 (♀) X DBA6 (♂)) were obtained from the Orient Bio (Korea). All animals were housed under controlled lighting and temperature conditions (13L:11D). The experimental protocols and animal-handling procedures were performed with approval of the Institutional Animal Care and Use Committee (IACUC) of Seoul National University Bundang Hospital (BA1506-178/028-01). Dissection, isolation, culture and evaluation process were performed according to the IACUC-approved method. Following sacrifice the mice by cervical dislocation, the ovaries were collected in collection medium [Dulbecco's phosphate buffered saline (D-PBS, Biowest, Korea) supplemented with 5% heat-inactivated fetal bovine serum (FBS, Gibco, Grand Island, NY, US)].

Isolation of secondary follicle and allocation

The ovaries were aseptically dissected from 2-week-old BDF-1 female mice (n=90) and then mechanically isolated using fine-needle (25-G). Early secondary follicle (diameter, 110-130 μm) were randomly divided into two different groups according to the culture methods (oil layer versus without oil layer). A total of 2,880 mouse ovarian follicle was used to compare the efficiency of conventional culture methods for secondary ovarian follicle. The

composition of puncture medium was D-PBS supplemented with 5% FBS, 1% penicillin-streptomycin (P/S, Gibco). Follicles with an intact basal membrane that showed no gaps between the oocyte and surrounding granulosa cells were selectively collected by observation under microscope for the present study.

Culture medium and conditions (oil layer versus without oil layer)

The culture medium for follicle culture was α–minimum essential medium (α-MEM, Life technologies, Carlsbad, CA, US) containing with 5% FBS, 5 μg/mL insulin, 5 μg/mL transferrin, 5 ng/mL sodium selenite (ITS, Sigma, St.Louis, MO, US), 1% P/S and 10 mIU/mL of recombinant human FSH (rhFSH, Gonal-F, Serono, Geneva, Switzerland).

Follicles were individually plated into two different culture plates in accordance with culture system. Firstly, the follicles were cultured under mineral oil overlay to minimize osmotic change which was applied by Cortvrindt's previous study [39]. In brief, culture dishes (60 mm petri dish, Falcon, Becton Dickinson, Franklin Lakes, NJ, US) contained 16 X 20 μL culture droplets and covered with 5 mL of mineral oil (Sigma). Selected follicles (n=96) were washed and seeded one by one in the culture droplets. Half of the culture medium (10 μL) was changed every other day. Follicles were grown in an incubator at 37 ℃, 100% humidity and 5% CO_2 in air.

The other culture system applied the Tarumi's previous study [38]. Briefly, selected secondary follicles (n=96) were plated at one follicle per well in 96-well plates (SPL, Pocheon, Korea) containing 75 μL/well of culture medium without a mineral oil overlay. Every four days, 30 μL of culture medium was

replenished to maintain culture environment. Follicles were grown in an incubator at 37 ℃, 100% humidity and 5% CO_2 in air. Follicles obtained from both culture systems were *in vitro* cultured for 10 days.

To assess the growth of individual follicle, two perpendicular diameters of follicle were measured using a calibrated ocular micrometer at x 50 magnification and viable follicle were defined as those that retained an oocyte completely embedded within the granulosa cell mass, and the survival rate was calculated as a percentage of all plated follicles as described previously [38]. In addition, antral-like cavity formation was calculated at the end of culture and considered as visible lucent space in granulosa cells complex around the oocyte.

Oocyte maturation and classification

On the 10^{th} day of culture, *in vitro* grown follicles was treated with 1.5 IU/mL of human chorionic gonadotropin (hCG, Sigma) and 5 ng/mL of murine epidermal growth factor (EGF, Sigma) to induce the maturation of oocytes at the GV stage. Following 16-18 h, mucified cumulus-oocyte complexes (COCs) were selected and then oocytes were denuded with 85 IU/mL hyaluronidase to assess the oocyte maturational status. Oocytes were individually classified into germinal vesicle (GV), germinal vesicle breakdown (GVBD) and metaphase II (MII) stages in accordance with the presence of GV or 1^{st} polar body extrusion.

For control, mature oocytes were obtained from 4-week-old BDF-1 mice superovulated with 5 IU of PMSG followed by 5 IU of hCG injection 48 h

later. Eggs were collected from the oviduct 16-18 h after hCG injection and cumulus cells were removed with 85 IU/mL hyaluronidase treatment as described previously [58].

Enzyme-linked immunosorbent assay (ELISA) for estradiol (E2) and progesterone (P4)

The concentrations of E2 (D4, D8 and D10) and P4 (D8, D10 and D11) in the spent medium were determined using ELISA (E2: Calbiotech, Spring Valley, CA, US and P4: DRG diagnostics, Springfield, NJ, US). The absorbance was measured at 450 nm, and the concentrations of E2 and P4 were calculated the corresponding concentration of E2 (pg/mL) and P4 (ng/mL) from standard curve.

***In vitro* fertilization (IVF)**

In vitro and *in vivo* ovulated COCs were completely denuded with 85 IU/mL hyaluronidase and maturity was checked. First polar body extruded oocytes were regarded as MII and selectively collected to fertilize *in vitro*. The epididymal spermatozoa were obtained from the cauda epididymis of sexually matured BDF-1 male mice (10-12 week-old aged). Sperm was incubated for 1 h in fertilization medium (KSOM/AA supplemented with 0.4% BSA) to capacitate and then added the sperm into selected oocytes for 4 h under 37℃ 5% CO_2 condition. Following insemination, the oocytes were washed with fertilization medium and further incubated for 120 h. Fertilization and blastulation were checked by the formation of two cells on day 1 after

insemination and blastocoel on 5th day of development [57].

Immunofluorescence to detect micro-organelles and reactive species oxygen (ROS) production in oocytes

To localize the nucleus, cortical granule (CGs), microfilaments and spindle, oocytes were immediately fixed with 4% paraformaldehyde for 30 min after denudation. Then, the oocytes were washed with 0.3% bovine serum albumin (BSA) twice, and permeabilized with Triton X-100 in D-PBS for 15 min. Following permeabilization, eggs were blocked in PBS containing 3% BSA at 4℃, overnight. And then the oocytes were incubated with rabbit anti-β-tubulin antibody (1:1:00, Cell Signaling, Danvers, MA, US) for 1 h at room temperature (RT). After incubation, the oocytes randomly divided into two groups according to the staining of micro-organelles, CGs or microfilaments. To visualize the CGs or microfilament, oocytes were stained with rhodamine-conjugated *Lens culinaris* agglutinin (1:200, Vector laboratories, Burlingame, CA, US) or rhodamine-conjugated phalloidin (Molecular Probes, Eugene, OR, US), respectively. Alexa Fluor 488-conjugated secondary goat anti-rabbit IgG (1:1,000, Thermo Fisher Scientific, Waltham, MA, US) and Hoechst 33342 (Sigma) were added at RT for 1 h to detect meiotic spindle and nucleus, respectively.

To determine the physiological activities in oocytes, ROS production and mitochondrial activities were detected and measured with fluorescence staining. *In vitro* and *in vivo* matured oocytes were separately incubated with 200 nM of ROS detection reagents (Molecular Probes), 100 nM of

Mitotracker® Mitochondrion-selective probes (Molecular Probe) and Hoechst 33342 at 37℃ for 30 min. *In vitro* grown and mature oocytes from both culture conditions were used as positive and negative control. Positive controls were treated with 1 mM hydrogen dioxide (H_2O_2) for 30 min to induce the artificial oxygenic stress and negative controls were omitted the probes. Images were detected and captured on a LSM 710 confocal microscope (Carl Zeiss, Oberkochen, Germany). The intensity of fluorescence was also measured with Zen 2012 software (Carl Zeiss) and presented as graphs.

Gene expression in oocytes

To evaluate the maturational ability, cell death and developmental competence in oocytes, gene expression was determined by quantitative reverse-transcription PCR (qRT-PCR). On 11th day of culture period, the oocytes were collected 16-18 h after hCG-triggering. Messenger RNAs were extracted from five oocytes in each groups using Dynabeads mRNA direct micro kit (Dynal, Oslo, Norway) according to the manufacturer's instructions. Then, cDNA was synthesized using Prime-script 1st strand cDNA synthesis kit (Takara Bio, Shiga, Japan) and qRT-PCR was performed with primer sets. BMP15-F, TCTGATTAGTTCGTATGCTACCTG, BMP15-R, CGAAAATGGTGAGGCTGGTA, Mater-F, TCACTAGCATACCAATCACCATC, Mater-R, AATGCCCTGTCTCTAACCTG, Hook1 F, GCTTAACCAAGATTCGCTGAAC, Hook1 R,

CATTCAAGACTGCCTCACCTT, Zar1-F, GCAGAACTGTTTGAAGTACACC, Zar1-R, GCCTGCGTTTCCAGTTCT, Bcl2-F, CCAGGAGAAATCAAACAGAGGT, Bcl2-R, GATGACTGAGTACCTGAACCG, Bax-F, GCCATCAGCAAACATGTCAG, Bax-R, GGAGATGAACTGGACAGCAAT. The threshold cycle (Ct) value represents the cycle number indicating increase in fluorescence above background levels. Reactions followed the steps of the SYBR® Premix Dimer Eraser™ (Takara) PCR kit. The PCR protocol used a denaturation step (95℃ for 10 m), followed by an amplification and quantification program that was repeated 40 times (95℃ for 15 s and 60℃ for 1 m), a melting curve program (60℃-95℃ with a heating rate of 0.34/second and continuous fluorescence measurement). Gene expression of each group was analyzed by generating a melting curve. The size of PCR products were confirmed by gel electrophoresis on 3% agarose gels stained with the Loading Star (Intronbio, Seongnam, Korea) and visualized by ultraviolet light using ethidium bromide staining as described previously [59]. The relative quantification of gene expression was analyzed using the 2^ddCt. In all qRT-PCR experiments, beta-actin mRNA served as an internal standard in analyzed oocytes as well as the gene expression was normalized to *in vivo* derived MII oocytes for comparison.

Statistical analysis

Data were analyzed by Chi-square test (for evaluation of oocyte nuclear

maturity, follicle development, oocyte diameter, and spindle normality) or analysis of variance (for follicle diameter, hormone levels, ROS and mitochondrial activity and gene-expression). The Statistical Package for the Social Sciences version 12.0 software (SPSS Inc., Chicago, IL, US) and GraphPad Prism 6.0 (GraphPad Software, La Jolla, CA, US) were used for statistical analysis. Values were considered significant at $p < 0.05$

RESULTS

I. Ovarian Injury during Cryopreservation and Transplantation: A Comparative Study between Cryoinjury and Ischemic Injury

Microscopic examination of the control OTs and grafts

In the present study, a microscopic examination of each group was performed to compare graft quality before/after cryopreservation and/or auto-transplantation. The quality of ovarian follicles and density of stroma in the vitri-con group decreased compared with those of the fresh controls (Figure 4A–B). Two days after transplantation, the quality of graft and stromal density in the FrOT-D2 and VtOT-D2 groups degenerated compared with those in the fresh and vitri-con groups, respectively, and red blood cells (RBCs) increased in both the FrOT-D2 and VtOT-D2 groups. Additionally, oocyte shrinkage and collapsed follicular structure were observed regardless of the presence or absence of OT vitrification (Figure 4C–D). The follicle integrity and stromal density at 7 days was improved compared with values at 2 days, and attachment to the kidney capsule was shown in both the FrOT-D7 and VtOT-D7 groups. These recovering tendencies also presented 21 days after transplantation, and many follicles developed into the advanced stages of folliculogenesis, even in the antral stage.

Follicle quality and quantity

Following vitrification-warming or transplantation procedures, the percentage of total G1 follicles in the vitri-con group was significantly reduced compared with that in the fresh control ($p < 0.0001$), and the proportion of total G1 follicles in the FrOT-D2 group was significantly lower than that in fresh controls ($p < 0.0001$). Additionally, there was a significant difference in the G1 follicle ratio between the vitri-con and FrOT-D2 groups (fresh: 350/545 (64.2%), vitri-con: 176/350 (50.3%), and FrOT-D2: 152/358 (42.5%); $p < 0.05$). However, no significant difference was detected between the FrOT-D2 and VtOT-D2 groups (152/358 (42.5%) and 139/281 (49.5%), respectively; $p = 0.077$). As the transplantation period increased, the total G1 ratio in the FrOT groups gradually increased, with significance (FrOT-D2: 152/358 (42.5%) and FrOT-D21: 198/280 (70.7%), $p < 0.0001$), whereas the G1 ratio in the VtOT groups was not significantly different according to the transplantation period (VtOT-D2: 138/281 (49.5%) and VtOT-D21: 88/152 (57.9%), $p < 0.0001$). A significant difference was noted between the FrOT and VtOT groups on days 7 and 21 (FrOT-D7: 206/367 (56.1%) and VtOT-D7: 187/408 (45.8%), $p < 0.05$; FrOT-D21: 198/280 (70.7%) and VtOT-D21: 88/152 (57.9%), $p < 0.05$; Figure 5A).

Regarding the number of ovarian follicles per section in each graft, a drastic reduction of ovarian follicles was observed in the vitri-con and FrOT-D2 groups compared with that in the fresh controls (fresh: 30.3 ± 3.6 (N=18), vitri-con: 20.6 ± 3.9 (N=17), and FrOT-2D: 17.9 ± 2.1 (N=20); $p < 0.05$). In contrast with the total G1 ratio, there were no significant differences between the FrOT and VtOT groups on each evaluation day (FrOT-D2: 17.9 ± 2.1

(N=20) and VtOT-D2: 14.8 ± 2.4 (N=19), p = 0.9892; FrOT-D7: 19.3 ± 2.8 (N=19) and VtOT-D7: 21.5 ± 2.7 (N=19), p = 0.9990; FrOT-D21: 15.6 ± 2.3 (N=18) and VtOT-D21: 10.9 ± 2.1 (N=14), p = 0.9406; Figure 5B).

The proportion of apoptotic follicles in the vitri-con group was significantly increased compared with that in the fresh control, and the apoptotic follicle ratio in the FrOT-D2 group was much higher than that in the vitri-con (fresh: 5/545 (0.9%), vitri-con: 21/350 (6.0%), and FrOT-D2: 96/358 (26.8%); p < 0.0001). Two days after transplantation, the apoptotic follicle ratio increased dramatically in both the FrOT-D2 and VtOT-D2 groups, but the values were comparable between groups (96/358 (26.8%) and 64/281 (22.8%), respectively; p = 0.242). These increased levels of apoptosis sharply decreased during the transplantation period in both the FrOT and VtOT groups, and no significant difference was noted between the FrOT and VtOT groups on days 7 and 21 (FrOT-D7: 10/367 (2.7%) and VtOT-D7: 17/408 (4.2%), p = 0.274; FrOT-D21: 15/280 (5.4%) and VtOT-D21: 11/152 (7.2%), p = 0.433, Figure 5C). Representative images of the TUNEL assay in each group are shown in Figure 6.

Follicle development

To investigate follicular development after vitrification and/or transplantation, further classification was performed according to the previous studies [52,53]. With respect to the primordial follicles in OTs, the proportion of primordial follicle in FrOT-D21 was significantly higher than that of VtOT-D21. However, there were no significant differences between fresh and

vitrified-warmed OT groups on each evaluation days (no transplantation, D2 and D7, Figure 7A). In primary follicle, no significant difference was observed regardless of tissue freezing status on all evaluation days (Figure 7B). On the other hand, the proportions of secondary follicle both in FrOT-D2 and VtOT-D2 were significantly higher than those of fresh and vitri-con, respectively ($p<0.05$). However, the percentage of secondary follicle in fresh OT groups was similar to those of vitrified-warmed OT in all time. Notably, secondary follicle ratio in VtOT-D7 and VtOT-D21 were slightly increased when compared with the FrOT-D7 and FrOT-D21, respectively ($p>0.05$, Figure 7C). Finally, the percentages of antral follicle both in FrOT-D7 and VtOT-D7 were respectively similar to the those of non-transplantation group (fresh and vitri-con). Twenty-one days after transplantation, antral follicle formation rate in FrOT-D21 was significantly higher than that of VtOT-D21 ($p<0.05$, Figure 7D).

Re-vascularization of the control OTs and grafts

Figure 8A shows a characteristic image for localization of CD31-positive blood vessels in transplants with immunohistochemistry. Figure 8B and C represent positive and negative control for CD31 IHC, respectively. Most brown-colored CD31-positive blood vessels were observed in interstitial spaces near the corpus luteum of OTs. Figure 8D indicates a significant reduction of the CD31-positive area in OTs after the vitrification-warming and transplantation procedures (fresh: 10.6 ± 1.3% (N=13), vitri-con: 5.7 ± 0.9 (N=11), and FrOT-D2: 4.2 ± 0.4% (N=16), $p < 0.05$). Twenty-one days

after transplantation, the CD31-positive area in the FrOT-D21 group was significantly increased compared with that in the FrOT-D2 group (4.2 ± 0.4% (N=11) vs. 7.5 ± 0.8% (N=18), p = 0.0242), whereas no significant difference was observed between the VtOT-D2 and VtOT-21D groups (3.3 ± 0.4% (N=19) vs. 5.8 ± 1.0% (N=15), respectively; p = 0.2062). This significant increase of CD31-positive areas was consistent with the increase of the total G1 ratio in the FrOT groups. However, there were no significant differences between the FrOT and VtOT groups on each evaluation day.

Serum FSH level in the fresh control, ovariectomized, and transplanted mice

Figure 9 shows a dramatic increase in the serum FSH level 1 wk after ovariectomy (fresh control (N=10): 0.94 ± 0.20 ng/mL and ovariectomized (N=7): 13.18 ± 0.87 ng/mL, p < 0.0001). The serum FSH levels gradually decreased with time after transplantation in both the FrOT and VtOT groups, and the concentration in the FrOT groups was comparable with that in the VtOT groups on each evaluation day (FrOT-D2 (N=9): 7.96 ± 1.50 ng/mL and VtOT-D2 (N=8): 11.96 ± 0.47 ng/mL, p = 0.0750; FrOT-D7 (N=9): 6.11 ± 1.22 ng/mL and VtOT-D7 (N=10): 5.46 ± 1.19 ng/mL, p = 0.9996; FrOT-D21 (N=8): 0.78 ± 0.11 ng/mL and VtOT-D21 (N=9): 1.66 ± 0.64 ng/mL, p = 0.9978). Twenty-one days after transplantation, the serum FSH levels recovered to the same level as that in the fresh control.

II. Effects of Three Different Types of Antifreeze Proteins on Mouse Ovarian Tissue Cryopreservation and Transplantation

Morphological evaluation of vitrified/warmed OT (Experiment I)

A total of 11 groups were examined; representative images are shown in Figure 10. The overall morphology of ovarian follicles in the fresh controls was superior to that seen in the other 10 groups. Most of the oocytes in follicles from the fresh control OT were intact and clear, and the interstitial tissues appeared denser in the fresh control OT than in the others (Figure 10). As shown in Figure. 10B, the vitrification/warming process may result in oocyte shrinkage and stromal damage. Similar to the OT from the vitrification control group, oocytes and stromal cells in OT treated with 0.1 mg/mL or 1.0 mg/mL AFP exhibited cryodamage (Figure. 10C–H). However, OT treated with 10 mg/mL AFP (Figure. 10I–K) had well-preserved follicles, as compared with the vitrification control OT and the OT treated with lower doses of AFP (Figure. 10C–H).

A total of 5,790 ovarian follicles (fresh control: 754; vitrification control: 1,003; FfIBP-treated: 1,161; LeIBP-treated: 1,333; and type III AFP-treated: 1,489 follicles) were counted and classified by developmental stage and grade. Figure 11A and B show the percentages of total and primordial G1 follicles in the fresh control OT, vitrification control OT, OT treated with 0.1 mg/mL AFP and OT treated with 1.0 mg/mL AFP. In the vitrification control OT and the AFP-treated OT, the total percentage of G1 follicles was significantly lower than that in the fresh control OT. However, the percentage of primordial

G1 follicles in the fresh control OT was not different from that in all the other OT groups except for the LeIBP-treated OT (Figure. 11A-B; fresh control OT: 314/472 (66.5%); vitrification control OT: 414/637 (65.0%); FfIBP-treated OT: 147/225 (65.3%); LeIBP-treated OT: 200/347 (57.6%), and type III AFP-treated OT: 178/294 (60.5%)).

Figure 11C shows the total percentage of G1 follicles and the percentage of primordial G1 follicles in the fresh control OT, the vitrification control OT, and the OT treated with 10 mg/mL of the different AFPs. Although in the vitrification control OT and most of the AFP-treated OT the total percentage of G1 follicles was lower than that for the fresh control group, that in OT treated with 10 mg/mL LeIBP was comparable with that in the fresh control OT (fresh control OT: 487/754 (64.6%); vitrification control OT: 524/1,003 (52.2%), FfIBP-treated OT: 250/435 (57.5%), LeIBP-treated OT: 289/480 (60.2%); and type III AFP-treated OT: 269/504 (53.4%)). In addition, all AFP-treated OTs had a significant increase in the percentage of primordial G1 follicles as compared with the vitrification control OT. Moreover, the percentage of primordial G1 follicles was higher in FfIBP-treated OT and LeIBP-treated OT than in fresh control OT (fresh control OT: 314/472 (66.5%); vitrification control OT: 414/637 (65.0%); FfIBP-treated OT: 204/275 (74.2%); LeIBP-treated OT: 233/301 (77.4%); and type III AFP-treated OT: 217/298 (72.8%)).

Analysis of apoptosis in vitrified/warmed OT

In the OT treated with 0.1 mg/mL of either FfIBP or LeIBP, the percentage

of apoptotic follicles was greater than that in the fresh OT and the vitrification control OT (Figure. 12). However, OT treated with 1.0 or 10 mg/mL of AFP had percentages of apoptotic follicles that were similar to that seen in the vitrification control OT. Moreover, the percentage of apoptotic follicles in the LeIBP-treated OT was significantly less than that in the vitrification control OT. (Fresh control OT: 23/381 (6.0%), vitrification control OT: 45/615 (7.3%), 0.1 mg/mL groups; FfIBP-treated: 28/238 (11.7%), LeIBP-treated: 37/273 (13.6%), type III AFP-treated:25/284 (8.8%), 1 mg/mL groups; FfIBP-treated: 10/231 (4.3%), LeIBP-treated: 6/195 (3.1%), type III AFP-treated: 8/195 (4.1%), 10 mg/mL groups; FfIBP-treated: 15/336 (4.5%), LeIBP-treated: 13/381 (3.4%), type III AFP-treated:19/296 (6.4%),

Immunohisotochemical analysis of vitrified/warmed OT

As seen in Figure. 13, the percentage of τH2AX positive follicle was significantly higher in the vitrification control OT and the AFP-treated OT than in the fresh control OT. AFP supplementation significantly decreased the percentage of τH2AX positive follicles, as compared with vitrification control OT (fresh control OT: 43/268 (16.0%); vitrification control OT: 150/301 (49.8%); FfIBP-treated OT: 131/339 (38.6%); LeIBP-treated OT: 124/329 (37.7%), and type III AFP-treated OT: 109/263 (41.4%)). A decreasing statistically non-significant tendency was also seen for the percentage of Rad51-positive follicles. However, the decrease was only statistically significant for FfIBP-treated OT and LeIBP-treated OT (fresh control OT: 40/262 (15.2%); vitrification control OT: 138/284 (48.6%); FfIBP-treated OT:

137/340 (40.3%); LeIBP-treated OT: 135/333 (40.5%); and type III AFP-treated OT: 111/265 (41.9%)).

Histology, apoptosis, immunohistochemical analysis, and serum FSH levels of recipient mice (Experiment II)

Figure 14 shows the histological assessment and immunohistochemical analysis for CD31 after auto-transplantation for both the vitrification control OT and OT treated with 10 mg/mL of LeIBP. There were many degraded follicles and damaged stromal cells in the vitrification control OT (Figure 15A, sham control: 106/232 (45.7%), LeIBP-treated: 90/140 (64.3%), $p<0.05$). In contrast, there were lower numbers of degraded follicles in the LeIBP-treated OT than in the vitrification control OT (Figure. 15B, sham control: 20/282 (7.1%), LeIBP-treated: 6/204 (2.9%), $p<0.05$). Figure 15C and D show the immunohistochemical detection of CD31 expression in endothelial cells in each graft; most of the expression was localized in late stage follicles and interstitial spaces (Figure 15C, sham control: 7.01 ± 0.82 (N=9), LeIBP-treated: 4.87 ± 0.36 (N=8), Figure 15D, sham control: 6.49 ± 1.14 (N=13), LeIBP-treated: 9.90 ± 07.7 (N=18), $p<0.05$). Figure 15 shows the percentages of G1 follicles and TUNEL-positive follicles in the graft, the levels of serum FSH in the recipient mice on day 7, and the area of CD31-labeled endothelial cells in the grafts. The LeIBP-treated OT had a statistically significant increase in the percentage of total G1 follicles, but there were no significant differences in the percentages of primary, secondary, or antral G1 follicles between the

control OT and the LeIBP-treated OT (data not shown). For the LeIBP-treated grafts, the percentage of apoptotic follicles in the OT was significantly lower, the serum FSH level in the recipient mice was significantly lower, and the area of CD31-positive cells in the graft was significantly greater than for the vitrification control grafts.

III. A Combination of Simvastatin and Methylprednisolone Improves the Quality of Vitrified-warmed Ovarian Tissue after Auto-transplantation

The effect of simvastatin and methylprednisolone on auto-transplantation of fresh OT (Experiment III-I)

With respect to the follicle quality in graft, the percentage of total grade 1 follicle in three treatment groups was significantly increased compared with sham control. In addition, the proportion of total grade 1 follicle in S+M group was significantly higher than Simv. and M.P. groups. (Figure 16A, sham: 226/450 (50.2%), Simv: 337/558 (60.4%), M.P.: 357/606 (58.9%) and S+M:498/733 (67.9%), $p<0.05$). S+M group showed significantly higher proportion of CD31-positive area in graft than that of sham control (Figure 16B, sham (N=7): 1.76±0.34, Simv (N=10): 2.43±0.30, M.P.(N=9): 2.98±0.43 and S+M (N=10):3.54.±0.29 $p<0.05$).

The effect of simvastatin and methylprednisolone on auto-transplantation of vitrified-warmed OT (Experiment III-II)

Gross observations and histological evaluation after transplantation

On day 2 after OT transplantation, the transplanted ovaries could be easily detached from the kidneys in all mice. Although plenty of red blood cells were present around the kidney capsule, angiogenesis was not detected in any group. However, adhesion between the grafts and kidneys was enhanced in a time-dependent manner. Most of the blood clot disappeared by days 7 and 21 after transplantation, and the blood vessels around the transplanted OT

increased with increasing time after transplantation (Figure 17A-L).

Figure 18. A and B depict the histological images of two different controls. After vitrification-warming procedure, the stromal density and normality of ovarian follicles was decreased. Moreover, grade 1 follicle ratios of all developmental stages except the antral follicle stage were significantly reduced when compared with the fresh control group (Table 2). The total follicle numbers were also dramatically decreased as a result of vitrification-warming process (Figure 19). Consistent with the gross observation, connection between the OT and kidney capsule was observed to be incomplete 2 days after transplantation (Figure 18C-F). In addition, stromal cells seemed to be loosely adhered to the capsule with only a few growing follicles. However, the primordial follicles were relatively well-preserved during the cryopreservation and transplantation procedures. Table 2 indicates the proportion of grade 1 follicles (morphologically intact according to Lundy's and Gandolfi's criteria) in the six different groups on day 2 after transplantation. The primordial and total grade 1 follicle ratio of the Simv. and S+M groups were significantly higher than those of the sham control group ($p < 0.05$). Total grade 1 follicle ratio was also significantly increased in the M.P. group as compared with that in the sham control group ($p < 0.05$).

On day 7, the density of stromal cells appeared higher on day 7 than on day 2, antral follicles were also detected and the OT was not completely detached from kidney capsules in all groups (Figure 18G–J). Moreover, the total grade 1 follicle ratio was also significantly higher in the M.P. and S+M groups than the sham control group (Table 3). With respect to the total grade 1 follicle

ratios, the S+M group was comparable to the fresh control group. Twenty-one days after transplantation, the density and quality of ovarian follicle were similar to the fresh control (Figure 18K-N), and the all treatment groups were significantly improved in terms of total and primordial grade 1 follicle ratios compared with the sham control (Table 4). The S+M group showed significantly higher grade 1 follicle ratio than the sham control group at all follicle stages, except the primary stage ($p < 0.05$). Although there were no significant differences in terms of total grade 1 follicle ratios between the fresh and other five groups, a massive reduction in the total number of follicles (~70%) was observed in the transplantation groups at each evaluation day (Figure 19).

Number of follicles in OT before/after cryopreservation and transplantation

Figure 19 A-C shows the mean number of follicles per section before and after cryopreservation and transplantation in the six different groups on day 2, 7 and 21, respectively. Following the vitrification-warming, 30% reduction in mean ovarian follicle number was observed in the vitrified-warmed control group when compared with the fresh control group (fresh: 31.2±2.7, N=19 and vitrified-warmed control: 21.7±2.5, N= 20). After auto-transplantation of OT, follicle number was reduced more in the four transplantation groups compared with the vitrification-warming control group although no significant differences were noted among the four transplantation groups at each evaluation day (Table.2-4) .

Evaluation for apoptotic follicles of transplanted OT

Table 5 depicts the proportion of apoptotic follicles in all groups 2, 7, and 21 days after tissue transplantation.. Although the percentage of apoptotic follicle was almost similar among the four groups after 2 and 7 days (day 2, sham: 6.1%, Simv.: 5.5%, M.P.: 5.0%, and S+M: 4.7%; day 7, sham: 4.7%, Simv.: 2.1%, M.P.: 3.5%, and S+M: 1.2%, respectively), the apoptotic follicle ratio in the S+M group was significantly lower than that in the other three groups after 21 days (day 21, Fresh: 6.1%, vitrified-warmed: 11.4%, sham: 5.7%, Simv.: 5.6%, M.P.: 8.7%, and S+M: 1.7%; $p < 0.05$). Most of the apoptotic follicle were observed in the growing phases from secondary to antral stage.

Density of CD31-positive endothelial cells in grafts

Figure 20A–C shows a representative image of immunohistochemistry for CD31 and CD31-positive area in each ovary in all groups 7 and 21 days after transplantation, respectively. A significant increase in the CD31-positive area in the S+M group was observed as compared with that in the sham control group (Figure 20B; sham (N=11): 2.45±0.53, Simv (N=13): 3.47±0.52, M.P.(N=7): 4.68±1.46 and S+M (N=9): 6.25±1.38, Figure 20C; sham (N=16): 7.34±0.96, Simv (N=12): 10.00±1.09, M.P.(N=11): 7.38±1.77 and S+M (N=11): 13.13±1.81 $p<0.05$). In contrast, no significant difference was noted in the CD31-positive area in the other three treated groups.

CD45-positive populations of transplanted OTs

The CD45-positive population of the transplanted ovary was assessed by flow cytometry 2, 7, and 21 days after auto-grafting to evaluate the anti-inflammatory effects of methylprednisolone and simvastatin. The CD45-positive cell proportion increased in most of the groups with time after the transplantation duration (Figure21A, 2 days; sham (N=5): 0.40±0.12, Simv. (N=5): 1.00±0.60, M.P.(N=5): 0.08±0.04 and S+M (N=5): 0.11±0.03, 7 days; sham (N=5): 1.64±0.58, Simv. (N=4): 1.41±0.22, M.P.(N=3): 1.72±0.15 and S+M (N=4): 2.22±0.53, 21 days; sham (N=5): 0.96±0.56, Simv. (N=4): 4.18±1.09, M.P.(N=5): 2.49±0.49 and S+M (N=4): 3.27±0.82) However, no effect was noted in the Simv., M.P., or S+M groups with respect to the numbers of graft-infiltrating inflammatory CD45 cells 2, 7, and 21 days after transplantation ($p = 0.3916$).

Measurement of AMH in the blood serum

To assess the ovarian reserves, the serum AMH level was measured by ELISA 2, 7, and 21 days after transplantation (Figure 21B). The serum AMH level 2 days after transplantation did not differ among the four groups (sham (N=9): 28.6 ± 4.1, Simv. (N=10): 28.9 ± 2.2, M.P. (N=10): 38.5 ± 4.4, and S+M (N=10): 32.1 ± 3.9 ng/mL). However, the serum AMH level was significantly improved in the S+M group on day 7 as compared with that in the other three groups (sham (N=10): 36.4 ± 3.7, Simv. (N=10): 37.0 ± 2.1,

M.P. (N=10): 39.7 ± 4.6, S+M (N=10):69.2 ± 8.2 ng/mL; $p < 0.05$). This difference in terms of the AMH level was not noted on day 21 (sham (N=10): 53.8 ± 5.1, Simv. (N=9): 49.6 ± 3.6, M.P. (N=10): 59.2 ± 8.0, and S+M (N=9): 41.8 ± 4.0 ng/mL).

IVM, IVF, *in vitro* embryonic development, and differential staining of blastocysts derived from transplanted ovaries

Table 6 represents the in vitro embryonic development and the total cell number of blastocyst. Allocation of inner cell mass and trophoectoderm in the blastocysts was determined by differential staining. Although the mature oocyte-retrieval rate was >70% in all groups, no significant difference was noted among the results for the four groups (sham: 71.7, Simv.: 75.0, M.P.:71.4, and S+M: 77.8). In addition, no significant difference was noted in the two-cell formation rate (sham: 47.4, Simv.: 47.6, M.P.: 65.0, and S+M: 57.1) and the blastocyst formation rate (sham: 61.1, Simv.: 50.0, M.P.: 50.0, and S+M: 55.0) at 72 h after insemination among the groups. In addition, the numbers of total blastomeres, inner cell mass (ICM), trophoectoderm (TE), and apoptotic cells analyzed by differential staining of blastocysts (Figure 22A-D) revealed no significant difference among the groups.

IV. Comparison of Conventional Follicle Culture Methods and Developmental Competence of an *in vitro* Grown and Mature Oocytes

Follicle survival, growth and development

A total of 2,880 ovarian follicles were *in vitro* cultured to compare the efficiency of different conventional culture method in the present study. Figure 23A shows morphological changes of ovarian follicle during culture period. In general, diameter of follicle in oil layer was seemed to be higher than that of without oil layer and the formation of pseudo-antral like cavity in oil layer (8^{th} day) was earlier than without oil layer (10^{th} day of culture period). To compare the follicle growth objectively, the perpendicular diameter of cultured follicle were measured every other day. Figure 23B indicates the growth curve of follicle in accordance with the culture period. From 8^{th} day of culture, diameter of follicle in oil layer significantly increased compared with without oil layer culture method ($p<0.05$). Figure 23C represents survival, development and ovulation rate on 10^{th} day of culture. All of these criteria in oil layer (N=384) were also significantly higher than those of without oil layer (N=384) (survival; 95.8% vs 90.1%, pseudo-antral like cavity formation; 66.9% vs 52.6%, and ovulation rate; 89.1% vs 66.4%, $p<0.05$).

Oocyte growth and maturation

On the 10^{th} day of culture period, hCG and EGF was treated for 16-18 h to induce oocyte nucleic maturation, *in vitro*. Following hCG-triggering, GVBD

and MII formation rate in oil layer (GVBD:320/384 (83.3%) and MII: 153/384 (39.8%)) significantly increased when comparing with that of without oil layer (GVBD: 225/384 (56.6%) and MII: 119/384 (31.0%)) while the percentage of GV oocyte was decreased with significance ($p<0.05$). After denudation of COCs, diameter of oocyte in both *in vitro* culture systems was significantly smaller than *in vivo* derived oocytes (oil layer (N=41): 69.82±0.45, without oil layer (N=36): 69.62±0.54 and *in vivo* control (N=22): 74.78±0.43 $p<0.05$). However, there was no significant difference between oil layer and without oil layer.

Estradiol and progesterone production

With respect to the E2 level in spent medium, there was no significant difference between both culture systems until the 8th day of culture (Figure 24A, day 4; oil layer (N=12): 970.65±43.6 and without oil layer (N=12): 1,847.26±133.1, day 8; oil layer (N=12): 6,487.2±449.3 and without oil layer (N=12): 5,753.17±830.47 pg/mL). However, E2 level in oil layer method was significantly higher than that of without oil layer on the 10th day of culture (day 10; oil layer (N=12): 3,365.16±441.07 and without oil layer (N=9): 1,236.95±418.61 pg/mL, $p<0.05$).

In contrast, no significant difference was observed until at the end of follicle

culture (8^{th} and 10^{th} day of culture, Figure 24B, day 8; oil layer (N=12): 0.23±0.38 and without oil layer (N=12): 0.06±0.07, day 10; oil layer (N=12): 2.87±1.27 and without oil layer (N=12): 0.26±0.21 ng/mL). Following hCG-triggering, P4 level in oil layer significantly increased while P4 level in without oil layer did not significantly increased compared with P4 level in oil layer on 11^{th} day of culture (Figure 24B, day 10; oil layer (N=12): 208.40±48.01 and without oil layer (N=12): 9.22±2.95 ng/mL) $p<0.05$).

Embryonic developmental competence after IVF

After collection of COCs, the oocytes were denuded and *in vitro* inseminated to evaluate the developmental competence. A total of 293 oocytes were used to fertilize *in vitro* and fertilization and blastulation were checked with time (Table 7.). With regard to the fertilization rate, MII oocytes from *in vivo* condition marked higher fertilization rate compared with those of both *in vitro* grown and matured oocyte (*in vivo*; 84.1%, oil layer; 3.8% and without oil layer; 4.5%, $p<0.05$). Five days after fertilization, blastulation rate of MII derived from *in vivo* was significantly higher than those of both *in vitro* derived oocytes oocyte (*in vivo*; 74.5%, oil layer; 0% and without oil layer; 0, $p<0.05$).

Microorganelles in oocyte

In the present study, fluorescence staining was performed to investigate the

microorganelles in oocytes. Figure 25A shows CGs, cytoskeleton and meiotic spindle in oocytes. Cortical granules in oocyte that was derived from *in vitro* culture were not evenly distributed and clumped. Most of GCs were marginal distributed in oocytes which was grown and matured *in vitro*. However, the distribution of CGs in oocyte that was derived from *in vivo* stimulation was evenly distributed at marginal side of oocyte.

In contrast, oocytes from all of three groups were similar in terms of actin filament localization while the fluorescent intensity in both *in vitro* derived oocytes were seemed to be stronger than that of oocytes derived from *in vivo milieu*.

On the other hand, there were no significant differences in spindle normality among three different groups when compared with each other (Figure 25B, oil layer (N=110): 81.0±3.5%, without oil layer (N=99): 82.4±4.48% and *in vivo* control (N=42): 92.9±4.13) .

Physiological changes in oocyte

Due to the follicles were cultured *in vitro*, we thought that oxygenic stress and alteration of mitochondrial activity would be induced. Figure 25C shows representative image of ROS production and mitochondrial activity both *in vitro* and *in vivo* matured oocytes (Figure 25C, ROS production; oil layer (N=100): 350.42±29.25, without oil layer (N=100): 384.71±31.94, *in vivo* control (N=29): 161.51±39.56, negative control (N=28): 1.86±0.15 and

positive control (N=26): 694.43±34.41 AU, $p<0.05$). When measuring oxygenic stress in oocytes in all three groups, oocytes derived from *in vivo* condition was statistically significant lower than those of both *in vitro* grown and matured oocytes while the mitochondrial activity in oocytes from *in vivo milieu* significantly increased compared with both *in vitro* derived oocytes (Figure 25D, mitochondrial activity; oil layer (N=135): 225.33±9.67, without oil layer (N=135): 246.85±11.12, *in vivo* control (N=41): 496.7±55.52, $p<0.05$).

Gene-expression

To find out the cause of impairment of developmental competence in oocytes that were derived from *in vitro* culture conditions, qRT-PCR was carried out to investigate the mRNA expression in oocytes. Various genes which were related to oocyte growth, maturation, embryonic development and cell-death were statistically not different among three different groups (Figure 25E).

Table 1. Characteristic of AFPs used in this study

Characteristics	Type III AFP (ref. Structure-function relationship in the globular type III AFP: identification of a cluster of surface residues required for binding to ice	LeIBP (ref. Characterization of the ice-binding protein from Arctic yeast Leucosporidium sp. AY30)	FfIBP (ref. Structure-based characterization and antifreeze properties of a hyperactive ice-binding protein from the Antarctic bacterium Flavobacterium frigoris PS1)
Mass (kDa)	6.5	~ 27	~ 25.3
Structure	globular 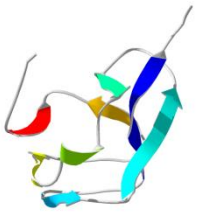	β-helix 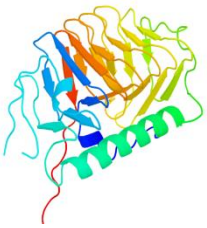	β-helix 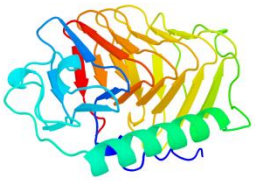
Natural source	Ocean pout, wolfish, eelpout	*Glaciozyma* sp.	*Flavobacterium frigoris*
TH	~ 1.5 ℃ at 3 mM	0.42 ℃ at 0.4 mM	2.5 ℃ at 50 μM

Table 2. The proportions of grade I follicles in fresh and vitrified-warmed control, sham, simvastatin, methylprednisolone and combined groups 2 days after mouse ovarian tissue transplantation

	Fresh Control	Vitrified-warmed Control	Sham	Simvastatin	Methyl-prednisolone	S+M
No. of ovaries	**19**	**20**	**18**	**18**	**15**	**18**
Primordial	**355 (66.2%) [a]**	**141/236 (59.7%) [b]**	**74/115 (64.3%) [abc]**	**137/179 (76.5%) [d]**	**88/118 (74.6%) [cd]**	**104/120 (86.7%) [e]**
Primary	**63/102 (61.8%) [a]**	**22/64 (34.4%) [b]**	**15/36 (41.7%) [bc]**	**16/29 (55.2%) [ab]**	**15/22 (68.2%) [ac]**	**20/33 (60.6%) [ac]**
Secondary	**37/64 (57.8%) [a]**	**29/75 (38.7%) [bc]**	**16/43 (37.2%) [bd]**	**17/39 (43.6%) [acd]**	**16/43 (37.2%) [bc]**	**15/31 (48.4%) [acd]**
Antral	**62/72 (86.1%)**	**21/29 (72.4%)**	**0/0 (0%)**	**0/0 (0%)**	**0/0 (0%)**	**0/0 (0%)**
Total	**397/593 (66.9%) [a]**	**213/404 (52.7%) [b]**	**105/194 (54.1%) [b]**	**170/247 (68.8%) [a]**	**119/183 (65.0%) [a]**	**139/184 (75.5%) [a]**

* A statistical analysis was performed by χ^2-test and different superscript letters indicate statistically significant differences ($p < 0.05$).
Fresh control: fixed ovarian tissue without vitrification or transplantation
Vitrified-warmed control: ovarian tissue fixed immediately after the vitrification-warming procedures
Sham: normal saline treatment 2 hours before ovariectomy and transplantation of vitrified-warmed ovarian tissue
Simvastatin: peroral Simvastatin treatment 2 hours before ovariectomy and transplantation of vitrified-warmed ovarian tissue
Methylprednisolone: i.v. Methylprednisolone treatment 2 hours before ovariectomy and transplantation of vitrified-warmed ovarian tissue
S+M: peroral Simvastatin and i.v. Methylprednisolone treated 2 hours before ovariectomy and transplantation of vitrified-warmed ovarian tissue
***Fresh and vitrified-warmed controls were used on days 2, 7 and 21.**

'The same experimental procedures were performed for the groups shown in Tables 2-5'

Table 3. The proportions of grade I follicles 7 days after mouse ovarian tissue transplantation

	Fresh Control	Vitrified-warmed Control	Sham	Simvastatin	Methyl-prednisolone	S+M
No. of ovary	**19**	**20**	**17**	**20**	**19**	**18**
Primordial	**235/355 (66.2%) [a]**	**141/236 (59.7%) [b]**	**62/93 (66.7%) [bc]**	**99/128 (77.3%) [c]**	**120/169 (71.1%) [c]**	**95/131 (72.5%) [c]**
Primary	**63/102 (61.8%) [ab]**	**22/64 (34.4%) [c]**	**27/51 (52.9%) [a]**	**35/57 (61.4%) [ab]**	**38/56 (67.9%) [ab]**	**44/61 (72.1%) [b]**
Secondary	**37/64 (57.8%) [a]**	**29/75 (38.7%) [b]**	**44/76 (57.9%) [a]**	**46/77 (59.7%) [a]**	**40/55 (72.7%) [a]**	**33/52 (63.5%) [a]**
Antral	**62/72 (86.1%)**	**21/29 (72.4%)**	**4/6 (66.7%)**	**0/0 (0%)**	**0/0 (0%)**	**5/8 (62.5%)**
Total	**397/593 (66.9%) [ac]**	**213/404 (52.7%) [b]**	**137/226 (60.6%) [ab]**	**180/262 (68.7%) [ac]**	**198/282 (70.2%) [c]**	**177/252 (70.2%) [c]**

* A statistical analysis was performed by χ^2-test and different superscript letters indicate statistically significant differences ($p < 0.05$).
Fresh control: fixed ovarian tissue without vitrification or transplantation
Vitrified-warmed control: ovarian tissue fixed immediately after the vitrification-warming procedures
Sham: normal saline treatment 2 hours before ovariectomy and transplantation of vitrified-warmed ovarian tissue
Simvastatin: peroral Simvastatin treatment 2 hours before ovariectomy and transplantation of vitrified-warmed ovarian tissue
Methylprednisolone: i.v. Methylprednisolone treatment 2 hours before ovariectomy and transplantation of vitrified-warmed ovarian tissue
S+M: peroral Simvastatin and i.v. Methylprednisolone treated 2 hours before ovariectomy and transplantation of vitrified-warmed ovarian tissue
***Fresh and vitrified-warmed controls were used on days 2, 7 and 21.**

Table 4. The proportions of grade I follicles 21 days after mouse ovarian tissue transplantation

	Fresh Control	Vitrified-warmed Control	Sham	Simvastatin	Methyl-prednisolone	S+M
No. of ovary	**19**	**20**	**18**	**17**	**19**	**18**
Primordial	**235/355 (66.2%) [a]**	**141/236 (59.7%) [bc]**	**71/131 (54.2%) [ab]**	**99/144 (68.8%) [cd]**	**69/96 (71.9%) [d]**	**99/133 (74.4%) [d]**
Primary	**63/102 (61.8%) [a]**	**22/64 (34.4%) [b]**	**24/52 (46.2%) [ab]**	**38/66 (57.6%) [b]**	**21/32 (65.6%) [a]**	**28/51 (54.9%) [a]**
Secondary	**37/64 (57.8%) [ac]**	**29/75 (38.7%) [b]**	**18/37 (48.6%) [ab]**	**31/45 (68.9%) [ac]**	**39/76 (51.3%) [ab]**	**39/53 (73.6%) [c]**
Antral	**62/72 (86.1%) [a]**	**21/29 (72.4%) [ab]**	**12/23 (52.2%) [b]**	**10/17 (58.8%) [bc]**	**9/16 (56.3%) [bc]**	**22/27 (81.5%) [bc]**
Total	**397/593 (66.9%) [ac]**	**213/404 (52.7%) [b]**	**125/243 (51.4%) [b]**	**178/272 (65.4%) [ac]**	**138/220 (62.7%) [a]**	**188/264 (71.2%) [c]**

* A statistical analysis was performed by χ^2-test and different superscript letters indicate statistically significant differences ($p < 0.05$).
Fresh control: fixed ovarian tissue without vitrification or transplantation
Vitrified-warmed control: ovarian tissue fixed immediately after the vitrification-warming procedures
Sham: normal saline treatment 2 hours before ovariectomy and transplantation of vitrified-warmed ovarian tissue
Simvastatin: peroral Simvastatin treatment 2 hours before ovariectomy and transplantation of vitrified-warmed ovarian tissue
Methylprednisolone: i.v. Methylprednisolone treatment 2 hours before ovariectomy and transplantation of vitrified-warmed ovarian tissue
S+M: peroral Simvastatin and i.v. Methylprednisolone treated 2 hours before ovariectomy and transplantation of vitrified-warmed ovarian tissue
***Fresh and vitrified-warmed controls were used on days 2, 7 and 21.**

Table 5. The number of apoptotic follicles at 2, 7 and 21 days after mouse ovarian tissue transplantation

	Fresh Control	Vitrified-warmed Control	Sham	Simvastatin	Methyl-prednisolone	S+M
Day 2	**27/441 (6.1%) [a]**	**46/405 (11.4%) [b]**	**6/99 (6.1%) [ab]**	**7/128 (5.5%) [ab]**	**5/101 (5.0%) [ab]**	**5/106 (4.7%) [a]**
Day 7		**46/405 (11.4%) [b]**	**8/171 (4.7%) [acd]**	**4/190 (2.1%) [cd]**	**7/201 (3.5 %) [acd]**	**2/162 (1.2%) [d]**
Day 21		**46/405 (11.4%) [b]**	**9/159 (5.7%) [ac]**	**11/195 (5.6%) [ac]**	**17/195 (8.7%) [ab]**	**3/172 (1.7%) [d]**

* A statistical analysis was performed by χ^2-test and different superscript letters indicate statistically significant differences ($p < 0.05$).
Fresh control: fixed ovarian tissue without vitrification or transplantation
Vitrified-warmed control: ovarian tissue fixed immediately after the vitrification-warming procedures
Sham: normal saline treatment 2 hours before ovariectomy and transplantation of vitrified-warmed ovarian tissue
Simvastatin: peroral Simvastatin treatment 2 hours before ovariectomy and transplantation of vitrified-warmed ovarian tissue
Methylprednisolone: i.v. Methylprednisolone treatment 2 hours before ovariectomy and transplantation of vitrified-warmed ovarian tissue
S+M: peroral Simvastatin and i.v. Methylprednisolone treated 2 hours before ovariectomy and transplantation of vitrified-warmed ovarian tissue
***Fresh and vitrified-warmed controls were used on days 2, 7 and 21.**

Table 6. The embryonic development of mouse oocytes retrieved from ovarian tissue grafts 21 days after transplantation

	Sham	Simvastatin	Methylprednisolone	S+M
No. of retrieved oocytes (from 8 ovaries/group)	**53**	**56**	**56**	**45**
No. of MII oocytes (ea)	**38 (71.7%)**	**42 (75.0%)**	**40 (71.4%)**	**35 (77.8%)**
No. of 2 cell embryos (ea)	**18 (47.4%)**	**20 (47.6%)**	**26 (65.0%)**	**20 (57.1%)**
No. of blastocysts (ea)	**11 (61.1%)**	**10 (50.0%)**	**13 (50.0%)**	**11 (55.0%)**
No. of total cells (ea)	**29.4±2.2**	**30.7±3.1**	**32.7±2.4**	**34.0±3.8**
No. of apoptotic blastomeres (ea)	**3.4±0.6**	**2.6±0.7**	**1.7±0.5**	**2.4±0.9**
ICM/TE (ea)	**7.9±1.9/ 21.5±1.7**	**7.3±2.6/ 23.4±2.7**	**7.9±1.9/ 25.4±2.6**	**9.1±2.4/ 24.9±2.5**

* Statistical analysis were performed by χ^2-test (for MII, fertilization and blastocyst formation rate) and one-way ANOVA (for the number of total, apoptotic blastomere and the ratio of ICM/TE)
ICM: Inner cell mass
TE: Trophoectoderm
MII: metaphase II

Table 7. Pre-implantation embryonic developmental competence in three different groups

	MII oocyte	**Two-cell embryo (24 h)**	**Two-cell embryos (48 h)**	**Blastocyst (120 h)**
In vivo control	126	106 (84.1%)		79 (74.5%)
Oil layer	79	3 (3.8%)	6 (7.6%)	0
Without oil layer	88	4 (4.5%)	17 (19.3%)	0

* Statistical analysis were performed by χ^2-test (for two-cell embryo and blastocyst formation rate).

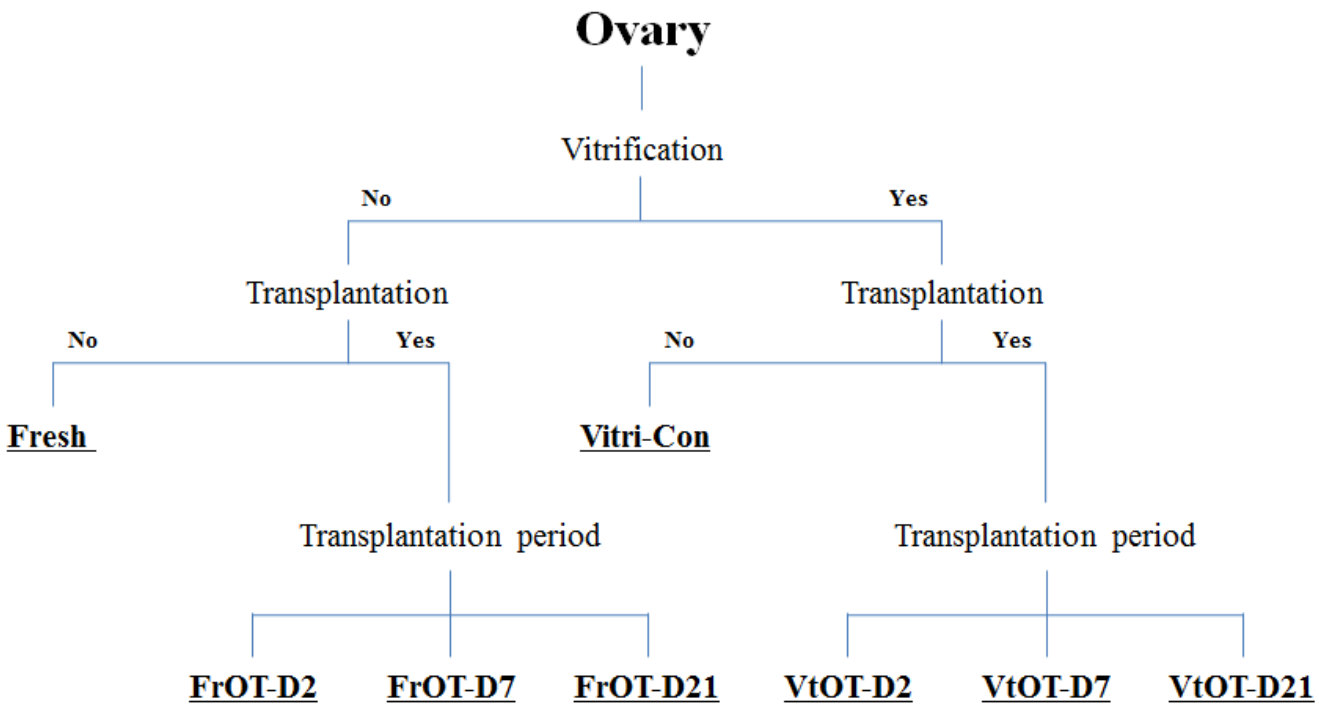

Figure 1. **Flowchart of the chapter I study**. Groups were randomly divided into eight different groups according to the cryopreservation and transplantation of ovarian tissue. Bold and underlined letters represent the eight different groups.

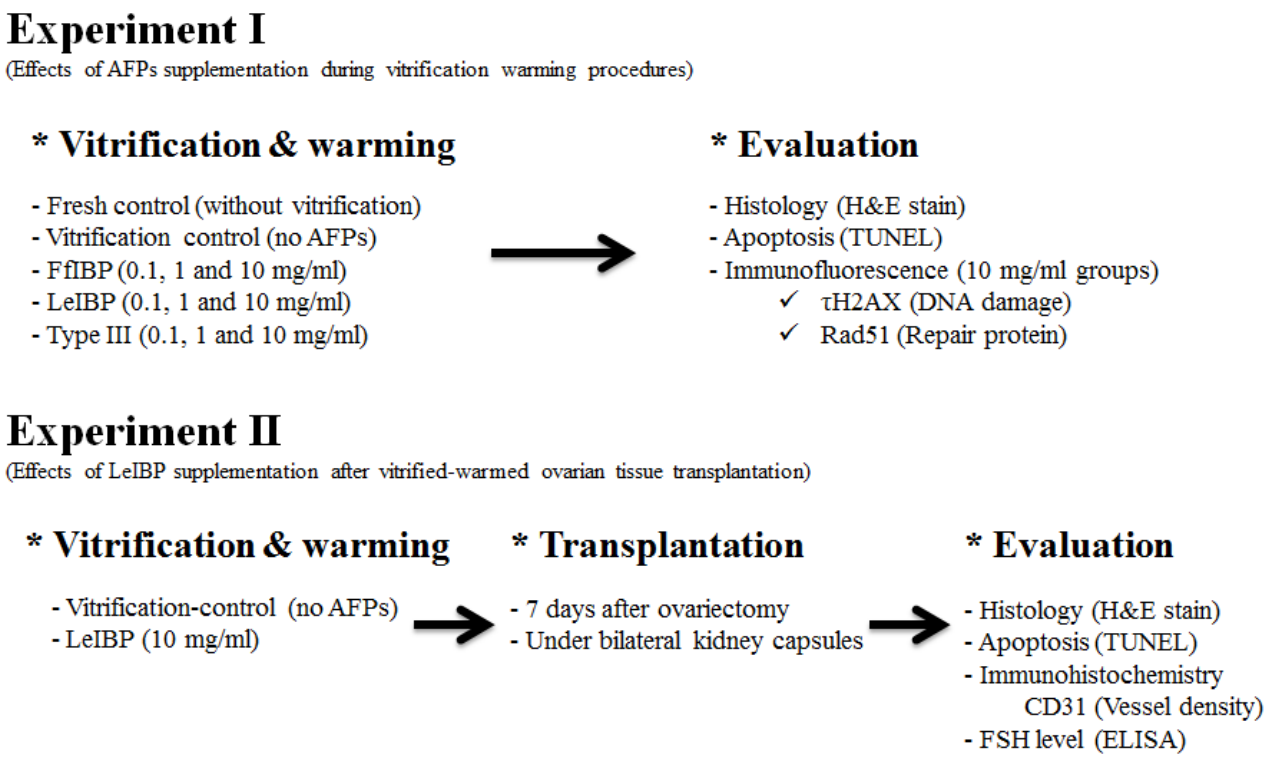

Figure 2. A schematic figure showing two experimental schemes of chapter II. This experimental flow was constructed to evaluate the effects of three different antifreeze proteins.

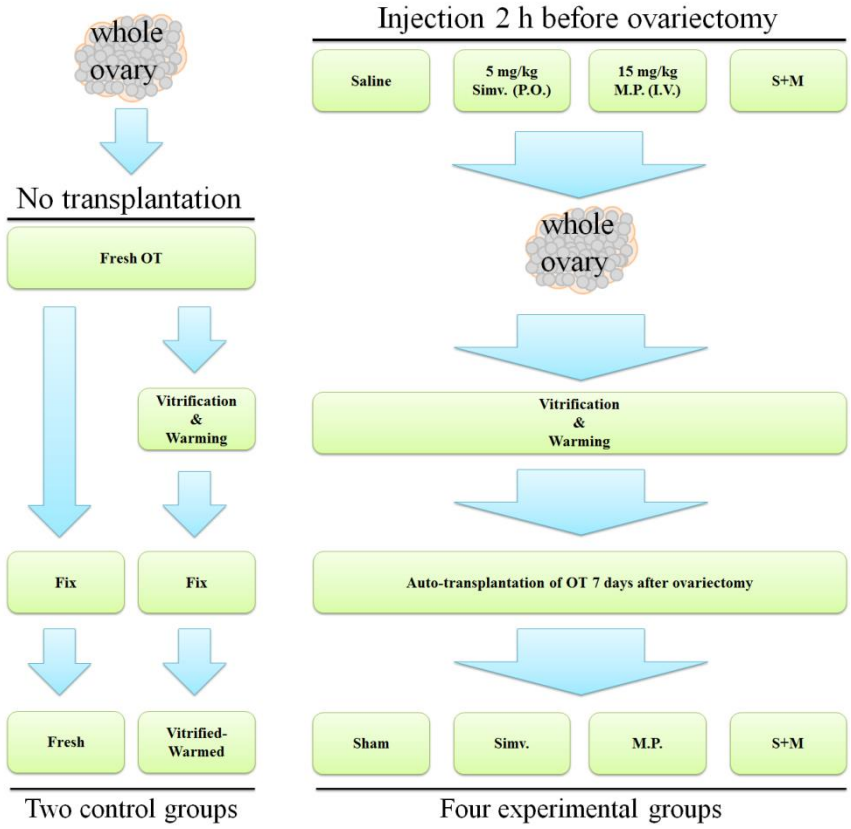

Figure 3. Schematic for the study design. The mice were divided into six groups: fresh control, vitrified-warmed control, sham control, simvastatin, methylprednisolone and a combination of simvastatin and methylprednisolone treatment. P.O. and I.V. indicate peroral and intravenous administration of drug, respectively.

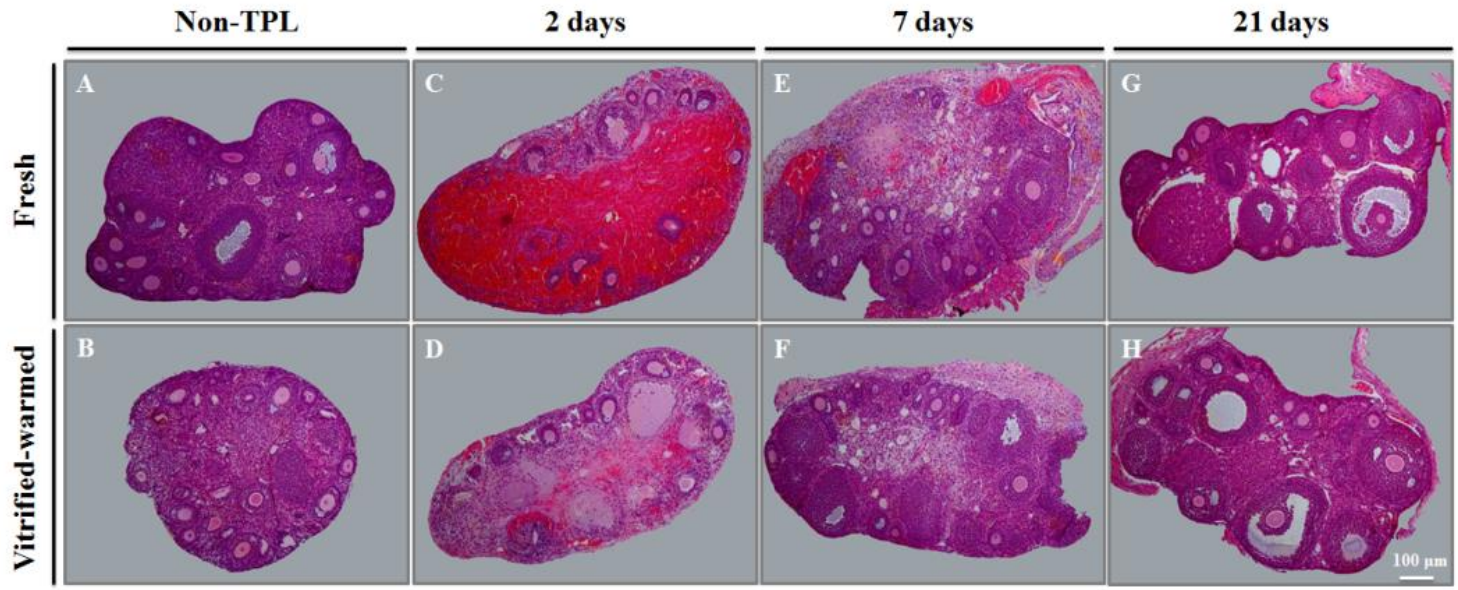

Figure 4. Representative images of the hematoxylin and eosin stain of ovarian tissue for eight different groups. (A) and (B) represent fresh and vitrified-warmed ovarian tissue without transplantation. (C, E, and G) represent groups that underwent transplantation of fresh ovarian tissue. (D, F, and H) show groups that underwent grafting of vitrified-warmed ovarian tissue during a different transplantation period. All magnifications are ×100, and the scale bar represents 100 μm.

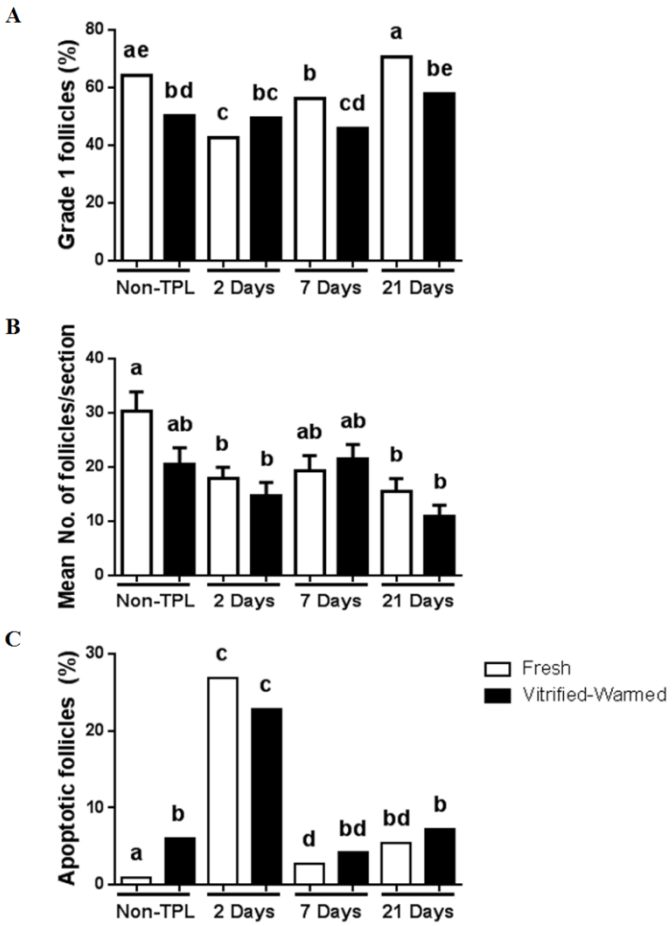

Figure 5. The proportion of grade 1 (G1) follicles, mean number of follicles per section, and apoptotic follicle ratio. (A, B, and C) represent the percentage of G1 follicles, mean number of ovarian follicles per single section, and percentage of apoptotic follicles after immediate fixation, and vitrified-warmed and transplanted ovarian tissue for each evaluation period, respectively. Statistically significant differences ($p < 0.05$) are indicated by different letters (e.g., a:b). Columns sharing the same letters (e.g., a:ab) are not significantly different.

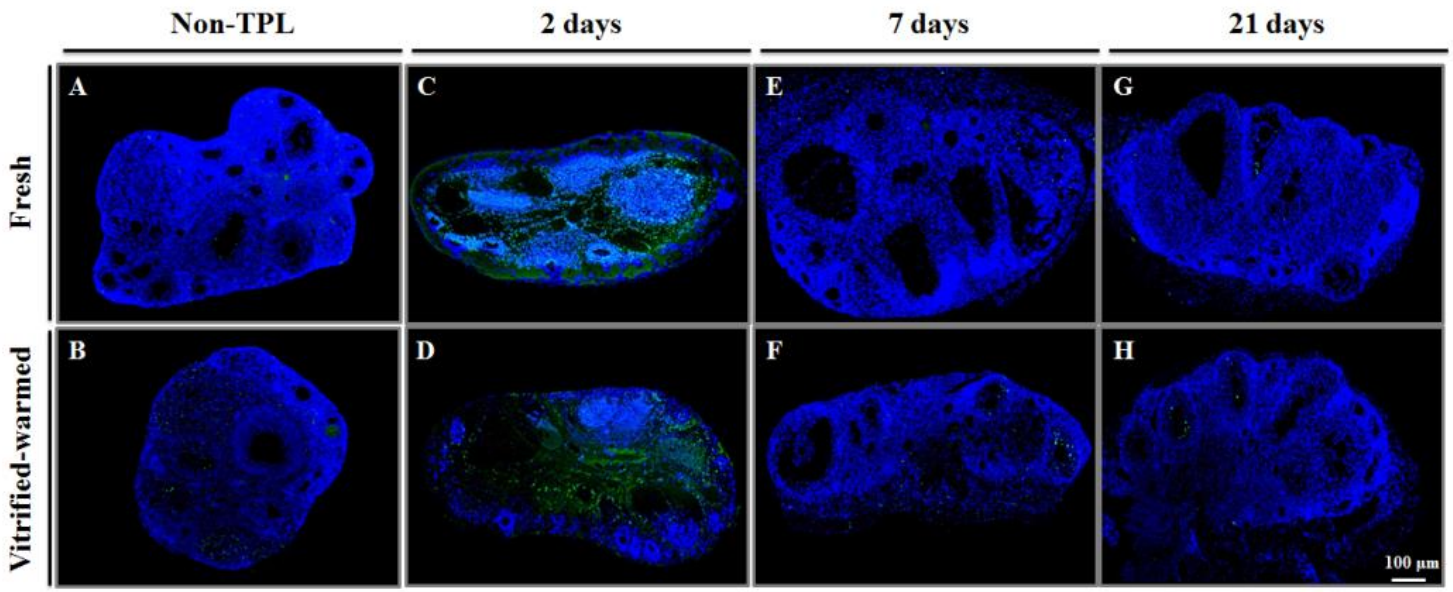

Figure 6. Terminal deoxynucleotidyl transferase mediated dUTP nick end labeling assay for detecting apoptosis in ovarian tissue. (A) and (B) represent fresh and vitrified-warmed ovarian tissue without transplantation. (C, E, and G) represent the fresh ovarian tissue groups. (D, F, and H) show the vitrified ovarian tissue groups at different periods. All magnifications are ×100, and the scale bar represents 100 μm.

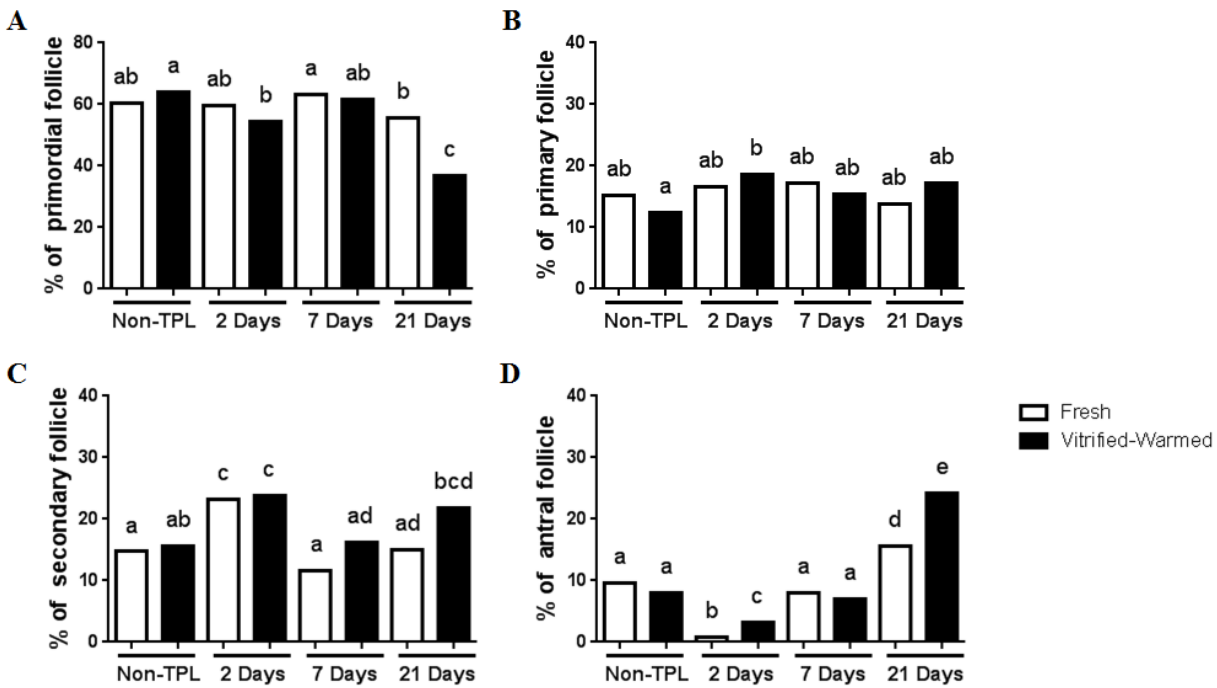

Figure 7. The proportion of ovarian follicle according to the developmental stage. Each panel (A-D) shows a percentage of ovarian follicles. (A) Primordial (B) Primary (C) Secondary and (D) Antral stage follicles. Statistically significant differences ($p < 0.05$) are indicated by different letters (e.g., a:b). Columns sharing the same letters (e.g., a:ab) are not significantly different.

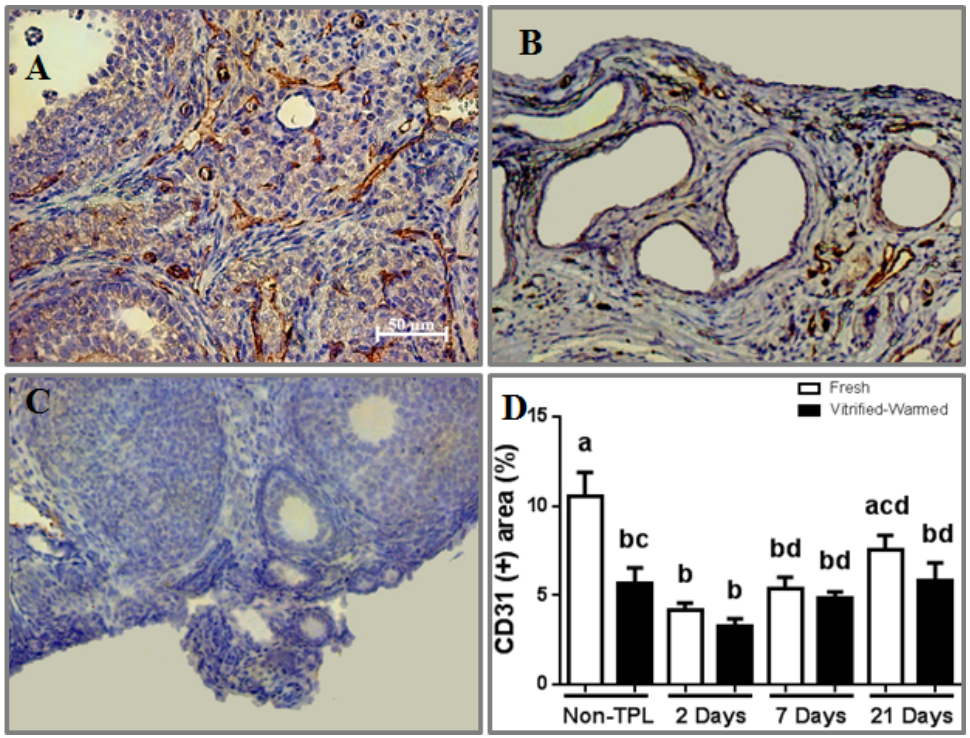

Figure 8. Immunohistochemical staining of ovarian tissue with CD31. (A) Brown-colored cells are the CD31(+) cells. White arrows represent CD31(+) blood vessels in the graft. Magnification is ×400, and the scale bar represents 50 μm. (B) The proportion of CD31-positive area in each ovarian tissue from eight different groups is represented as the mean ± standard error of mean. Statistically significant differences ($p < 0.05$) are indicated by different letters (e.g., a:b). Columns sharing the same letters (e.g., a:ab) are not significantly different.

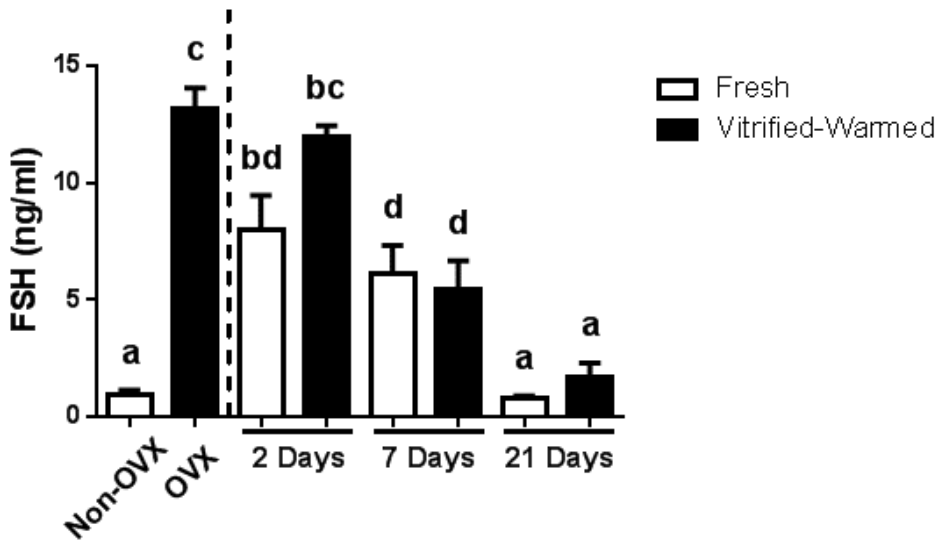

Figure 9. Serum follicle-stimulating hormone (FSH) level. Serum FSH levels are estimated by enzyme-linked immunosorbent assay in eight different groups. Data are represented as the mean ± standard error of mean. Statistically significant differences ($p < 0.05$) are indicated by different letters (e.g., a:b). Columns sharing the same letters (e.g., a:ab) are not significantly different.

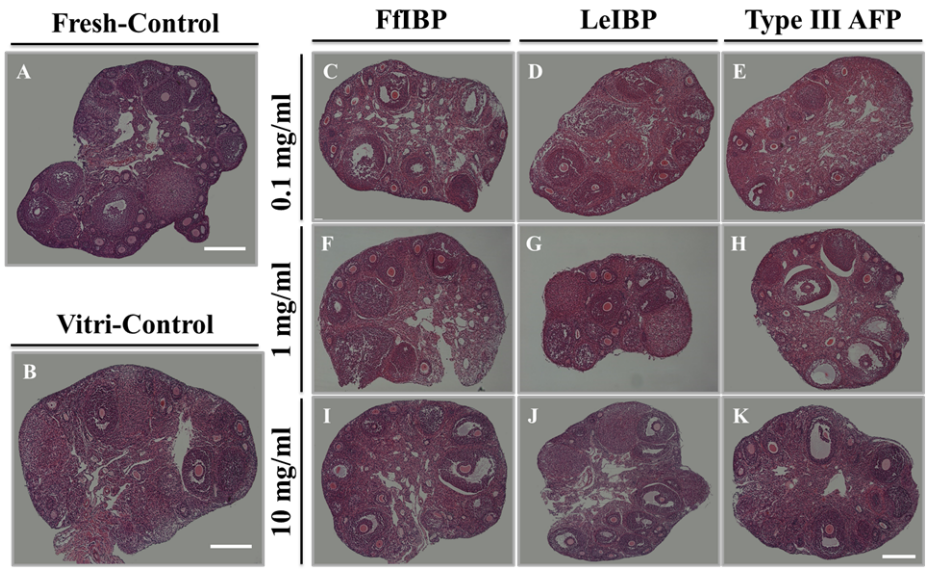

Figure 10. Representative images of hematoxylin and eosin stain for 11 groups according to type of antifreeze protein (AFP) and dose. (A) Fresh control (without cryopreservation); (B) vitrification control (cryopreservation without any AFP supplementation); (C–E) groups treated with 0.1 mg/mL AFP; (F–H) groups treated with 1.0 mg/mL AFP; (I–K) groups treated with 10 mg/mL AFP. (C, F, I) The FfIBP-treated group; (D, G, J) the LeIBP-treated group; and (E, H, K) the group treated with type III AFP. White bars indicate 500 μm; the magnification was 100×.

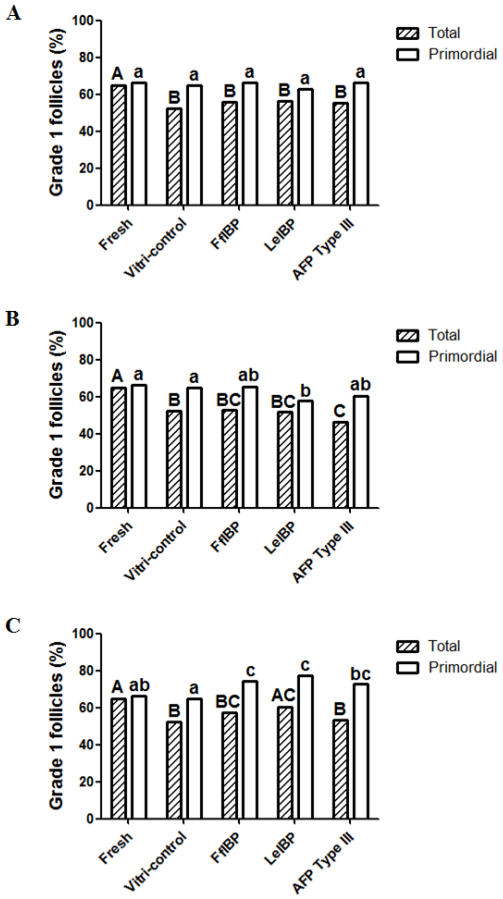

Figure 11. Percentages of total grade 1 follicles and primordial stage follicles in groups treated with (A) 0.1 mg/mL antifreeze protein (AFP), (B) 1.0 mg/mL AFP, and (C) 10 mg/mL AFP. Different of upper and lower case letters respectively indicate statistically significant differences among five groups in terms of total and primordial grade 1 follicle ratio, respectively ($p<0.05$). Statistically significant differences ($p < 0.05$) are indicated by different letters (e.g., a:b). Columns sharing the same letters (e.g., a:ab) are not significantly different.

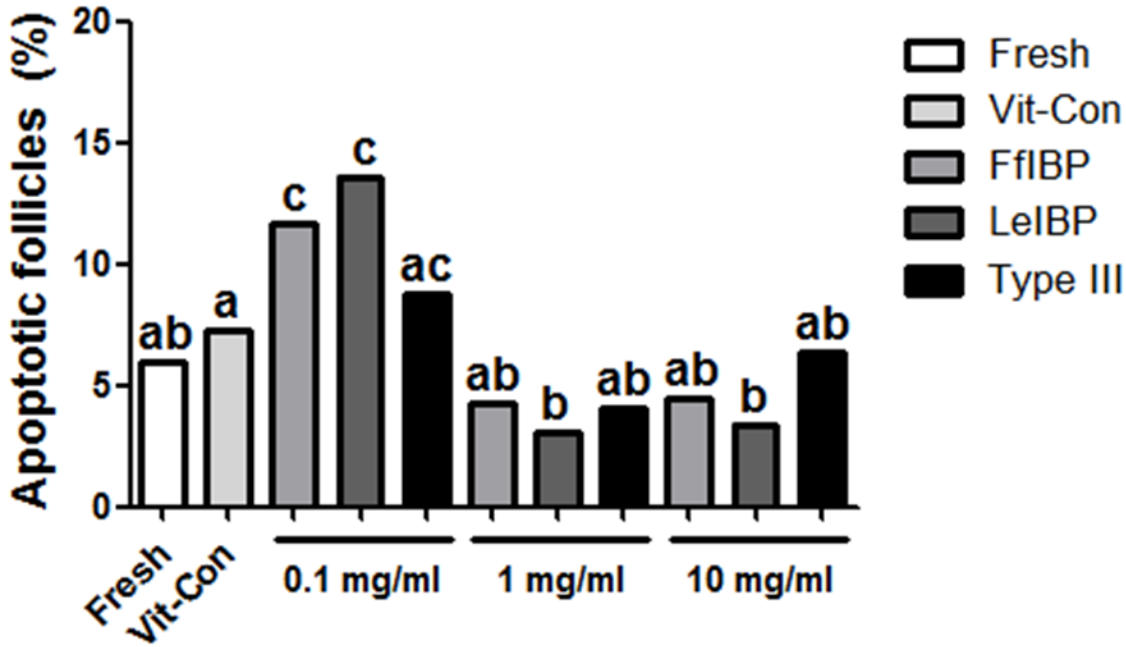

Figure 12. Percentage of apoptotic follicles in 11 groups after vitrification and warming procedures. Statistically significant differences ($p < 0.05$) are indicated by different letters (e.g., a:b). Columns sharing the same letters (e.g., a:ab) are not significantly different.

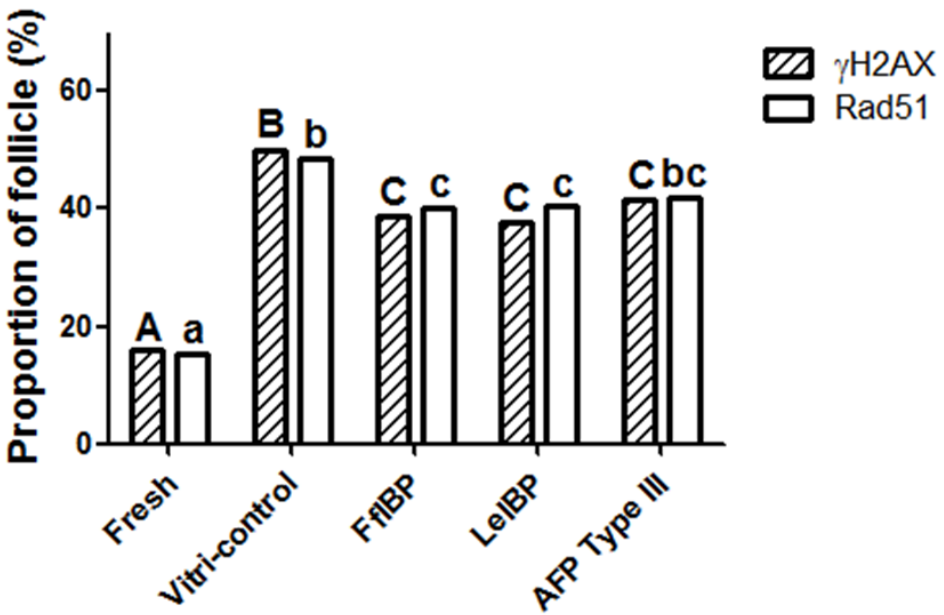

Figure 13. The percentage of τH2AX- and Rad51-positive follicles in the two control groups and the groups treated with 10 mg/mL of the different antifreeze proteins. Upper case and lower case letters respectively indicate significant differences among five groups in terms of τH2AX and Rad51, respectively ($p<0.05$). Statistically significant differences ($p < 0.05$) are indicated by different letters (e.g., a:b). Columns sharing the same letters (e.g., a:ab) are not significantly different.

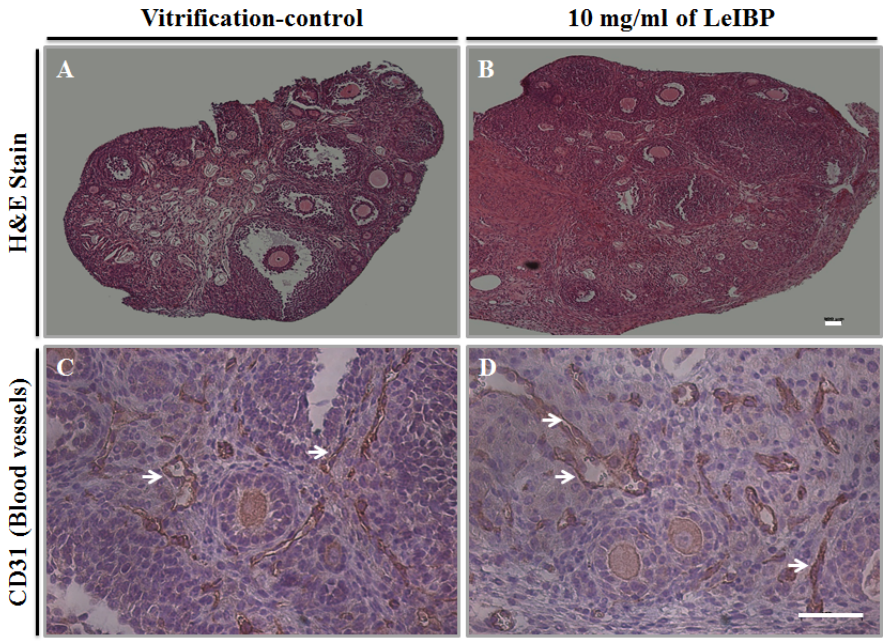

Figure 14. Histological assessment and immunohistochemical analysis for blood vessels (using the marker CD31) in transplanted ovarian tissue. Hematoxylin and eosin staining of grafts in (A) the vitrification-control group and (B) the LeIBP-treated group (100×). (C) CD31 expressed in endothelial cells in the vitrification-control group and (D) the LeIBP group (400×). Arrows indicate blood vessels, and white bars represent 100 μm.

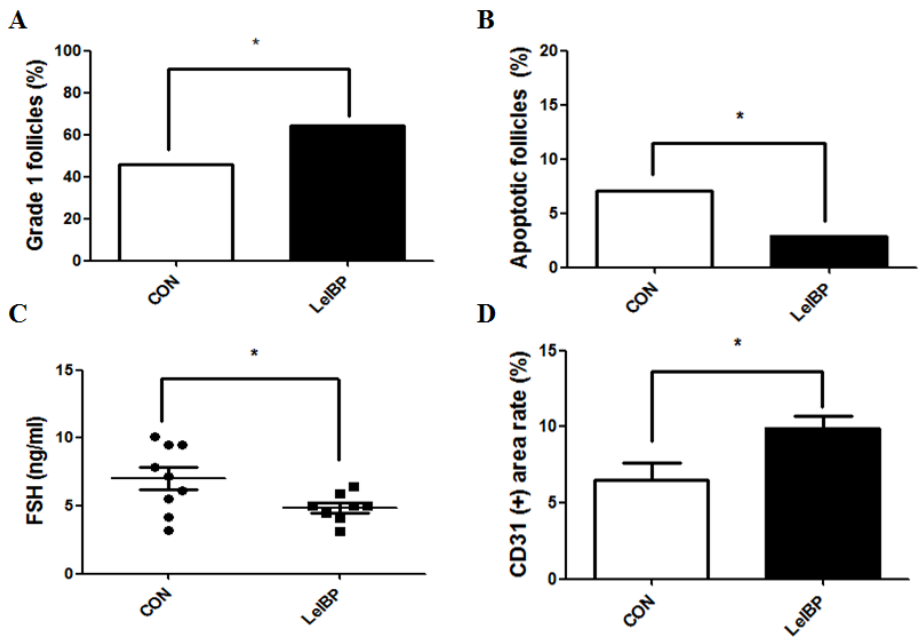

Figure 15. Comparisons of various parameters in the vitrification-control group and the LeIBP-treated group after ovarian tissue transplantation. (A) Percentage of total grade 1 follicles, (B) percentage of apoptotic follicles, (C) serum follicle stimulating hormone levels, and (D) CD31-positive area in both transplantation groups. Asterisks indicate significant differences compared with the vitrification-control.

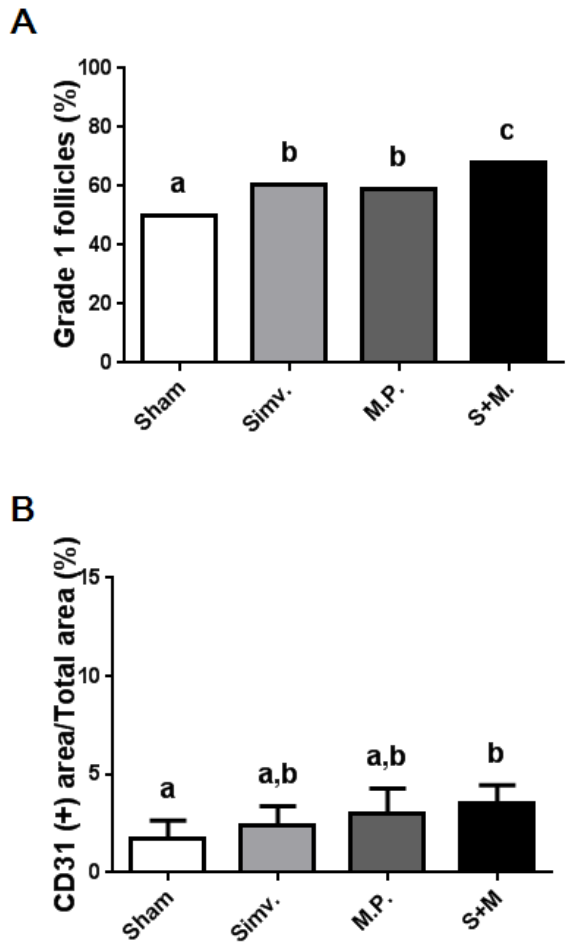

Figure 16. The proportion of Grade 1 follicle and CD31-positive area in graft 7 days after transplantation of normal ovarian tissue. The preventive effect of simvastatin and/or methylprednisolone was evaluated in terms of (A) Grade 1 follicle ratio and (B) CD31-positive area in graft, respectively. Data are represented as mean ± SEM and different letters indicate statistically significant differences ($p < 0.05$).

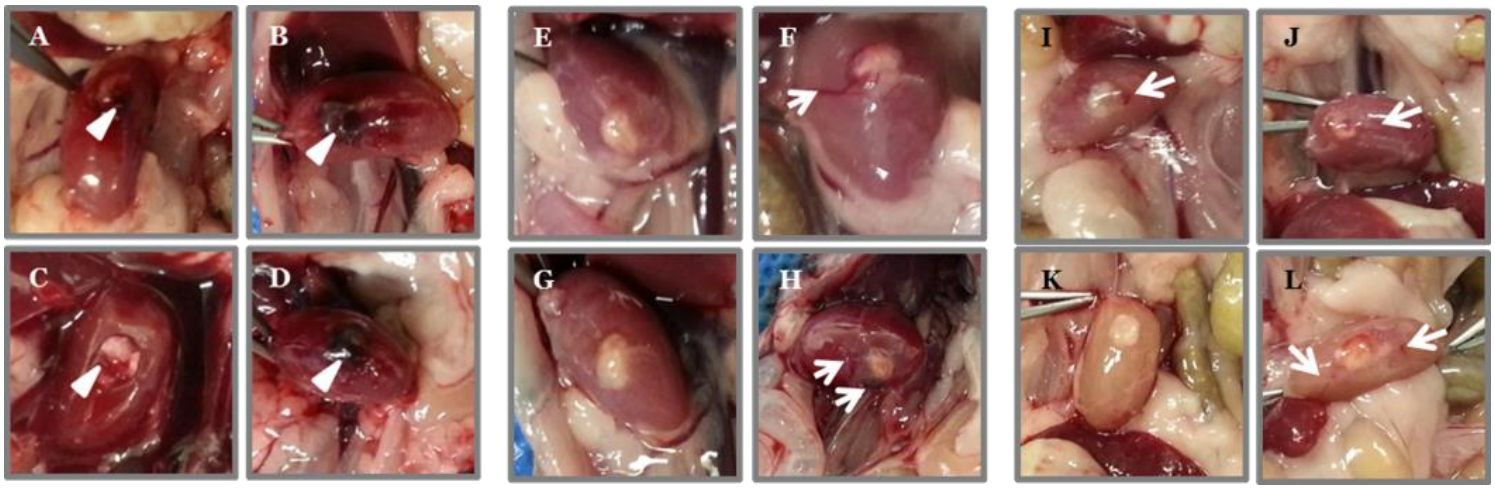

Figure 17. Representative images of mouse ovarian tissue grafts according to the duration of transplantation. A, E, I: sham control, B, F, J: simvastatin, C, G, K: methylprednisolone, and D, H, L: simvastatin and methylprednisolone combination treated. A–D: 2 days, E–H: 7 days, and I–L: 21 days after transplantation. The arrowhead and arrow indicate blood clot and blood vessel, respectively.

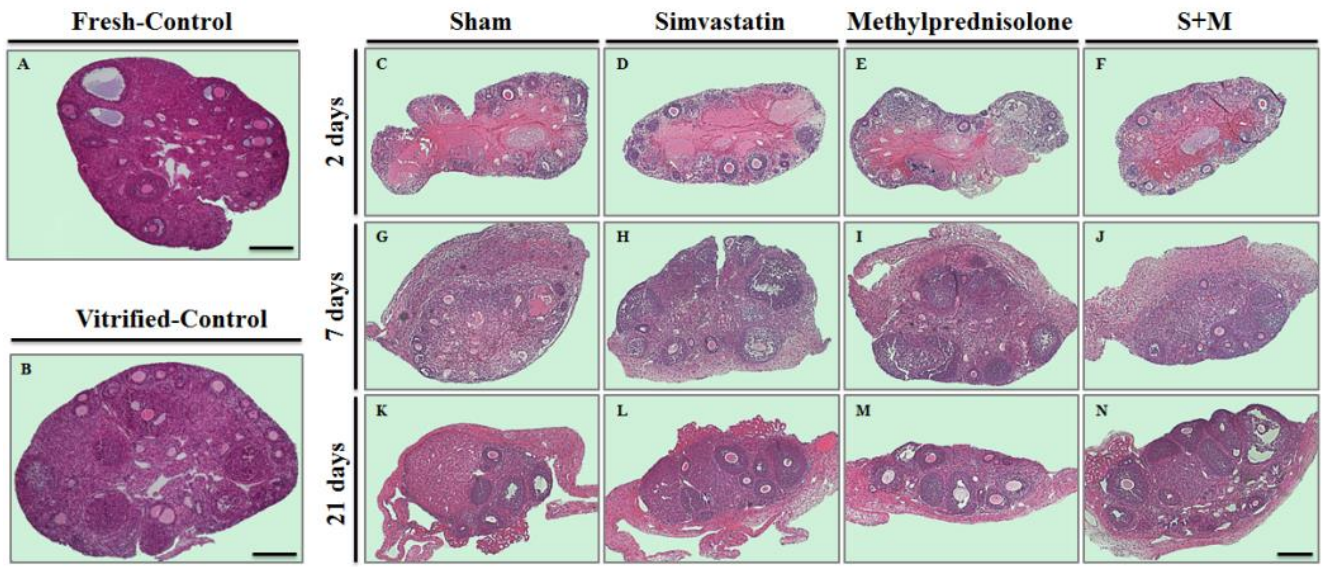

Figure 18. Representative images of hematoxylin and eosin stained ovarian tissue from mice. X-axis shows the different groups (A: fresh ovarian tissue, B: vitrified-warmed ovarian tissue C, G, K: sham, D, H, L: simvastatin, E, I, M: methylprednisolone and F, J, N: simvastatin and methylprednisolone combination treated.) and Y –axis represents days after ovarian tissue transplantation (A-D: 2 days, E-H: 7 days and I-L: 21 days after transplantation). The magnification was x100 and the scale bar indicates 200 μm.

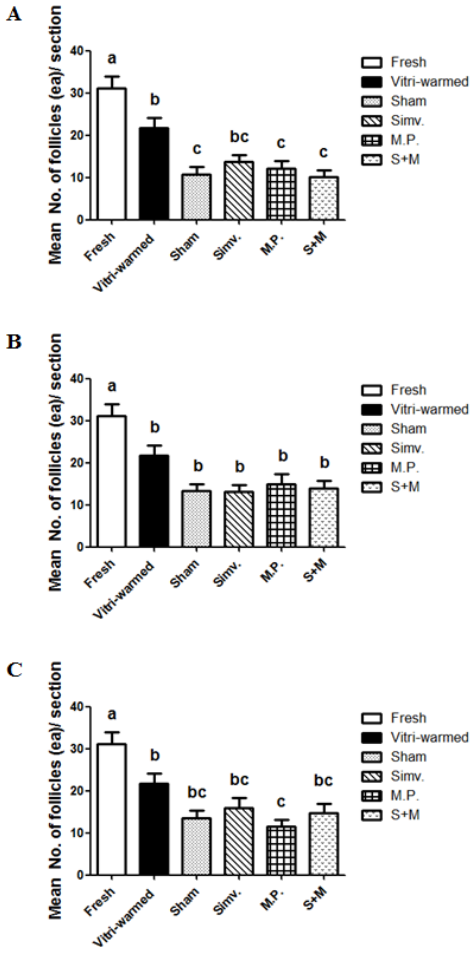

Figure 19. Mean follicle number per section of mouse ovary. (A-C) represents the average follicle number in one section from each ovary on day 2, 7 and 21, respectively. Data from fresh and vitrified-warmed controls were used as same value on day 2, 7 and 21. Data was analyzed by one-way analysis of variance (ANOVA). Graphs are presented as mean ± SEM and different letters indicate statistically significant differences ($p < 0.05$).

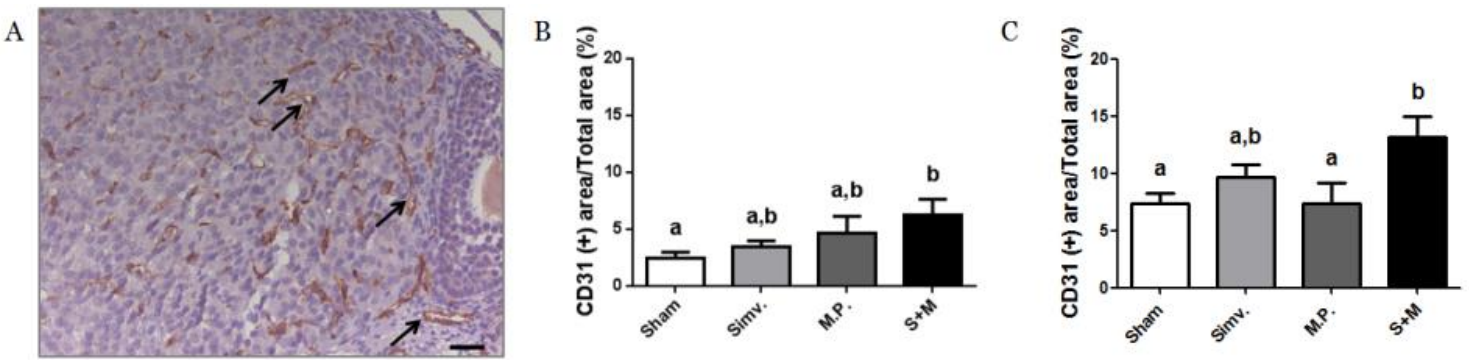

Figure 20. Immunohistochemical staining of ovarian tissue with CD31. (A) Brown-colored cells are the CD31-positive cells. Magnification was 400× and scale bar represents 100 μm. (B) and (C) indicate the CD31-positive area in each ovarian tissue 7 and 21 days after transplantation, respectively. The area was measured and analyzed by I-solution image analysis program and data was analyzed by one-way ANOVA. Graphs are presented as mean ± SEM and different letters indicate statistically significant differences ($p < 0.05$).

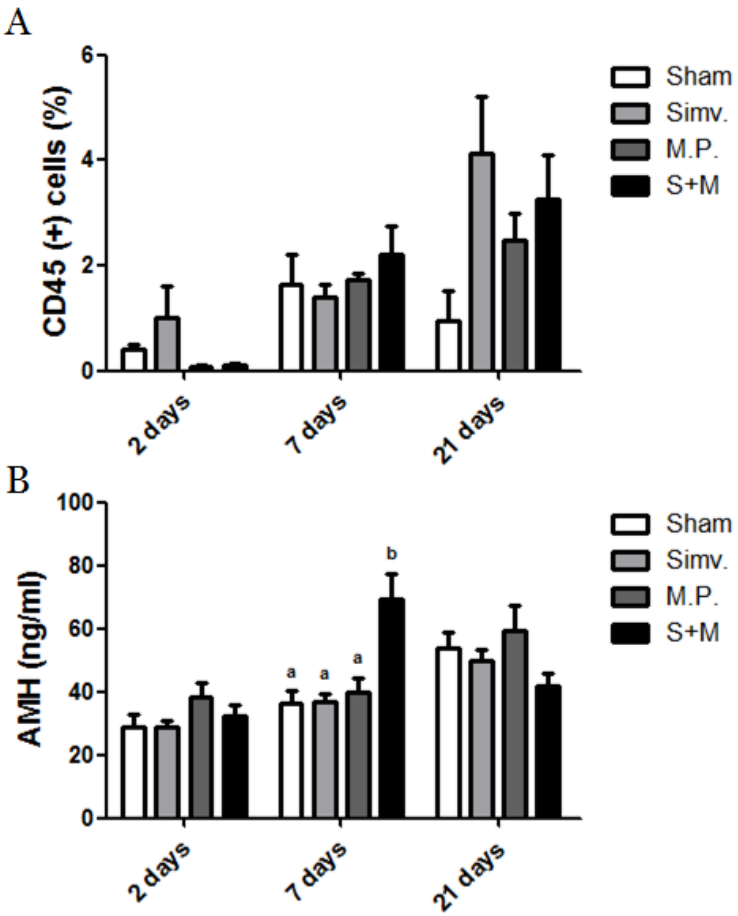

Figure 21. The proportion of infiltrated CD45-positive cells in transplanted ovarian tissues and serum AMH levels in mice. (A) The percentage of CD45-positive cells and the serum AMH levels was detected by flow cytometry and (B) enzyme-linked immunosorbent assay, respectively. Data was analyzed by one-way analysis of variance (ANOVA). Graphs are presented as mean ± SEM and different letters indicate statistically significant differences ($p < 0.05$).

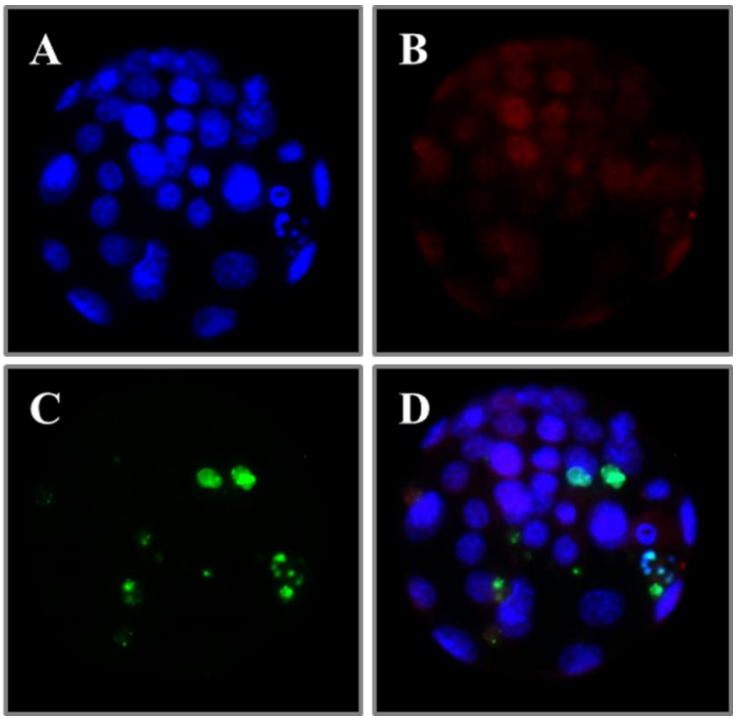

Figure 22. Differential staining of *in vitro*-developed mouse blastocysts. Blastocysts were stained with (A) DAPI (blue), (B) Oct-4 (red) and (C) TUNEL (green) for counting total blastomeres, the number of ICM, apoptotic blastomeres, and stained blastocysts, respectively. Panel (D) shows the merged image. Magnification was 400× and scale bar represents 100 µm.

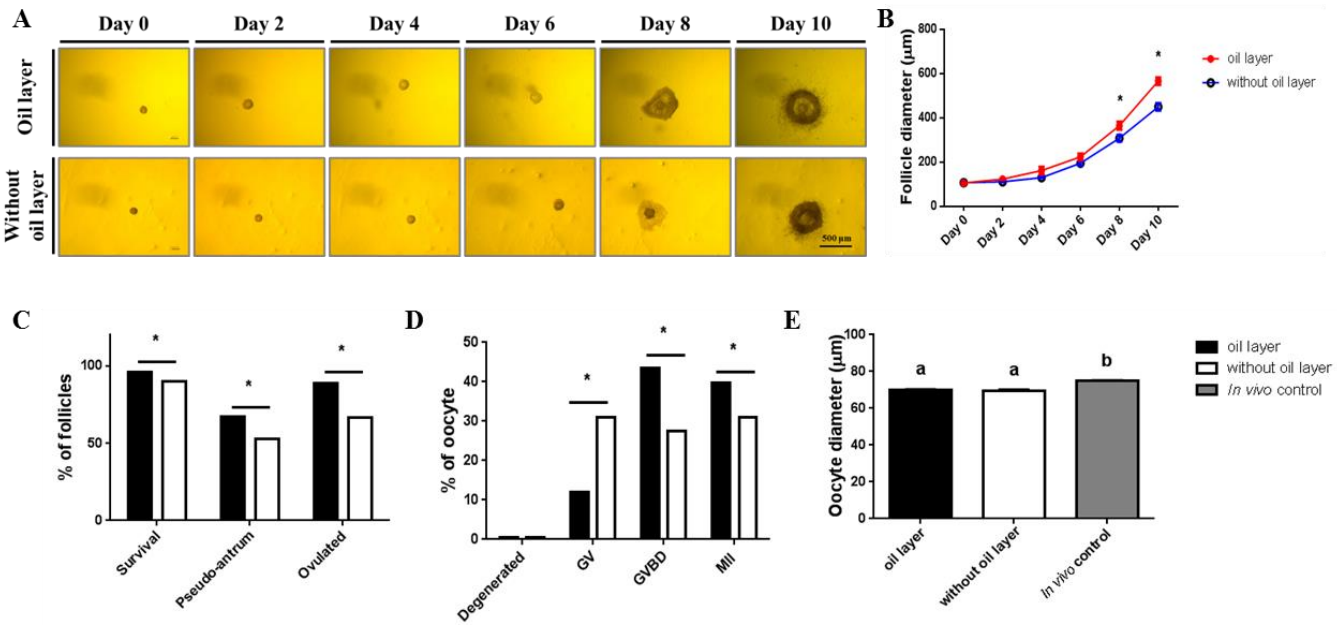

Figure 23. **Follicle growth, development, and oocyte growth and development according to the conventional culture methods.** (A-B) shows a representative image of follicle growth and growth curve during culture period. (C) indicates follicular development on 10th day of culture. (D) and (E) respectively mean the developmental stages and diameter of oocyte. Asterisks and different letter means statistical different ($p<0.05$).

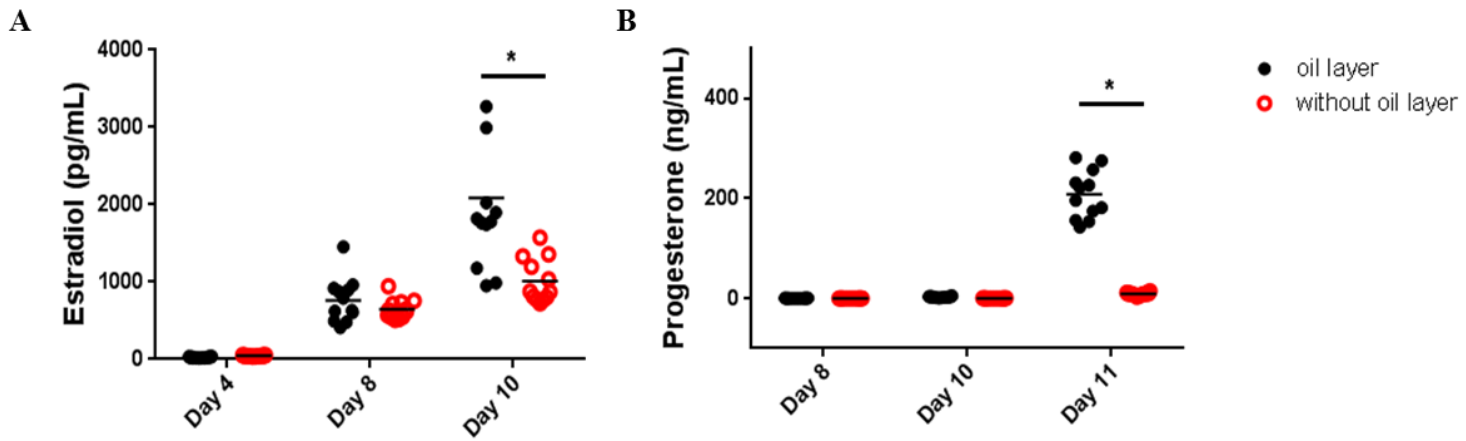

Figure 24. Hormone production during culture period in accordance with culture method. (A) and (B) represent estradiol and progesterone level in spent culture medium at each evaluation days. Each plot indicate each hormone value and asterisk means statistical different ($p<0.05$).

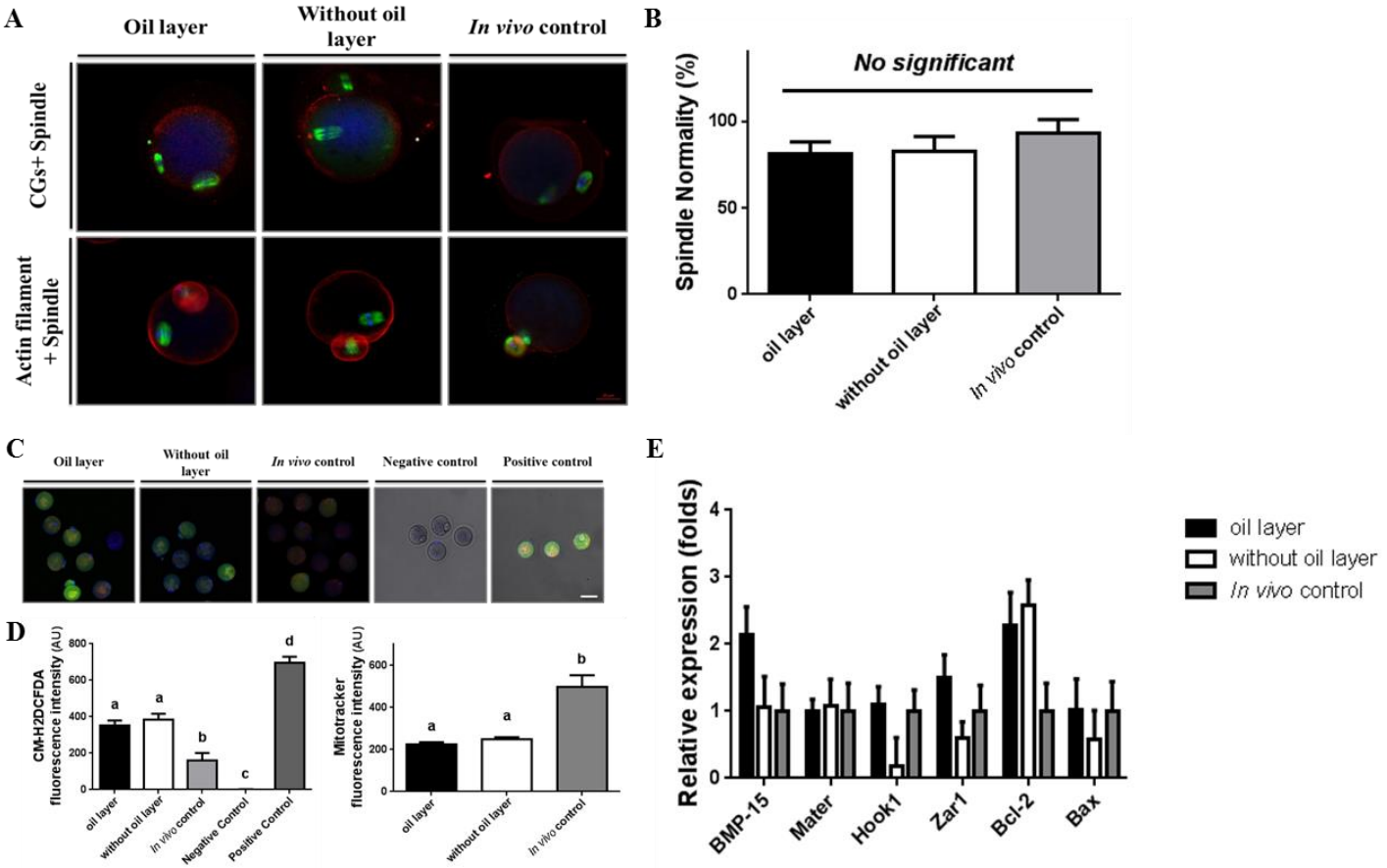
A
Oil layer
Without oil layer
In vivo control
CGs+ Spindle
Actin filament + Spindle
B
No significant
Spindle Normality (%)
100
50
0
oil layer
without oil layer
In vivo control
C
Oil layer
Without oil layer
In vivo control
Negative control
Positive control
D
CM-H2DCFDA fluorescence intensity (AU)
800
600
400
200
0
a
a
b
c
d
oil layer
without oil layer
In vivo control
Negative Control
Positive Control
Mitotracker fluorescence intensity (AU)
600
400
200
0
a
a
b
oil layer
without oil layer
In vivo control
E
Relative expression (folds)
4
3
2
1
0
BMP-15
Mater
Hook1
Zar1
Bcl-2
Bax
oil layer
without oil layer
In vivo control

Figure 25. Quality of cytoplasmic and nucleic maturation depending on the conventional culture methods. (A) represents the distribution of cortical granule, actin filament and meiotic spindle in both *in vitro* derived groups. (B) shows a normality of spindle organization. (C) shows a reactive oxygen species (ROS) production and mitochondrial activities in all five different groups. (D) indicates a graphs for quantitative fluorescent intensity of ROS and mitochondrial activities. Different letters indicate statistically significant differences among groups. (E) means mRNA expression in oocyte derived from three different culture environment.

DISCUSSIONS

In study 1, cryoinjury during OTC and ischemic injury after OTT are two major causes that impair OT quality during fertility preservation treatment using ovaries. We directly compared the deleterious effects between cryoinjury and ischemic injury to help understand tissue damage after cryopreservation and transplantation to devise a strategy to enhance the quality of OT for clinical application. Furthermore, this study showed the effect of both injuries on the quality of follicle, stromal density, blood vessel in OT and serum FSH level over time after the transplantation period.

Until now, there are two major ways to cryopreserve the OT in human, either controlled-rate freezing (slow freezing) or vitrification method. Of two methods, slow freezing of OT has been mostly applied to fertility preservation using ovarian tissue in human. Aforementioned in introduction, >60 babies have been born from female cancer patients after transplantation of frozen-thawed OT when the OT was cryopreserved by slow freezing method. In addition, Dittrich and Maltaris suggest that a simple freezing protocol for the use of an open freezing system for cryopreservation of ovarian tissue [60]. Contrast to the slow freezing, only two live births have been reported by Suzuki's studies [61]. Although vitrification protocol made successful live birth, further studies would be required to apply to clinic more than now. To widen the application of vitrification protocol in human OT, a few research teams

including us have attempted to provide insights of the method.

To date, few studies have reportedly investigated whether the main cause of ovarian injury is cryoinjury or ischemic injury [62-67]. However, the main reason for tissue injury has not been fully established. In Nisolle et al.'s previous study, fresh and frozen-thawed human OTs were xeno-transplanted subcutaneously and intraperitoneally, respectively [64]. Regardless of the transplantation site, there were no significant differences between fresh-transplantation and frozen-thawed-transplantation groups in terms of follicular density and capillary relative surface area. The authors assumed that post-transplantation ischemia is much more harmful on OT than cryoinjury. However, they could not investigate the negative effects of those injuries during the early phase of the ischemic period since they killed the mice only 24 days after transplantation [64]. In contrast, Liu and colleagues allo-transplanted fresh or frozen-thawed newborn mouse ovaries in recipients' kidney capsules and sacrificed the mice 14 days after transplantation. They also postulated that transplantation rather than cryopreservation accounts for the major and early loss of primordial follicles in grafted newborn mouse ovaries [63]. In 2012, expression of kit-ligand (KL) and anti-Mullerian hormone (AMH) was found in primordial and primary follicles after xeno-grafting of both fresh and slow frozen-thawed tissue [67]. However, those previous studies are not suitable for direct comparison of those injuries because a frozen-thawed control was not included. A Belgium research group demonstrated

that freezing does not appear to have a major impact on human early follicular growth and expression of C-kit, KL, growth differentiation factor 9 (GDF-9). However, they cryopreserved the human ovarian tissue using 10% DMSO and slow freezing-thawing protocols [65,66]. In 2015, Jafarabadi et al. also demonstrated that ischemic injury seems to be more detrimental than cryoinjury by evaluating follicle normality, cell-death related gene expression, and TUNEL reaction. Even though we think the design of their study is reasonable for comparing those injuries directly, they could not evaluate the harmful effects of those two major injuries during the early phase of the ischemic periods [62]. In addition to these limitations of previous studies, xeno- or allo-transplantation models were used. Because xeno- and allo-transplantation rather than auto-transplantation may result in an immune response in the recipient mouse, we used the auto-transplantation model to reduce possible bias from donor-recipient immune responses, with a view on clinical application.

In the present study, we evaluated OT quality in fresh and vitrified-warmed ovaries with and without transplantation. After transplantation, we evaluated ovarian graft quality according to time at 2, 7, and 21 days after transplantation (Fig 1.1). A comparison among the fresh control, vitri-con, and FrOT-D2 groups showed which of the two, cryoinjury or ischemic injury, had more detrimental effects on ovarian morphology and function. Histologically, cryoinjury and ischemic injury caused severe destruction of

the follicles and stroma in OT after vitrification-warming and transplantation procedures compared with fresh ovaries. A significant reduction of the G1 follicle ratio in both vitri-con and FrOT-D2 was observed when compared with the fresh as well as the proportion of G1 follicle in FrOT-D2 was also significantly lower than that of vitri-con. The reduced G1 ratio in the FrOT-D2 group gradually improved with significance over time after transplantation, whereas no such significant improvement was noted in the VtOT groups. Actually, we could not correctly explain this difference between follicle grading and number because we did not further investigate the exact mechanism of those two injuries. However, we assumed that only post-transplantation ischemic injury seems to be reversible injury while the quality of follicle (G1) could not recovered from a combination of those two injuries. We thought that this difference probably derived from extent of tissue damage (cryoinjury + ischemic injury ≥ cryoinjury alone, Figure. 5A). With regard to the mean number of follicles in tissue, cryoinjury and/or ischemic injury might decrease the number of follicles (Figure. 5B). On the contrast to the G1, irreversible damaged in number was shown in even FrOT groups. Based on these results, we suggest that recovery of ovarian follicle after cryopreservation and/or transplantation may occur according to the extent of tissue damage and status through different mechanisms. These finding suggest that ischemic injury immediately after transplantation is more harmful than cryoinjury. In addition, the detrimental effect of ischemic injury can be

overcome with time after transplantation, but a combination of cryoinjury and ischemic injury significantly interferes with this recovery.

In the current study, the recovery of the G1 follicle ratio in the FrOT groups was consistent with the increase of the CD31-positive area in graft. Kizuka-Shibuya et al. reported that locally existing endothelial cells in the stroma play a central role in neovascularization during follicular growth [68]. In addition, Soleimani et al. demonstrated that the number of blood vessels positively correlated with the graft survival rate and the size of follicles in grafts [16]. In the VtOT groups, the CD31(+) area showed a statistically non-significant increasing tendency. This non-significant increase in vascularization may result in the non-significant improvement of follicle quality in the VtOT groups. In the VtOT groups, the combination of both injuries caused more harmful effects on OT and interfered with vascular recovery after transplantation. In contrast to the G1 ratio, the mean number of follicles following cryopreservation and transplantation did not increase in either the FrOT or VtOT groups. These and our other results also correspond with Soleimani's previous study. This means that re-vascularized CD31-positive cells play a crucial role in the restoration of ovarian follicle quality, not in the mean number of follicles after the cryopreservation/transplantation process.

In Skuli's previous study, they demonstrated that activated primordial follicles need 19-21 days to become pre-ovulatory follicles in murine model [50]. However, secondary follicle ratios both in FrOT-D2 and VtOT-D2 were

respectively significant different compared with the fresh and vitri-con as well as the proportion of antral follicle both in FrOT-D7 and VtOT-D7 recovered as fresh control. It means transplantation process may cause spontaneously massive activation and growth of residual primordial follicle in graft which already shown by previous reports [69-71]. Accordingly, such spontaneous follicular-activation seems to be derived from elimination of AMH-secreted follicle during avascular period after transplantation. In other words, removal of negative regulation may affect the dormant follicle growth and development [67,71,72]. Interestingly, both FrOT-D21 and VtOT-D21 increased the antral follicle ratio than before with significance. We suggest that excessive antral follicle would inhibit the massive follicle growth and development 21 days after transplantation and then estrous cycle in graft be returned as normal.

Following the vitrification and transplantation process, destruction of the stroma was also observed in both the vitri-con and FrOT-D2 groups, and the density of the stroma in the FrOT-D2 and VtOT-D2 groups appeared lower than that in the vitri-con group. Two days after transplantation, the accumulation of RBCs in the FrOT-D2 group was greater than that in the VtOT-D2 group. Stroma and follicles in grafts were severely damaged in both the FrOT-D2 and VtOT-D2 groups. As aforementioned, Soleimani et al. demonstrated that there is a substantial positive correlation between the mean blood vessel density and stromal cell density [16]. In addition, Wu et al.

suggested that the accumulation of those RBCs in the vessel and the ruptured endothelial cell junctions on day 2 indicate that severe damage occurred in the vascular system of the grafted tissue [73]. From this viewpoint, we suggest that damaged blood vessels in OT exacerbate the deterioration in OT quality following the cryopreservation and transplantation process.

Apoptosis of ovarian follicles from cryoinjury and ischemic injury has been reported, and numerous researchers have made efforts to minimize these injuries in various animal models [1,10,15,74,75]. However, only one report made a direct comparison of apoptosis in ovarian follicles between cryopreserved and xeno-transplanted human OT [62]. Similar to our G1 ratio, the percentage of apoptotic follicles in the FrOT-D2 group was much higher than that in the vitri-con group. According to Jafarabadi et al., the transplantation of human OT into gamma-irradiated mice surprisingly increased the number of TUNEL signals per 1,000 μm^2 compared with non-vitrified and vitrified human OT. Moreover, they reported no significant difference between transplanted fresh and vitrified-warmed OT [62]. Our results in the present study are also consistent with their study. Based on these findings, ovarian follicles and stroma were severely damaged by cryoinjury, and post-transplantation ischemia showed much more detrimental effects than cryoinjury.

The apoptotic follicle ratio and serum FSH level in both the FrOT and VtOT groups gradually recovered to the level of that in the non-transplanted control. Liu et al. also demonstrated that follicular apoptosis increased

remarkably in the early phase of the ischemic period, and it recovered to normal levels 4 days after grafting [63]. Moreover, the serum FSH level was the highest on day 2, and it gradually recovered with time. This trend also corresponded with our previous study [54]. Wu et al. reported that angiogenesis of the frozen-thawed rodent's OT begins within 48 h after transplantation, and it takes >7 days to complete this process [73]. Additionally, Kim et al. demonstrated that the messenger ribonucleic acid expression of angiotensin-2 and vascular endothelial growth factor-A 189 increased on day 2 [76]. The present study also showed an increase of angiogenesis with time after transplantation. These findings indicate that early phase neo-angiogenesis in grafts is responsible for improving ovarian quality via the reduction of apoptosis and restoration of ovarian function.

The present study showed that ischemic injury has more impact; therefore, reducing ischemic injury appears more important for enhancing transplanted OT. However, minimizing cryoinjury is also important. In our previous study, we tried to reduce cryoinjury during the vitrification-warming process using AFPs, and we also compared transplantation efficiency according to the presence or absence of AFPs in cryomedia [77]. The addition of high dose AFPs in vitrification and warming media decreased cryodamage during the vitrification-warming procedure, and it significantly improved the ovarian reserve and tissue quality compared with those of the control even after transplantation. Taking our previous and present findings together, we suggest

that minimizing cryoinjury promotes the restoration of OT quality after transplantation via enhancement of the recovery process.

Several limitations are present in the current study. We counted the number of ovarian follicles from one section per graft. However, bias from the uneven distribution of the follicles was minimized because we randomly divided the mice into each group, and we randomly selected the section from each ovary. We evaluated the deleterious impacts of cryoinjury and ischemic injury through vitrification and the auto-transplantation of mouse OT. Nonetheless, verifying the exact mechanisms of this impact was beyond the scope of this study, and this point remains a limitation of our research. In addition, the limitation posed by the difference between mouse and human OT in terms of structural and physiological characteristics such as follicle population present in biopsies and constitution of the OT must be considered in planning for further clinical studies.

In summary, the results of the present study indicated that inevitable post-transplantation ischemia seems to be more deleterious than cryoinjury, and cryoinjury during cryopreservation hinders the recovery process after transplantation by reducing vascularization. Additionally, angiogenesis in grafts after transplantation plays a crucial role in the reduction of apoptosis and the restoration of function. Therefore, minimizing cryoinjury and reducing ischemic injury by enhancing vascularization is needed to improve ovarian function after cryopreservation and transplantation.

In study 2, we set out to; we compared the cryoprotective efficiency of three types of recombinant AFPs in the vitrification of mouse OT. One of the main causes of cell death during cryopreservation seems to be IR [78]. IR takes place constantly in nature due to moderate cooling and temperature fluctuations of frozen substances. In cryopreservation, IR during the thawing process causes cell membrane ruptures and cell dehydration, underling lethal damage cell and tissue. It is believed that many freezing-tolerant organisms inhabiting cold environments have developed AFPs to ensure survival [79]. Since AFPs are effective at inhibiting IR, AFPs are beneficial for the cryopreservation of cells and tissues [80-83]. Based on previous studies, 1.0 mg/mL of AFPs was set as the initial dose, and doses that were 10 times lower and higher, respectively, (0.1 and 10 mg/mL) were also used [25]. At both 0.1 mg/mL and 1.0 mg/mL, there were no significant differences between the AFPs in terms of follicular preservation at each of the different developmental stages examined. However, 10 mg/mL of the AFPs provided cryoprotective effects in primordial follicle preservation, as compared with the vitrification control. This result indicates for the three types of AFPs 10 mg/mL was sufficient to prevent cryodamage derived from the vitrification and warming process.

In view of primordial follicle preservation, the lowest grade 1 ratio was marked in 1 mg/ml of LeIBP supplemented group. In fact, the reason why 1 mg/ml LeIBP decreased the percentage of primordial grade 1 follicle is

unclear because we did not investigate the exact mechanism of LeIBP on ovarian tissue vitrification. However, we are able to postulate some possible mechanisms based on other studies. Biphasic effects of antifreeze proteins were demonstrated by Wen and Laursen [84]. Moreover, other investigators already proved that various antifreeze proteins have different characteristics such as TH activity, ice-binding affinities, molecular weights and structural features [25,85,86]. We assumed that these differences and biphasic effects deriving from different types of antifreeze proteins may result in obscure data.

With respect to the apoptotic follicle ratio, the higher rate of TUNEL-positive follicles in 0.1 mg/ml of FfIBP and LeIBP were observed compared with that in fresh and vitrification-control. In demonstrating the function of 'type I antifreeze polypeptide (AFP type I)', and its double-sided character in ice-growth inhibition [87]. Wen and Laursen showed in 1992 that at low concentration, AFP molecules bind randomly and, presumably, reversibly to the surface; at high concentrations, intermolecular interactions occur and the surface becomes covered, either completely or in a patchwork pattern [88,89]. Based on these previous studies, we could suggest that the changeable actions (a somewhat presumably binding randomly and reversibly to the surface) of low dose AFPs could be the cause of high ratio of apoptotic follicles in the 0.1mg/ml FfIBP and LeIBP group. However, further study for the exact mechanisms of various AFPs is required.

Because high doses of three different AFPs reduced the percentage of

apoptotic follicles, we performed immunohistochemistry for τH2AX and Rad51 to detect DNA DBS and DDR, respectively, because τH2AX is expressed at the site of DNA DSB and Rad51 is localized at the repair proteins [90]. The percentage of τH2AX-labeled follicles was significantly decreased in the AFPs-treated groups compared with vitrification control. In addition, the percentage of Rad51-expressing follicles was also significantly lower in FfIBP-treated and LeIBP-treated OT than in the vitrification control OT. In 2005, Sak et al., demonstrated that there is a positive correlation between τH2AX and Rad51 expression as well as Paull et al., reported histone H2AX plays a critical role in recruitment of Rad51 to nuclear foci after DNA damage [91,92]. Our data are consistent with these previous studies. According to these results, we can assume that the more DNA DSB occurs, the more DNA DDR also activated and therefore cryodamage-induced Rad51 expression positively correlated with τH2AX expression. These findings indicate that the anti-apoptotic effects of AFPs during cryopreservation derived from prevention of DNA DSBs

In Experiment I, we used three AFPs with different properties. As shown in Table 1, FfIBP has the highest TH activity but the lowest IR inhibitory activity, while LeIBP has the lowest TH activity but the highest IR inhibitory activity. This comparison is consistent with the previous report by Yu et al [93], who demonstrated that there was no obvious correlation between high TH activity and high IR inhibitory activity. In their IR inhibition experiment,

moderately active type III AFP has higher (or comparable) IR inhibitory activity than hyperactive AFPs do. However, it is still unclear how AFPs inhibit IR and why hyperactive AFPs do not show high IR inhibitory activity or vice versa. Our observation clearly showed that all AFPs are effective for cryopreserving OT and that the AFP with the highest IR inhibitory activity is the most beneficial. Lee et al. demonstrated that the ice-binding site in LeIBP is different from that in other AFPs and IBPs [86]. Although LeIBP has a conserved β-helical fold similar to that in canonical hyperactive AFPs, the ice-binding site is more complex and does not have a simple ice-binding motif.

In Experiment 2, we analyzed the efficacy of 10 mg/mL LeIBP 7 days after transplantation, because reperfusion ischemia and hypoxia play a major role in follicle depletion in the first days after transplantation and for about a week afterward [9,14,94,95]. There were statistically significant improvements with regard to the percentage of G1 follicles, the percentage of apoptotic follicles, the serum FSH levels in recipient mice, and in the extent of the CD31-positive areas in each of the ovaries in the LeIBP-treated group as compared with the vitrification control group. Shikanov et al. described FSH concentration ranges in normal, ovariectomized, and transplant-recipient mice. Normal FSH levels ranged from 2 to 10 ng/mL, 0 to 50 ng/mL in the absence of ovaries, and then started to decrease rapidly 7 days post-transplantation due to restored hormonal cyclicity [96]. Previous studies have suggested elevation of FSH indicates the reduction of ovarian reserve in the graft [97]. In our study, the

serum FSH level was lower in mice transplanted with the LeIBP-treated OT than in mice transplanted with the vitrification control OT, but remained within the normal range in both groups. Based on these results, we conclude that supplementation of LeIBP (10 mg/mL) during vitrification/warming procedures not only prevents cryoinjury to the grafts, but also provides beneficial effects to the ovarian function even after transplantation.

When Bagis et al. generated transgenic mice carrying a type III fish AFP gene, testicular and OT in the F3 generation were protected from damage during hypothermic storage [13]. In addition, Bagis et al. evaluated the cryogenic effect of AFP type III on vitrified transgenic mouse OT and the production of live offspring by orthotopic transplantation of cryopreserved mouse ovaries [20]. Their results indicated that the application of AFPs for cryobiology for mammalian reproductive cells and tissues seems to be safe and stable, as they also showed that AFP genes were stably transcribed and expressed even in the seventh generation of transgenic mice [80]. Nonetheless, even though Bagis et al. provided a useful transgenic mouse model for investigating the biological functions of AFP in mammalian systems, more investigation are required to assess the function of AFPs. In the present study, we observed the restoration of function (hormonal assay), and used immunohistochemical and other analyses to verify the cryoprotective effects of three different AFPs.

This study contains some limitations. We did not investigate the exact

mechanism of beneficial effects deriving from AFPs during vitrification-warming in the transplantation process. Moreover, we also did not evaluate the impact of AFPs on oocyte quality and embryonic development. There was also no slow freezing control in this study.

In study 3, after transplantation, ovarian revascularization occurs and numerous ovarian follicles are lost during the ischemic period [98,99]. Therefore, reducing the ischemic damage during OT transplantation is crucial for its success. To date, multifarious studies have reported successful shortening of the ischemic period and improvement of ovarian function after OT transplantation with selective transplantation sites [100], administration of anti-oxidants [19,76], hormonal factors [101], angiogenic factors [18,102], and other factors [103]. Despite a lot of research efforts in this direction, further optimization studies are required for improve tissue grafting.

Based on the results of previous studies, we attempted to reduce the ischemic injury after transplantation through administration of simvastatin and/or methylprednisolone in order to preserve ovarian functions and fertility in mice. Although we did not quantify the blood vessels surrounding the kidney capsules precisely, gross observation revealed that there were more the blood vessels in the S+M group than in the sham control group (Figure 3.3). These results were consistent with the quantitative results of CD31-positive areas in the OT 7 and 21 days after transplantation (Figure 3.6 B and C). Because CD31-positive areas indicate re-vascularized blood vessels in grafts, it was

crucially significant in terms of reduction of the ischemia period. Several studies have demonstrated that simvastatin promotes angiogenesis, microvascular remodeling and VEGF expression [104-106]. Moreover, Tuuminen et al. demonstrated that a high dose (15 mg/kg) of methylprednisolone significantly reduces the inflammatory response and donor methylprednisolone treatment may directly contribute to cardioprotection via up-regulation of endothelin-1 and VEGF [35].

It has also been suggested that minimizing the microvascular injury and activation of innate immunity may prevent IRI and positively affect the survival rate of rat cardiac allografts [35]. In the present study, combined treatment with simvastatin and methylprednisolone synergistically improved blood vessel formation after transplantation. IRI may occur during the time period required for revascularization of the transplanted tissue [107], which consequently leads to cytokine and free radical release, platelet activation, and apoptosis, causing massive primordial follicle loss and shortening of the lifespan of the transplanted ovary [108].

In the present study, the proportion of primordial grade 1 follicles on day 2 in the S+M group was significantly higher than that in the sham control group. Synergistic effects of simvastatin and methylprednisolone diminished ischemic injury during the vascular period through promotion of neo-angiogenesis, resulting in improvement of the quality of primordial and total follicles (Table 2). After 7 days, the proportion of primary grade 1 follicles in

the S+M group increased significantly compared with that in the sham control group (Table 3). Better preserved primordial follicles were detected on day 2, and better preserved primary follicles were detected on day 7 after transplantation. Improvement in the ratio of primary grade 1 follicle was shifted to the secondary and antral follicle grade 1 ratios on day 21 after transplantation (Table 4). This trend suggests the presence of swift revascularization that created a trophic environment for folliculogenesis through reduction of ischemic injury in the S+M group.

CD45 is known as a leukocyte common antigen, and it is also expressed on activated T cells, on a subset of dendritic cells, and other antigen-presenting cells, besides the B cells. De Vito et al. postulated that the inflammatory infiltrate can be characterized by immunuohistochemical analysis of CD45, CD3, and CD163 as markers of leukocytes, T cells, and activated Kupffer cells/macrophages, respectively [109]. Accordingly, we investigated the CD45-positive population in transplanted OT to determine the anti-inflammatory effects of methylprednisolone. However, no significant differences were noted in the population of infiltrated CD45-positive cells (Figure 3.7A). Moriyama et al. demonstrated that lymphocyte infiltration causes more proliferative changes in fresh allografts than in fresh auto-grafts [110]. Moreover, Solanes et al. demonstrated that the population of CD3-positive cells, LC1-positive cells, and polymorphonuclear granulocytes (per mm^2 area) of the intimal and medial layers decreased in auto-grafts [111]. Based on the results of these studies, the

discrepancy with regard to the significance of infiltrating cells between the present study and a previous study [112] is believed to be related to the difference in the grafting technique used (autograft versus allograft).

In the present study, we measured serum AMH levels in the OT transplanted mice because AMH is expressed and secreted by granulosa cells of growing follicles [113,114]. Serum AMH has been demonstrated by many researchers as a reliable indicator of ovarian reserve since its levels are not affected by the estrous cycle in mouse and human [115]. In the present study, the serum AMH level was significantly higher in the S+M group on day 7 than in the other three groups (Figure 3.7B), indicating a higher ovarian reserve. In light of these results, we propose that the AMH-secreting growing follicles were significantly increased in the S+M group compared with the other three groups, indicating that S+M treatment has beneficial effects on restoration of vitrified-transplanted ovarian function 7 days after transplantation.

In the present study, we obtained meiotic-competent oocytes from transplanted ovaries, and the eggs were fertilized *in vitro*. After IVF, no significant differences in the embryonic development were noted among the four groups. After 21 days of transplantation, the appearance of grafted OTs was almost and the grafts seemed to be more stable at 21 than at 2 or 7 days after transplantation. The hormonal dosage for superovulation in the present study was too high to allow comparisons with ovarian functions in the natural cycles, therefore, it is difficult to compare transplanted tissue quality on the

basis of embryonic developmental criteria. In the present study, the purpose of COH was to evaluate whether or not the treatment has any harmful effects on the quality of oocytes and embryo. According to the COH outcome, preoperative simvastatin and/or methylprednisolone treatment does not have any harmful effects on the competency of oocyte and embryonic development.

In the present study we did not consider the stage of the estrous cycle because of our original experimental design and to avoid having too many study groups. However, the mice were randomly assigned to each group, thus a possible bias originating from any differences according to the estrous cycle will have been minimized. In addition, we counted follicle number in only one section of each ovary and this could introduce bias because the ovarian follicle population is not evenly distributed in the ovary even in one ovary. However, this possible bias also could be minimized because we randomly assigned mice to each experimental group.

In conclusion, in mice the combined treatment with simvastatin and methylprednisolone prior to ovariectomy can prevent ovarian follicle damage and restore ovarian function promptly through the rapid construction of blood vessels of the ovary. However, further studies are necessary to identify the mechanisms involved in minimizing ischemic injury in the ovaries of other domestic animals and humans.

In final study, due to the risk which is re-implantation of malignancy cells after transplantation of ovarian tissue, *in vitro* follicle culture has been studied

to provide as an alternative instead of ovarian tissue cryopreservation and transplantation for fertility preservation in female cancer patients [48]. Even though several studies have tried to establish the *in vitro* follicle culture system, only mouse model was achieved success to delivery live birth. To date, most of follicle culture literatures have applied the conventional culture including oil layer, without oil layer for individual follicle culture and other methods for multiple follicle culture. Moreover, three-dimensional culture using extracellular matrix (ECM) has been also adopted to mimic three-dimensional structures for follicle growth and maturation. In 2006, Xu and his colleagues reported 3D-culture based folliculogenesis, embryonic development and live birth in mice [41]. Despite these efforts, lots of hurdles are still remains to overcome the maturational and developmental errors in follicle culture system, especially conventional culture.

In the present study, we applied two different conventional follicle culture systems for individual follicle culture to improve the efficiency of conventional culture method. Although there are different conventional culture systems for multiple follicle culture, we did not use it because multiple follicle culture could not trace growth maturation of follicle, individually. In addition, we could not also accurately measure the follicle diameter and rule out the paracrine effects from multiple follicle culture system. Therefore, we tried to compare only two different conventional culture methods for individual culture in this study.

With respect to the follicle growth, development, oocyte maturation and even in somatic cell proliferation and function, oil layer method for individual culture seems to be superior to those of without oil layer method. In fact, there were three minor different between oil layer and without oil layer culture methods. First, the presence or absence of oil layer on the culture medium. We assumed that oil layer prevent severe pH change and osmolality during handling and culture period. It can positively affect the follicular growth, maturation and oocyte nucleic maturation. Eggs are well-known to be very sensitive to external changes such as pH, osmolality, temperature and others [81,101,116-119]. Second, the volume of culture medium in oil layer (20 μL) is smaller than that of without oil layer (75 μL). We thought that smaller volume of culture medium for single follicle culture is much more favorable environment in terms of autocrine effect. Ovarian follicle and oocyte shows autocrine effect during folliculogenesis and oocyte development, respectively. Secretomes by autocrine manner may exist in higher concentration in smaller volume of medium compared with larger volume. It may also influence on the development of follicles and oocytes. Finally, the volume of replenishment medium was also different between oil layer and without oil layer. Fifty percent of culture medium in oil layer (10 μL) was exchanged every other day while forty percent of culture medium in without oil layer (40 μL) was refreshed every four days according to the previous studies [38,39]. We suggest that these three minor differences showed a significant difference in the

present study.

As mentioned above, embryonic development and healthy live birth has been reported using mouse model. However, a Japanese research group showed that impairment of developmental competence in oocytes which were *in vitro* grown and matured of same strain mice (BDF-1) we used [120]. Their result was consistent with our present study (Table 7). They overcome the impaired developmental competence via nuclear transfer and IVF. Finally, they concluded that an *in vitro* follicle culture and denudation of cumulus cells caused zona hardening and critical cytoplasmic deficiency. Therefore, we attempted to find out the reason for embryonic development damage.

We separately analyzed the nucleic and cytoplasmic status to determine the cause of developmental failure. In terms of cytoplasmic deficiency, we firstly checked distribution of GCs in oocyte according to the Mainigi's previous report [58]. Oocytes from *in vitro* culture showed abnormal CG distribution and with clumping CGs compared with *in vivo* derived oocytes. It was consistent with our data. CG plays a role in inducing the zona pellucida block to poly spermy. Based on this finding, CG biogenesis and localization would be impaired from *in vitro* derived oocytes. On the other hand, we did not recognize the significant difference among three groups with respect to the distribution of actin filament and spindle organization.

Next, we also investigated the physiological alteration including ROS production and mitochondrial expression in these oocytes. In both *in vitro*

derived oocytes, ROS production was significantly higher than *in vivo* oocytes while expression of mitochondrial activity significantly decreased compared with that of *in vivo* control. We suggest that massive production of ROS may cause decrease of mitochondrial activity and it may negatively influence on pre-implantation embryonic development. According to the previous study, mitochondrial activity is correlated with two-cell block and the use of mitochondrial nutrients such as co-enzyme Q10 could improve the outcome of infertility treatment in older patients [121,122].

According to the previous studies, cytoplasmic replacement following nuclear transfer could overcome impairment of developmental failure and restores meiotic maturation and spindle assembly [120,123]. It means that the nucleus of egg is thought to possess enough potential for maturation and embryonic development. Our results also showed nucleic normality and gene-expression in both *in vitro* derived oocytes. Taken together, the impairment of developmental ability in oocyte which is derived from *in vitro milieu* may be caused by cytoplasmic deficiency.

The present study has several limitations. We just compared two culture methods only for conventional culture conditions and we did not overcome the developmental failure. The most important thing to consider for clinical application is species-specific difference between mouse and human. Finally, a further study for the exact mechanisms and optimization of culture condition to improve the efficiency of follicle culture and embryonic development

would be needed.

Collectively, we compared the efficiency of different conventional follicle culture systems using mouse model and demonstrated the cytoplasmic deficiency of an *in vitro* derived oocyte. In the near future, an *in vitro* follicle culture would provide the valuable alternative instead of ovarian tissue transplantation for fertility preservation in human.

REFERENCES

1 Dath, C. *et al.* Endothelial cells are essential for ovarian stromal tissue restructuring after xenotransplantation of isolated ovarian stromal cells. *Human reproduction* **26**, 1431-1439, doi:10.1093/humrep/der073 (2011).

2 Demeestere, I. *et al.* Ovarian function and spontaneous pregnancy after combined heterotopic and orthotopic cryopreserved ovarian tissue transplantation in a patient previously treated with bone marrow transplantation: case report. *Human reproduction* **21**, 2010-2014, doi:10.1093/humrep/del092 (2006).

3 Hovatta, O. Methods for cryopreservation of human ovarian tissue. *Reproductive biomedicine online* **10**, 729-734 (2005).

4 Oktay, K. & Sonmezer, M. Ovarian tissue banking for cancer patients: fertility preservation, not just ovarian cryopreservation. *Human reproduction* **19**, 477-480, doi:10.1093/humrep/deh152 (2004).

5 Donnez, J. & Dolmans, M. M. Transplantation of ovarian tissue. *Best practice & research. Clinical obstetrics & gynaecology* **28**, 1188-1197, doi:10.1016/j.bpobgyn.2014.09.003 (2014).

6 Keros, V. *et al.* Vitrification versus controlled-rate freezing in cryopreservation of human ovarian tissue. *Human reproduction* **24**, 1670-1683, doi:10.1093/humrep/dep079 (2009).

7 Kim, G. A. *et al.* Effectiveness of slow freezing and vitrification for long-term preservation of mouse ovarian tissue. *Theriogenology* **75**, 1045-1051, doi:10.1016/j.theriogenology.2010.11.012 (2011).

8 Rahimi, G. *et al.* Apoptosis in human ovarian tissue after conventional freezing or vitrification and xenotransplantation. *Cryo letters* **30**, 300-309 (2009).

9 Arav, A. & Natan, D. Directional freezing of reproductive cells and organs. *Reproduction in domestic animals = Zuchthygiene* **47 Suppl 4**, 193-196, doi:10.1111/j.1439-0531.2012.02075.x (2012).

10 Youm, H. W. *et al.* Optimal vitrification protocol for mouse ovarian tissue cryopreservation: effect of cryoprotective agents and in vitro culture on vitrified-warmed ovarian tissue survival. *Human reproduction* **29**, 720-730, doi:10.1093/humrep/det449 (2014).

11 Bos-Mikich, A. Marques, L. Rodrigues, J., L. Lothhammer & N.

Frantz, N. The use of a metal container for vitrification of mouse ovaries, as a clinical grade model for human ovarian tissue cryopreservation, after different times and temperatures of transport. *Journal of assisted reproduction and genetics* **29**, 1267-1271, doi:10.1007/s10815-012-9867-y (2012).

12 Lee, J. R. *et al.* Effect of antifreeze protein on mouse ovarian tissue cryopreservation and transplantation. *Yonsei medical journal* **56**, 778-784, doi:10.3349/ymj.2015.56.3.778 (2015).

13 Bagis, H. *et al.* Stable transmission and transcription of newfoundland ocean pout type III fish antifreeze protein (AFP) gene in transgenic mice and hypothermic storage of transgenic ovary and testis. *Molecular reproduction and development* **73**, 1404-1411, doi:10.1002/mrd.20601 (2006).

14 Newton, H., Aubard, Y., Rutherford, A., Sharma, V. & Gosden, R. Low temperature storage and grafting of human ovarian tissue. *Human reproduction* **11**, 1487-1491 (1996).

15 Abir, R. *et al.* Improving posttransplantation survival of human ovarian tissue by treating the host and graft. *Fertility and sterility* **95**, 1205-1210, doi:10.1016/j.fertnstert.2010.07.1082 (2011).

16 Soleimani, R., Heytens, E. & Oktay, K. Enhancement of neoangiogenesis and follicle survival by sphingosine-1-phosphate in human ovarian tissue xenotransplants. *PloS one* **6**, e19475, doi:10.1371/journal.pone.0019475 (2011).

17 Wang, Y. *et al.* Effects of HMG on revascularization and follicular survival in heterotopic autotransplants of mouse ovarian tissue. *Reproductive biomedicine online* **24**, 646-653, doi:10.1016/j.rbmo.2012.02.025 (2012).

18 Wang, L., Ying, Y. F., Ouyang, Y. L., Wang, J. F. & Xu, J. VEGF and bFGF increase survival of xenografted human ovarian tissue in an experimental rabbit model. *Journal of assisted reproduction and genetics* **30**, 1301-1311, doi:10.1007/s10815-013-0043-9 (2013).

19 Nugent, D., Newton, H., Gallivan, L. & Gosden, R. G. Protective effect of vitamin E on ischaemia-reperfusion injury in ovarian grafts. *Journal of reproduction and fertility* **114**, 341-346 (1998).

20 Bagis, H., Akkoc, T., Tass, A. & Aktoprakligil, D. Cryogenic effect of antifreeze protein on transgenic mouse ovaries and the production of live offspring by orthotopic transplantation of cryopreserved mouse ovaries. *Molecular reproduction and development* **75**, 608-613, doi:10.1002/mrd.20799 (2008).

21 Hemadi, M. *et al.* Melatonin promotes the cumulus-oocyte

complexes quality of vitrified-thawed murine ovaries; with increased mean number of follicles survival and ovary size following heterotopic transplantation. *European journal of pharmacology* **618**, 84-90, doi:10.1016/j.ejphar.2009.07.018 (2009).

22 Leinala, E. K. *et al.* . *The Journal of biological chemistry* **277**, 33349-33352, doi:10.1074/jbc.M205575200 (2002).

23 DeVries, A. L. & Wohlschlag, D. E. Freezing resistance in some Antarctic fishes. *Science (New York, N.Y.)* **163**, 1073-1075 (1969).

24 Yeh, Y. & Feeney, R. E. Antifreeze Proteins: Structures and Mechanisms of Function. *Chem Rev* **96**, 601-618 (1996).

25 Lee, S. G., Koh, H. Y., Lee, J. H., Kang, S. H. & Kim, H. J. Cryopreservative effects of the recombinant ice-binding protein from the arctic yeast Leucosporidium sp. on red blood cells. *Applied biochemistry and biotechnology* **167**, 824-834, doi:10.1007/s12010-012-9739-z (2012).

26 Garnham, C. P. *et al.* A Ca2+ -dependent bacterial antifreeze protein domain has a novel beta-helical ice-binding fold. *The Biochemical journal* **411**, 171-180, doi:10.1042/bj20071372 (2008).

27 Raymond, J. A., Christner, B. C. & Schuster, S. C. A bacterial ice-binding protein from the Vostok ice core. *Extremophiles : life under extreme conditions* **12**, 713-717, doi:10.1007/s00792-008-0178-2 (2008).

28 Fletcher, G. L., Hew, C. L. & Davies, P. L. Antifreeze proteins of teleost fishes. *Annual review of physiology* **63**, 359-390, doi:10.1146/annurev.physiol.63.1.359 (2001).

29 Kristiansen, E. *et al.* Hyperactive antifreeze proteins from longhorn beetles: some structural insights. *Journal of insect physiology* **58**, 1502-1510, doi:10.1016/j.jinsphys.2012.09.004 (2012).

30 Middleton, A. J. *et al.* Antifreeze protein from freeze-tolerant grass has a beta-roll fold with an irregularly structured ice-binding site. *Journal of molecular biology* **416**, 713-724, doi:10.1016/j.jmb.2012.01.032 (2012).

31 Kim, S. S., Battaglia, D. E. & Soules, M. R. The future of human ovarian cryopreservation and transplantation: fertility and beyond. *Fertility and sterility* **75**, 1049-1056 (2001).

32 Lefer, A. M. *et al.* Simvastatin preserves the ischemic-reperfused myocardium in normocholesterolemic rat hearts. *Circulation* **100**, 178-184 (1999).

33 Wolfrum, S. *et al.* Simvastatin acutely reduces myocardial reperfusion injury in vivo by activating the phosphatidylinositide 3-kinase/Akt pathway. *Journal of cardiovascular pharmacology* **44**, 348-355 (2004).

34 Tuuminen, R. *et al.* Donor simvastatin treatment abolishes rat cardiac allograft ischemia/reperfusion injury and chronic rejection through microvascular protection. *Circulation* **124**, 1138-1150, doi:10.1161/circulationaha.110.005249 (2011).

35 Tuuminen, R. S., S. Krebs, R. Arnaudova, R. Rouvinen, E. Nykanen, A. I. Lemstrom, K. B. Combined donor simvastatin and methylprednisolone treatment prevents ischemia-reperfusion injury in rat cardiac allografts through vasculoprotection and immunomodulation. *Transplantation* **95**, 1084-1091, doi:10.1097/TP.0b013e3182881b61 (2013).

36 Sloka, J. S. & Stefanelli, M. The mechanism of action of methylprednisolone in the treatment of multiple sclerosis. *Multiple sclerosis (Houndmills, Basingstoke, England)* **11**, 425-432 (2005).

37 Eppig, J. J. & Schroeder, A. C. Capacity of mouse oocytes from preantral follicles to undergo embryogenesis and development to live young after growth, maturation, and fertilization in vitro. *Biology of reproduction* **41**, 268-276 (1989).

38 Tarumi, W., Itoh, M. T. & Suzuki, N. Effects of 5alpha-dihydrotestosterone and 17beta-estradiol on the mouse ovarian follicle development and oocyte maturation. *PloS one* **9**, e99423, doi:10.1371/journal.pone.0099423 (2014).

39 Cortvrindt, R., Smitz, J. & Van Steirteghem, A. C. In-vitro maturation, fertilization and embryo development of immature oocytes from early preantral follicles from prepuberal mice in a simplified culture system. *Human reproduction* **11**, 2656-2666 (1996).

40 Cortvrindt, R., Smitz, J. & Van Steirteghem, A. C. A morphological and functional study of the effect of slow freezing followed by complete in-vitro maturation of primary mouse ovarian follicles. *Human reproduction* **11**, 2648-2655 (1996).

41 Xu, M., Kreeger, P. K., Shea, L. D. & Woodruff, T. K. Tissue-engineered follicles produce live, fertile offspring. *Tissue engineering* **12**, 2739-2746, doi:10.1089/ten.2006.12.2739 (2006).

42 Desai, N. *et al.* Mouse ovarian follicle cryopreservation using vitrification or slow programmed cooling: assessment of in vitro

development, maturation, ultra-structure and meiotic spindle organization. *The journal of obstetrics and gynaecology research* **37**, 1-12, doi:10.1111/j.1447-0756.2010.01215.x (2011).

43 Nagano, M. *et al.* Effects of isolation method and pre-treatment with ethylene glycol or raffinose before vitrification on in vitro viability of mouse preantral follicles. *Biomedical research (Tokyo, Japan)* **28**, 153-160 (2007).

44 Trapphoff, T., El Hajj, N., Zechner, U., Haaf, T. & Eichenlaub-Ritter, U. DNA integrity, growth pattern, spindle formation, chromosomal constitution and imprinting patterns of mouse oocytes from vitrified pre-antral follicles. *Human reproduction* **25**, 3025-3042, doi:10.1093/humrep/deq278 (2010).

45 Xing, W. *et al.* Solid-surface vitrification is an appropriate and convenient method for cryopreservation of isolated rat follicles. *Reproductive biology and endocrinology : RB&E* **8**, 42, doi:10.1186/1477-7827-8-42 (2010).

46 Bao, R. M. *et al.* Development of vitrified bovine secondary and primordial follicles in xenografts. *Theriogenology* **74**, 817-827, doi:10.1016/j.theriogenology.2010.04.006 (2010).

47 Barrett, S. L., Shea, L. D. & Woodruff, T. K. Noninvasive index of cryorecovery and growth potential for human follicles in vitro. *Biology of reproduction* **82**, 1180-1189, doi:10.1095/biolreprod.109.082933 (2010).

48 Vanacker, J. *et al.* Should we isolate human preantral follicles before or after cryopreservation of ovarian tissue? *Fertility and sterility* **99**, 1363-1368.e1362, doi:10.1016/j.fertnstert.2012.12.016 (2013).

49 Pedersen, T. Follicle kinetics in the ovary of the cyclic mouse. *Acta endocrinologica* **64**, 304-323 (1970).

50 Skuli, N. *et al.* Endothelial HIF-2alpha regulates murine pathological angiogenesis and revascularization processes. *The Journal of clinical investigation* **122**, 1427-1443, doi:10.1172/jci57322 (2012).

51 Youm, H. W. *et al.* Transplantation of mouse ovarian tissue: comparison of the transplantation sites. *Theriogenology* **83**, 854-861, doi:10.1016/j.theriogenology.2014.11.026 (2015).

52 Lundy, T., Smith, P., O'Connell, A., Hudson, N. L. & McNatty, K. P. Populations of granulosa cells in small follicles of the sheep ovary. *Journal of reproduction and fertility* **115**, 251-262 (1999).

53 Gandolfi, F. *et al.* Efficiency of equilibrium cooling and vitrification procedures for the cryopreservation of ovarian

tissue: comparative analysis between human and animal models. *Fertility and sterility* **85 Suppl 1**, 1150-1156, doi:10.1016/j.fertnstert.2005.08.062 (2006).

54 Lee, J., Lee, J. R., Youm, H. W., Suh, C. S. & Kim, S. H. Effect of preoperative simvastatin treatment on transplantation of cryopreserved-warmed mouse ovarian tissue quality. *Theriogenology* **83**, 285-293, doi:10.1016/j.theriogenology.2014.09.027 (2015).

55 Huang, Y. *et al.* Role for caspase-mediated cleavage of Rad51 in induction of apoptosis by DNA damage. *Molecular and cellular biology* **19**, 2986-2997 (1999).

56 Brown, E. T. & Holt, J. T. Rad51 overexpression rescues radiation resistance in BRCA2-defective cancer cells. *Molecular carcinogenesis* **48**, 105-109, doi:10.1002/mc.20463 (2009).

57 Jo, J. W., Jee, B. C., Lee, J. R. & Suh, C. S. Effect of antifreeze protein supplementation in vitrification medium on mouse oocyte developmental competence. *Fertility and sterility* **96**, 1239-1245, doi:10.1016/j.fertnstert.2011.08.023 (2011).

58 Mainigi, M. A., Ord, T. & Schultz, R. M. Meiotic and developmental competence in mice are compromised following follicle development in vitro using an alginate-based culture system. *Biology of reproduction* **85**, 269-276, doi:10.1095/biolreprod.111.091124 (2011).

59 Lee, J., Kim, J., Kim, S. H., Kang, H. G. & Jun, J. H. Effects of Coculture With Immune Cells on the Developmental Competence of Mouse Preimplantation Embryos in Vitro and in Utero. *Reproductive sciences* **22**, 1252-1261, doi:10.1177/1933719115574342 (2015).

60 Dittrich, R. & Maltaris, T. A simple freezing protocol for the use of an open freezing system for cryopreservation of ovarian tissue. *Cryobiology* **52**, 166, doi:10.1016/j.cryobiol.2005.11.005 (2006).

61 Suzuki, N. *et al.* Successful fertility preservation following ovarian tissue vitrification in patients with primary ovarian insufficiency. *Human reproduction* **30**, 608-615, doi:10.1093/humrep/deu353 (2015).

62 Jafarabadi, M., Abdollahi, M. & Salehnia, M. Assessment of vitrification outcome by xenotransplantation of ovarian cortex pieces in gamma-irradiated mice: morphological and molecular analyses of apoptosis. *Journal of assisted reproduction and genetics* **32**, 195-205, doi:10.1007/s10815-014-0382-1 (2015).

63 Liu, J., Van der Elst, J., Van den Broecke, R. & Dhont, M. Early

massive follicle loss and apoptosis in heterotopically grafted newborn mouse ovaries. *Human reproduction* **17**, 605-611 (2002).

64 Nisolle, M., Casanas-Roux, F., Qu, J., Motta, P. & Donnez, J. Histologic and ultrastructural evaluation of fresh and frozen-thawed human ovarian xenografts in nude mice. *Fertility and sterility* **74**, 122-129 (2000).

65 Amorim, C. A. *et al.* Impact of freezing and thawing of human ovarian tissue on follicular growth after long-term xenotransplantation. *Journal of assisted reproduction and genetics* **28**, 1157-1165, doi:10.1007/s10815-011-9672-z (2011).

66 David, A., Dolmans, M. M., Van Langendonckt, A., Donnez, J. & Amorim, C. A. Immunohistochemical localization of growth factors after cryopreservation and 3 weeks' xenotransplantation of human ovarian tissue. *Fertility and sterility* **95**, 1241-1246, doi:10.1016/j.fertnstert.2010.06.007 (2011).

67 David, A. *et al.* Effect of cryopreservation and transplantation on the expression of kit ligand and anti-Mullerian hormone in human ovarian tissue. *Human reproduction* **27**, 1088-1095, doi:10.1093/humrep/des013 (2012).

68 Kizuka-Shibuya, F. *et al.* Locally existing endothelial cells and pericytes in ovarian stroma, but not bone marrow-derived vascular progenitor cells, play a central role in neovascularization during follicular development in mice. *Journal of Ovarian Research* **7**, 10 (2014).

69 Gavish, Z., Peer, G., Hadassa, R., Yoram, C. & Meirow, D. Follicle activation and 'burn-out' contribute to post-transplantation follicle loss in ovarian tissue grafts: the effect of graft thickness. *Human reproduction*, doi:10.1093/humrep/deu015 (2014).

70 Smitz, J. *et al.* Current achievements and future research directions in ovarian tissue culture, in vitro follicle development and transplantation: implications for fertility preservation. *Human reproduction update* **16**, 395-414, doi:10.1093/humupd/dmp056 (2010).

71 Dolmans, M. M. *et al.* Short-term transplantation of isolated human ovarian follicles and cortical tissue into nude mice. *Reproduction (Cambridge, England)* **134**, 253-262, doi:10.1530/rep-07-0131 (2007).

72 Kalich-Philosoph, L. *et al.* Cyclophosphamide triggers follicle activation and "burnout"; AS101 prevents follicle loss and

preserves fertility. *Science translational medicine* **5**, 185ra162, doi:10.1126/scitranslmed.3005402 (2013).

73 Wu, D. *et al.* Angiogenesis of the frozen-thawed human fetal ovarian tissue at the early stage after xenotransplantation and the positive effect of Salviae miltiorrhizae. *Anatomical record* **293**, 2154-2162, doi:10.1002/ar.21228 (2010).

74 Chang, H. J. *et al.* Optimal condition of vitrification method for cryopreservation of human ovarian cortical tissues. *Journal of Obstetrics and Gynaecology Research* **37**, 1092-1101, doi:10.1111/j.1447-0756.2010.01496.x (2011).

75 Liu, L. *et al.* Restoration of fertility by orthotopic transplantation of frozen adult mouse ovaries. *Human reproduction* **23**, 122-128, doi:10.1093/humrep/dem348 (2008).

76 Kim, S. S. *et al.* Quantitative assessment of ischemic tissue damage in ovarian cortical tissue with or without antioxidant (ascorbic acid) treatment. *Fertility and sterility* **82**, 679-685, doi:10.1016/j.fertnstert.2004.05.022 (2004).

77 Lee, J. *et al.* Effects of three different types of antifreeze proteins on mouse ovarian tissue cryopreservation and transplantation. *PloS one* **10**, e0126252, doi:10.1371/journal.pone.0126252 (2015).

78 Gage AA, B. J. Mechanisms of Tissue Injury in Cryosurgery. *Cryobiology* **37**, 171-186 (1998).

79 Knight, C. A., Hallett, J. & DeVries, A. L. Solute effects on ice recrystallization: an assessment technique. *Cryobiology* **25**, 55-60 (1988).

80 Bagis, H., Tas, A. & Kankavi, O. Determination of the expression of fish antifreeze protein (AFP) in 7th generation transgenic mice tissues and serum. *Journal of experimental zoology. Part A, Ecological genetics and physiology* **309**, 255-261, doi:10.1002/jez.455 (2008).

81 Jo, J. W., Jee, B. C., Suh, C. S. & Kim, S. H. The beneficial effects of antifreeze proteins in the vitrification of immature mouse oocytes. *PloS one* **7**, e37043, doi:10.1371/journal.pone.0037043 (2012).

82 Kamijima, T., Sakashita, M., Miura, A., Nishimiya, Y. & Tsuda, S. Antifreeze protein prolongs the life-time of insulinoma cells during hypothermic preservation. *PloS one* **8**, e73643, doi:10.1371/journal.pone.0073643 (2013).

83 Rubinsky, L. *et al.* Antifreeze protein suppresses spontaneous neural activity and protects neurons from hypothermia/re-warming injury. *Neuroscience research* **67**, 256-259,

doi:10.1016/j.neures.2010.04.004 (2010).
84 Wen, D. & Laursen, R. A. Structure-function relationships in an antifreeze polypeptide. The role of neutral, polar amino acids. *The Journal of biological chemistry* **267**, 14102-14108 (1992).
85 Do, H., Lee, J. H., Lee, S. G. & Kim, H. J. Crystallization and preliminary X-ray crystallographic analysis of an ice-binding protein (FfIBP) from Flavobacterium frigoris PS1. *Acta crystallographica. Section F, Structural biology and crystallization communications* **68**, 806-809, doi:10.1107/s1744309112020465 (2012).
86 Lee, J. H. *et al.* Structural basis for antifreeze activity of ice-binding protein from arctic yeast. *The Journal of biological chemistry* **287**, 11460-11468, doi:10.1074/jbc.M111.331835 (2012).
87 Wen, D. & Laursen, R. A. A model for binding of an antifreeze polypeptide to ice. *Biophysical journal* **63**, 1659-1662, doi:10.1016/s0006-3495(92)81750-2 (1992).
88 DeLuca, C. I., Comley, R. & Davies, P. L. Antifreeze proteins bind independently to ice. *Biophysical journal* **74**, 1502-1508, doi:10.1016/s0006-3495(98)77862-2 (1998).
89 Salvay, A. G. *et al.* Structure and interactions of fish type III antifreeze protein in solution. *Biophysical journal* **99**, 609-618, doi:10.1016/j.bpj.2010.04.030 (2010).
90 Kryeziu, K. *et al.* Synergistic anticancer activity of arsenic trioxide with erlotinib is based on inhibition of EGFR-mediated DNA double-strand break repair. *Molecular cancer therapeutics* **12**, 1073-1084, doi:10.1158/1535-7163.mct-13-0065 (2013).
91 Paull, T. T. *et al.* A critical role for histone H2AX in recruitment of repair factors to nuclear foci after DNA damage. *Current biology : CB* **10**, 886-895 (2000).
92 Sak, A., Stueben, G., Groneberg, M., Bocker, W. & Stuschke, M. Targeting of Rad51-dependent homologous recombination: implications for the radiation sensitivity of human lung cancer cell lines. *British journal of cancer* **92**, 1089-1097, doi:10.1038/sj.bjc.6602457 (2005).
93 Yu, S. O. *et al.* Ice restructuring inhibition activities in antifreeze proteins with distinct differences in thermal hysteresis. *Cryobiology* **61**, 327-334, doi:10.1016/j.cryobiol.2010.10.158 (2010).
94 Soleimani, R. Heytens, E. & Oktay, K. Enhancement of neoangiogenesis and follicle survival by sphingosine-1-phosphate in human ovarian tissue xenotransplants. *PloS one* **6**,

e19475, doi:10.1371/journal.pone.0019475 (2011).
95 Yang, H., Lee, H. H., Lee, H. C., Ko, D. S. & Kim, S. S. Assessment of vascular endothelial growth factor expression and apoptosis in the ovarian graft: can exogenous gonadotropin promote angiogenesis after ovarian transplantation? *Fertility and sterility* **90**, 1550-1558, doi:10.1016/j.fertnstert.2007.08.086 (2008).
96 Shikanov, A. *et al.* Fibrin encapsulation and vascular endothelial growth factor delivery promotes ovarian graft survival in mice. *Tissue engineering. Part A* **17**, 3095-3104, doi:10.1089/ten.TEA.2011.0204 (2011).
97 Campbell BK, T. E., Webb R, Baird DT. Evidence of a role for follicle-stimulating hormone in controlling the rate of preantral follicle development in sheep. *Endocrinology* **145**, 1870-1879 (2004).
98 Israely, T. *et al.* Vascular remodeling and angiogenesis in ectopic ovarian transplants: a crucial role of pericytes and vascular smooth muscle cells in maintenance of ovarian grafts. *Biology of reproduction* **68**, 2055-2064, doi:10.1095/biolreprod.102.011734 (2003).
99 Jeremias, E. *et al.* Heterotopic autotransplantation of the ovary with microvascular anastomosis: a novel surgical technique. *Fertility and sterility* **77**, 1278-1282 (2002).
100 Dath, C. *et al.* Xenotransplantation of human ovarian tissue to nude mice: comparison between four grafting sites. *Human reproduction* **25**, 1734-1743, doi:10.1093/humrep/deq131 (2010).
101 Yang, H. Y. *et al.* Graft site and gonadotrophin stimulation influences the number and quality of oocytes from murine ovarian tissue grafts. *Reproduction (Cambridge, England)* **131**, 851-859, doi:10.1530/rep.1.00916 (2006).
102 Labied, S. *et al.* Isoform 111 of vascular endothelial growth factor (VEGF111) improves angiogenesis of ovarian tissue xenotransplantation. *Transplantation* **95**, 426-433, doi:10.1097/TP.0b013e318279965c (2013).
103 Lee, J. R. *et al.* Effect of necrostatin on mouse ovarian cryopreservation and transplantation. *European journal of obstetrics, gynecology, and reproductive biology* **178**, 16-20, doi:10.1016/j.ejogrb.2014.04.040 (2014).
104 Tuuminen, R. *et al.* Donor simvastatin treatment prevents ischemia-reperfusion and acute kidney injury by preserving microvascular barrier function. *American journal of*

transplantation : official journal of the American Society of Transplantation and the American Society of Transplant Surgeons **13**, 2019-2034, doi:10.1111/ajt.12315 (2013).

105 Li, Y., Zhang, D., Zhang, Y., He, G. & Zhang, F. Augmentation of neovascularization in murine hindlimb ischemia by combined therapy with simvastatin and bone marrow-derived mesenchymal stem cells transplantation. *Journal of biomedical science* **17**, 75, doi:10.1186/1423-0127-17-75 (2010).

106 Zhang, Y. *et al.* Simvastatin augments the efficacy of therapeutic angiogenesis induced by bone marrow-derived mesenchymal stem cells in a murine model of hindlimb ischemia. *Molecular biology reports* **39**, 285-293, doi:10.1007/s11033-011-0737-y (2012).

107 Demeestere, I., Simon, P., Emiliani, S., Delbaere, A. & Englert, Y. Orthotopic and heterotopic ovarian tissue transplantation. *Human reproduction update* **15**, 649-665, doi:10.1093/humupd/dmp021 (2009).

108 Van Eyck, A. S. *et al.* Both host and graft vessels contribute to revascularization of xenografted human ovarian tissue in a murine model. *Fertility and sterility* **93**, 1676-1685, doi:10.1016/j.fertnstert.2009.04.048 (2010).

109 De Vito, R. *et al.* Markers of activated inflammatory cells correlate with severity of liver damage in children with nonalcoholic fatty liver disease. *International journal of molecular medicine* **30**, 49-56, doi:10.3892/ijmm.2012.965 (2012).

110 Moriyama, S. *et al.* Clinical controversy concerning the use of cryopreserved allografts in cardiovascular surgery. *Transplantation proceedings* **32**, 336-338 (2000).

111 Solanes, N. *et al.* Cryopreservation alters antigenicity of allografts in a porcine model of transplant vasculopathy. *Transplantation proceedings* **36**, 3288-3294, doi:10.1016/j.transproceed.2004.10.053 (2004).

112 Tuuminen, R. *et al.* Combined donor simvastatin and methylprednisolone treatment prevents ischemia-reperfusion injury in rat cardiac allografts through vasculoprotection and immunomodulation. *Transplantation* **95**, 1084-1091, doi:10.1097/TP.0b013e3182881b61 (2013).

113 Dewailly, D. *et al.* The physiology and clinical utility of anti-Mullerian hormone in women. *Human reproduction update* **20**, 370-385, doi:10.1093/humupd/dmt062 (2014).

114 Weenen, C. *et al.* Anti-Mullerian hormone expression pattern in

the human ovary: potential implications for initial and cyclic follicle recruitment. *Molecular human reproduction* **10**, 77-83 (2004).

115 Broer, S. L. *et al.* Anti-mullerian hormone predicts menopause: a long-term follow-up study in normoovulatory women. *J Clin Endocrinol Metab* **96**, 2532-2539, doi:10.1210/jc.2010-2776 (2011).

116 Wang, F. *et al.* Beneficial effect of resveratrol on bovine oocyte maturation and subsequent embryonic development after in vitro fertilization. *Fertility and sterility*, doi:10.1016/j.fertnstert.2013.10.041 (2013).

117 Huang, J. Y., Chen, H. Y., Park, J. Y., Tan, S. L. & Chian, R. C. Comparison of spindle and chromosome configuration in in vitro- and in vivo-matured mouse oocytes after vitrification. *Fertility and sterility* **90**, 1424-1432, doi:10.1016/j.fertnstert.2007.07.1335 (2008).

118 Lin YH, H. J., Seow KM, Huang LW, Chen HJ. Effects of growth factors and granulosa cell co-culture on in-vitro maturation of oocytes. *Reproductive biomedicine online* **19**, 165-170 (2009).

119 Van den Abbeel, E. *et al.* Osmotic responses and tolerance limits to changes in external osmolalities, and oolemma permeability characteristics, of human in vitro matured MII oocytes. *Human reproduction* **22**, 1959-1972, doi:10.1093/humrep/dem083 (2007).

120 Obata, Y., Maeda, Y., Hatada, I. & Kono, T. Long-term effects of in vitro growth of mouse oocytes on their maturation and development. *The Journal of reproduction and development* **53**, 1183-1190 (2007).

121 Bentov, Y., Esfandiari, N., Burstein, E. & Casper, R. F. The use of mitochondrial nutrients to improve the outcome of infertility treatment in older patients. *Fertility and sterility* **93**, 272-275, doi:10.1016/j.fertnstert.2009.07.988 (2010).

122 Wang, S. *et al.* Correlation of the mitochondrial activity of two-cell embryos produced in vitro and the two-cell block in Kunming and B6C3F1 mice. *Anatomical record* **292**, 661-669, doi:10.1002/ar.20890 (2009).

123 Zhang, J. & Liu, H. Cytoplasm replacement following germinal vesicle transfer restores meiotic maturation and spindle assembly in meiotically arrested oocytes. *Reproductive biomedicine online* **31**, 71-78, doi:10.1016/j.rbmo.2015.03.012 (2015).

국문 초록

서론: 여성 암 환자의 생존율은 증가함에 따라 생존을 넘어서는 삶의 질 향상을 위한 가임력 보존이 각광받고 있다. 현재 여성의 가임력 보존 방법은 난자 및 배아의 동결이 주를 이루나 이러한 방법은 사춘기 성 성숙 이전의 여성이나 배우자가 없는 여성에게는 적용하는 데에 한계가 있다. 난소조직을 이용할 시 이러한 단점을 극복할 수 있는 것으로 알려져 있고, 연구가 활발히 진행되고 있다. 난소조직의 동결보존 시 발생하는 동결손상, 이식 후 발생하는 허혈성 손상, 난소조직 직접 이식 시 암의 재발 가능성이라는 문제점을 지니고 있다. 본 문제점들을 극복하고자 생쥐 난소조직 유리화 동결-해동-자가이식 모델과 체외 난포배양을 적용하였다.

방법: 동결손상과 허혈성 손상을 비교하고자 유리화동결 및 자가이식 시행 여부에 따라, 총 8 군으로 분류하였다. 비교 연구 후

동결 손상과 허혈성 손상을 줄이고자 유리화동결-해동 시 항동결단백을 사용하여 동결손상을 감소시키고자 하였고, 난소 적출 2 시간 전 심바스타틴과 메틸프레드니솔론을 생쥐에 투여하여 허혈성 손상을 줄이고자 하였다. 유리화동결-해동-이식에 관련된 실험의 분석을 위해 6 주령의 생쥐를 이식 2, 7, 21 일 후에 희생하였고, 난소조직과 혈청을 회수하여 조직학적 관찰, 세포자멸사, 면역조직화학염색, 효소결합 면역흡착 분석법 (ELISA), 체외수정 등을 통해 분석하였다. 난포의 체외배양 조건을 개선하고자 2 주령 생쥐로부터 난포를 획득한 후 두 가지의 방법으로 10 일간 체외배양을 진행하였으며, 배양 10 일째 인간 융모선 자극호르몬 (hCG)과 표피성장인자 (EGF)를 처리하여 배란을 유도하였다. 난포의 생장 및 발달, 난자의 배 발달능, 유전자 발현 및 세포소기관의 기능 및 활성 등을 형광염색을 통하여 확인하였다.

결과: 유리화 동결과정은 난소 내 난포의 양과 질 측면에서 정상

대조군에 비해 감소하였으며, 이러한 결과는 이식 후 허혈성 손상에서 더 큰 감소폭을 나타내었다. 항동결단백을 이용하여 동결손상을 감소시킨 결과 고농도의 LeIBP를 사용하였을 때 난포의 상태, 세포자멸사 측면 등에서 높은 효과를 보였고, 개선된 동결보존 방법은 해동 및 이식 후까지 영향을 미치는 것으로 확인되었다. 심바스타틴과 메틸프레드니솔론을 난소 적출 전 같이 처리한 군에서는 허혈성손상을 감소시켜 난포의 상태, 세포자멸사, 이식체 내 혈관의 형성 및 항뮐러리안 호르몬 수치가 개선되는 것을 확인하였다. 체외난포배양 시 미네랄 오일을 사용한 군에서 난포의 생장 및 발달 등이 개선되었으나, 배아 발달능이 급감하였다. 원인을 체내 성숙된 난자와 비교·분석한 결과, 난자의 핵 내 유전자 발현에는 차이가 없었으나, 세포질 내 소기관 및 생리학적 기능 측면에서 문제가 발생하는 것을 확인하였다.

결론: 난소조직을 이용한 가임력 보존에서 발생되는 동결손상과

허혈성 손상을 최소화하기 위한 지속적인 연구들이 필요하며, 항동결단백을 이용한 동결손상의 감소 및 심바스타틴과 메틸 프레드니솔론을 이용한 허혈성 손상의 감소를 통해 유리화동결-해동 후 이식된 난소조직의 손상 정도를 감소시킬 수 있음을 제시하였다. 난소조직 내 혈관의 분포 정도가 중요한 요소임을 추가적으로 판단할 수 있었다. 난포의 체외 배양은 난소조직을 직접 이식하는 경우 발생할 수 있는 암의 재발을 사전에 예방할 수 있는 매우 유용한 방법으로 제시하였다. 앞으로 난포의 체외배양조건의 개선, 대동물 및 인간 난소에서의 효용성 확인 등과 같은 추가적인 연구가 필요하다.

주요어 : 가임력보존 / 난소조직 / 유리화동결 / 동결손상 / 이식 / 허혈성 손상/ 난포 체외배양

학 번 : 2013-30597